Quarterly Report, Volume I

PLANETARY SOLAR ARRAY DEVELOPMENT

Prepared for
Jet Propulsion Laboratory
California Institute of Technology
4800 Oak Grove Drive
Pasadena, California
Attention: M. Beckstrom

Contract 952035

EOS Report 7254-Q-3 15 April 1968

Prepared by
R. Wizenick, Program Manager

Approved by

W. Menetrey, Manager
Space Electronics Division

This work was performed for the Jet Propulsion Laboratory, California Institute of Technology, as sponsored by the National Aeronautics and Space Administration under Contract No. NAS7-100.

ELECTRO-OPTICAL SYSTEMS, INC.
A XEROX COMPANY

ABSTRACT

This is the third quarterly report describing the work completed at EOS on the Planetary Solar Array Development Study Program, JPL Contract No. 952035.

This report finalizes the requirements of Task III, and is presented in three volumes.

CONTENTS

1.	INTRODUCTION	1-1
2.	PACKAGING AND DEPLOYMENT	2-1
	2.1 Packaging	2-1
	2.2 Deployment	2-7
3.	ELECTRICAL ANALYSIS	3-1
	3.1 Solar Cells	3-1
	3.2 Solar Cell Covering	3-2
	3.3 Solar Cell Radiation Degradation	3-10
	3.4 Circuit Design	3-17
	3.5 Electrical Power Analysis	3-23
	3.6 Magnetic Field Analysis	3-43
	3.6.1 Sun at Zenith of Spacecraft	3-46
	3.6.2 Sun-Shade Condition	3-49
	3.6.3 Conclusion	3-51
4.	STRUCTURAL DESIGN AND ANALYSIS	4-1
	4.1 Substrate	4-2
	4.1.1 Description	4-2
	4.1.2 Material Selection	4-2
	4.1.3 Mathematical Model	4-2
	4.1.4 Loads and Deflection Analysis	4-8
	4.1.5 Substrate Stress Analysis	4-9
	4.1.6 Conclusions and Recommendations	4-12
	4.2 Peripheral Frame of the Substrate	4-12
	4.2.1 Functional Description	4-12
	4.2.2 Material Selection Criteria	4-12
	4.2.3 Mathematical Model(s)	4-12
	4.2.4 Critical Loads Analysis	4-13
	4.2.5 Stress Analysis	4-13
	4.2.6 Conclusion	4-14

CONTENTS (contd)

5.	SYSTEM ANALYSIS	5-1
	5.1 Environmental Interaction	5-1
	5.1.1 Earth Environmental Interaction	5-1
	5.1.2 Launch, Flight, and Landing	5-4
	5.1.3 Mars Environmental Interaction	5-5
	5.2 Materials Evaluation	5-7
	5.3 Thermal Analysis, Nontracking Conical Array	5-10
	5.4 Weight Analysis, Nontracking Conical Array	5-16
	5.5 Reliability Considerations for the Nontracking Conical Array	5-16
	5.5.1 Reliability Definition	5-16
	5.5.2 Power Capability	5-16
	5.5.3 Failure Mode Discussion	5-22
	5.5.4 Calculations	5-23
	5.5.5 Conclusions	5-25
6.	PRELIMINARY MANUFACTURING PLAN	6-1
	6.1 Facilities	6-1
	6.1.1 Location	6-1
	6.1.2 Whiteroom Facilities	6-2
	6.1.3 Storage Areas	6-2
	6.1.4 Resident Offices	6-3
	6.2 Manufacturing Flow Plan	6-3
	6.2.1 Incoming Cell Test and Matching	6-3
	6.2.2 Submodule Fabrication	6-5
	6.2.3 Module Series Strings	6-5
	6.2.4 Substrate Fabrication	6-6
	6.2.5 Handling Procedures	6-6
	6.2.6 Module Bonding to Substrate	6-7
	6.3 Material Status Control	6-7
	6.4 Document Preparation and Its Use	6-10

CONTENTS (contd)

7.	PRELIMINARY TEST PLAN	7-1
	7.1 Introduction	7-1
	7.1.1 Definitions	7-1
	7.2 Solar Array Tests	7-2
	7.2.1 Development Engineering Test Evaluation	7-2
	7.2.2 Acceptance Test	7-10
	7.2.3 Qualification Test	7-10
	7.2.4 Reliability Test	7-14
	7.2.5 Shipping Container Test	7-14
	7.3 Test Equipment and Fixtures	7-16
	7.4 Performance Testing	7-16
	7.4.1 Single Cell Testing	7-16
	7.4.2 Submodule Testing	7-17
	7.4.3 Sample Module Testing	7-17
	7.4.4 Panel Testing	7-17
8.	SUMMARY	8-1
	APPENDIX A — ANGLE OF INCIDENCE OF SUNLIGHT ON TRUNCATED CONE FOR SEVERAL LOCATIONS AND ORIENTATIONS ON THE MARTIAN SURFACE	A-1
	APPENDIX B — SOLAR PANEL HEAT BALANCE EQUATIONS	B-1

SECTION 1

INTRODUCTION

This report is Volume I of three volumes of the third quarterly report. It represents the detailed study of the nontracking conical solar array.

SECTION 2

PACKAGING AND DEPLOYMENT

This section details the mechanical packaging and deployment of the non-tracking, deployable, conical solar array.

2.1 PACKAGING

The following is a discussion of the mechanical aspects of a conceptual design for a photovoltaic power system which meets the design constraints of Jet Propulsion Laboratory Drawing Number 1002 3236A, and Electro-Optical Systems Drawing Number 7254-100 (Fig. 2-1). It provides for solar cell circuits being permanently affixed to the outer surface of a substrate in the form of a frustrum of a right cone. For convenience in manufacture and testing, the substrate is divided into six 60 degree segments. Each segment, or panel, is in the form of an aluminum hollow core substrate, with integral beryllium tubing frames around the periphery of the panel. The two 180 degree sections of the cone will be mounted into the sterilization canister with their ends mated and securely latched to form a 360 degree frustrum of a right cone during the launch and flight mode.

The support and deployment structure consists of three major elements for each 180 degree section of the conical array. These sets of elements are situated on opposite sides of the spacecraft body and are not only capable of supporting the array in both the launch and landed modes, but are also capable of deploying each 180 degree half-section out away from the spacecraft body so that the other two sides of the spacecraft are completely unobstructed after the solar array has been deployed.

SECURITY CLASSIFICATION

NOTES:

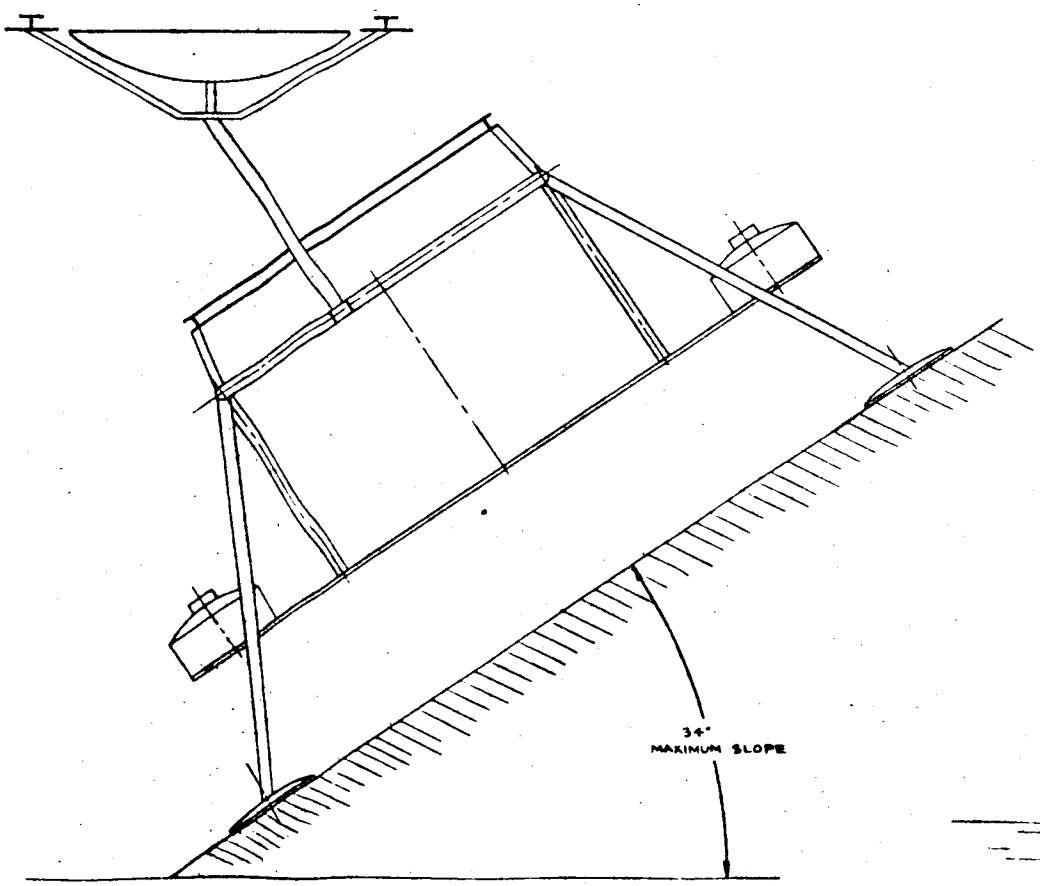

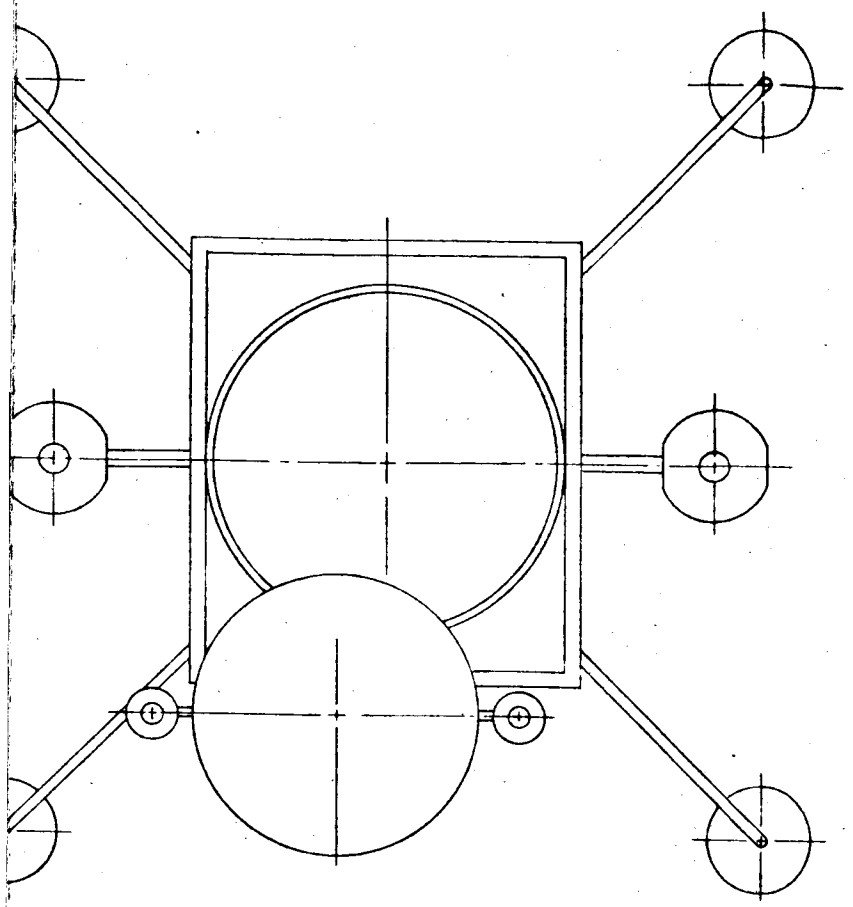

EXTENDED POSITION

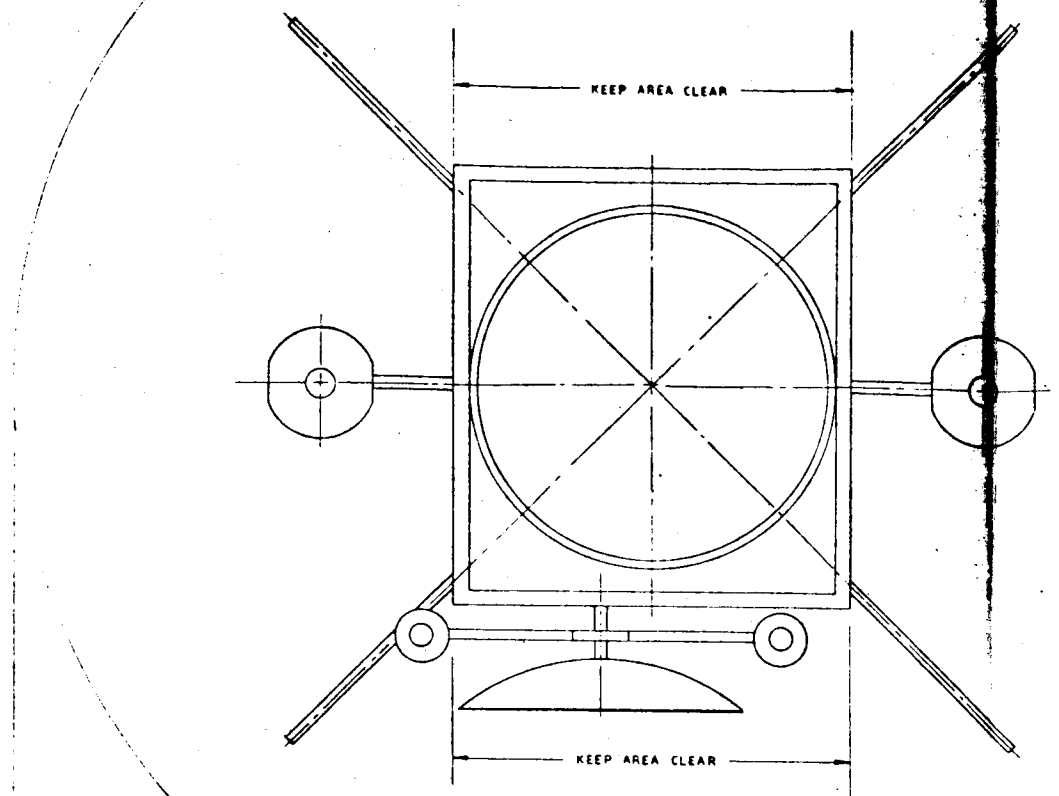

TOP VIEW
STOWED CONDITION

AREA AVAILABLE FOR S.P. IN STRAIGHT OUT POSITION. 107°E FROM S.C. CENTER IN STOWED POSITION.

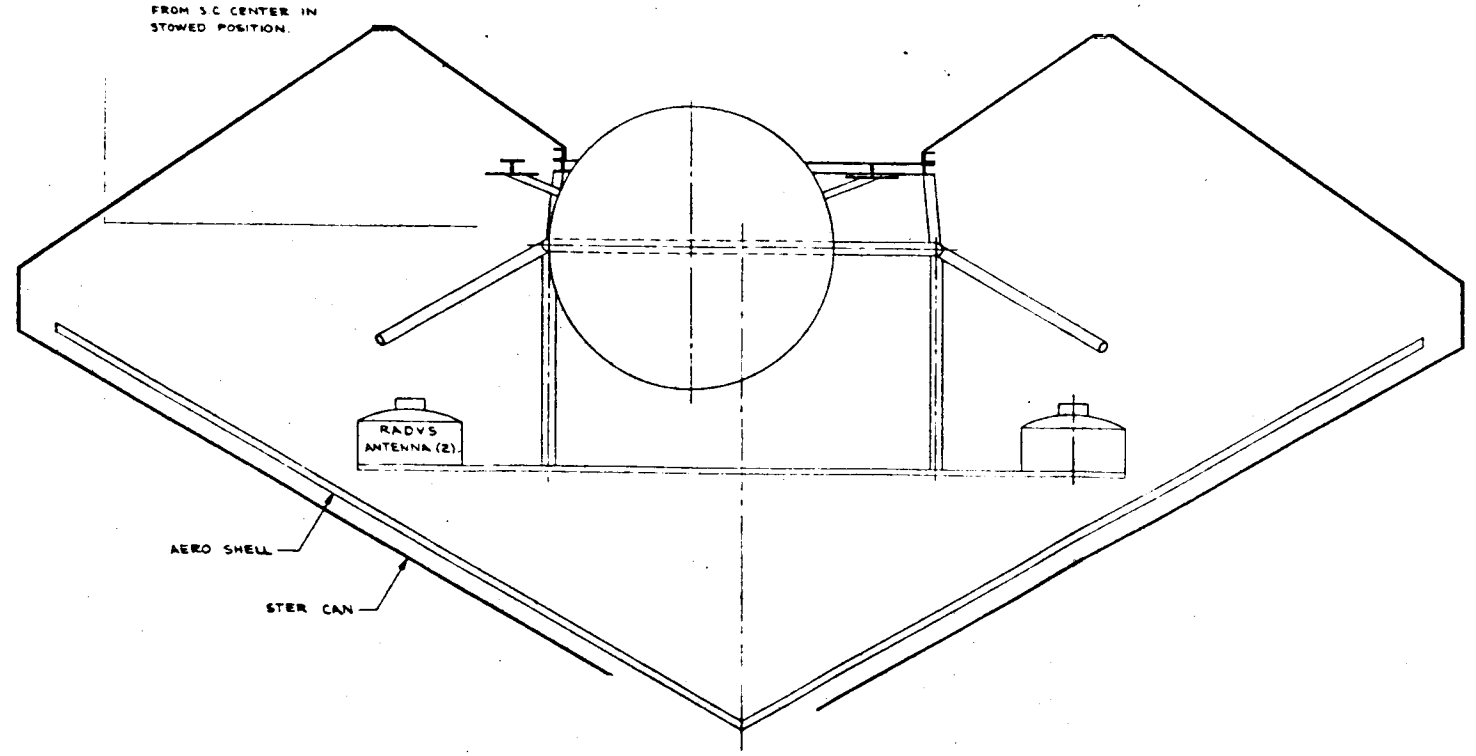

SIDE VIEW
STOWED CONDITION

SCALE - INCHES

REVISIONS			
ZONE	LTR	DESCRIPTION	DATE

SYM	CODE IDENT	PART OR IDENTIFYING NO.	NOMENCLATURE OR DESCRIPTION	MATERIAL	SPECIFICATION	UNIT WT.	ZONE	ITEM NO.

LIST OF MATERIALS

UNLESS OTHERWISE NOTED LARGER DIGIT IN INCHES. TOLERANCES DECIMAL .XX ± .XXX ± FINISH ANGULAR ± DO NOT SCALE

MATERIAL

TREATMENT / FINISH

DRAWING NO.

NEXT ASSY | USED ON | APPLICATION

DRAWING LEVEL

CONTRACT NO.

DRAWN | DATE

CHECKED R.L. Ferrand 2-10-65

DESIGN

STRESS

RELIABILITY ACTIVITY APPD

CUSTOMER

ELECTRO-OPTICAL SYSTEMS, INC.
a subsidiary of Xerox Corporation
300 N. Halstead St., Pasadena, California 91107

TITLE
LAYOUT -
SOLAR PANEL CLEARANCE

SIZE	CODE IDENT NO.	DWG NO.
J	12705	7254-100

SCALE NONE | RELEASE DATE | SHEET 1 OF 1

7254-100 REV

FOLDOUT FRAME 2 | FOLDOUT FRAME 3 | FOLDOUT FRAME 4

SECURITY CLASSIFICATION

NOTES: UNLESS OTHERWISE SPECIFIED

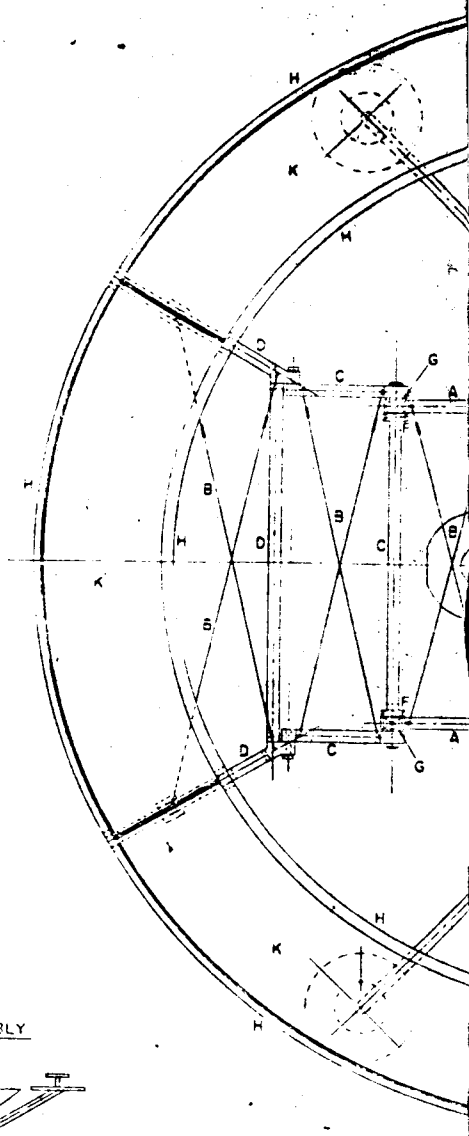

TRANSMITTING ANTENNA ASSEMBLY

SOLAR ARRAY HALF-SECTION
IN HALF DEPLOYED CONDITION

SPACECRAFT BODY

SIDE VIEW OF
PLANETARY SOLAR ARRAY
IN LANDED MODE

FOLDOUT FRAME 2-3

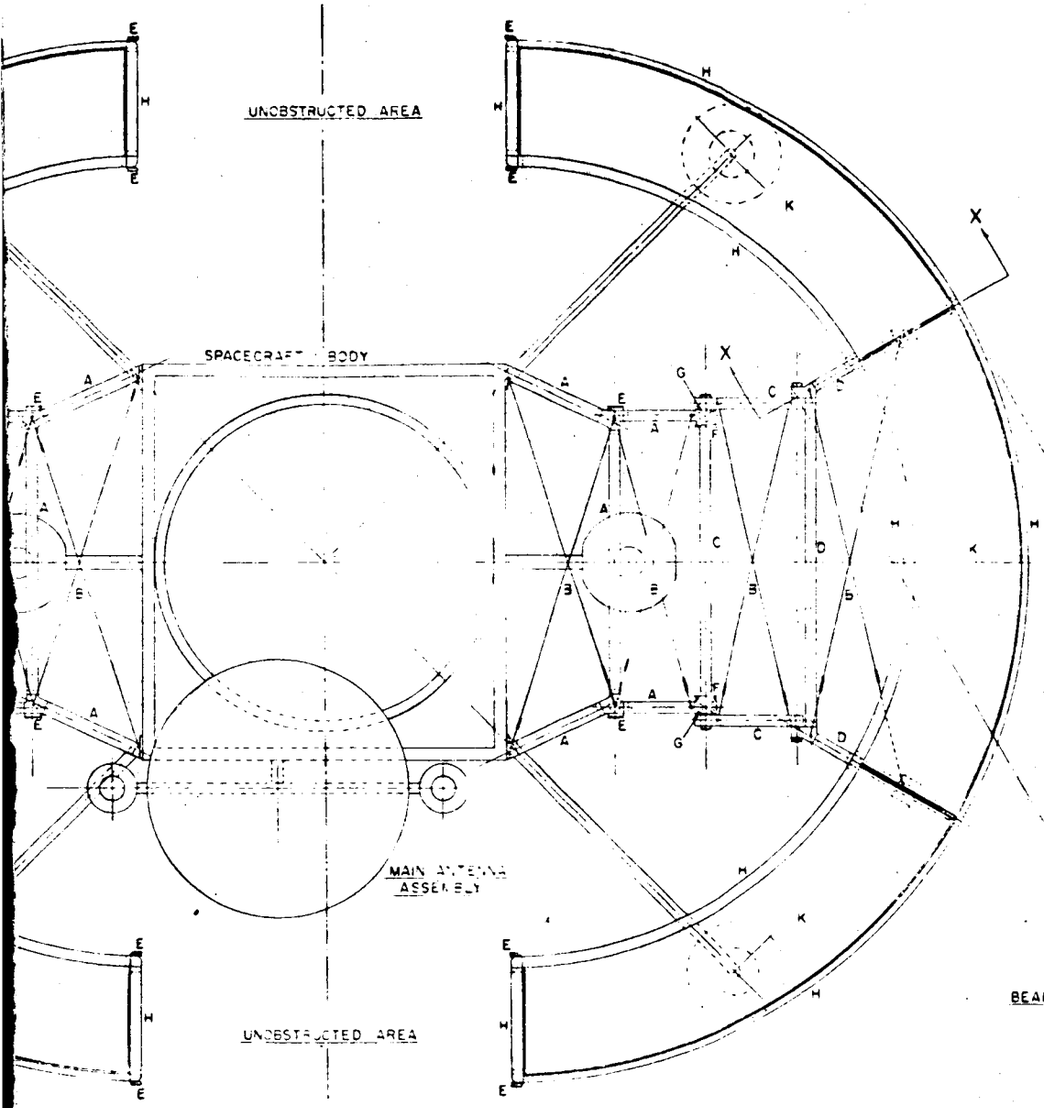

TOP VIEW OF PLANETARY SOLAR ARRAY
IN FULLY DEPLOYED CONDITION

LEGEND

A-SOLAR ARRAY SUPPORT STRUCTURE
B-TENSION CABLE
C-DEPLOYMENT YOKE
D-DEPLOYABLE ARRAY TRUSS
E-LAUNCH MODE LATCH
F-CABLE-DRUM ASSEMBLY — DEPLOYMENT YOKE SYNCHRONIZER
G-DEPLOYMENT DRIVE TORSION SPRINGS
H-ARRAY FRAME
K-SUBSTRATE
M-SOLAR CELL CIRCUIT

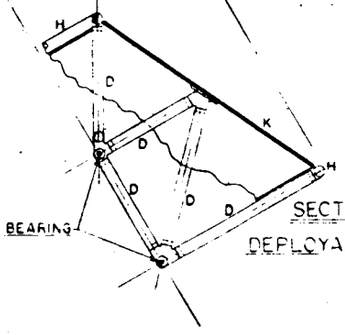

SECTION X-X
DEPLOYABLE ARRAY TRUSS

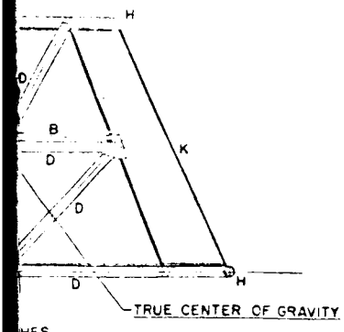

HES
LAR ARRAY HALF-SECTION
FULLY DEPLOYED CONDITION

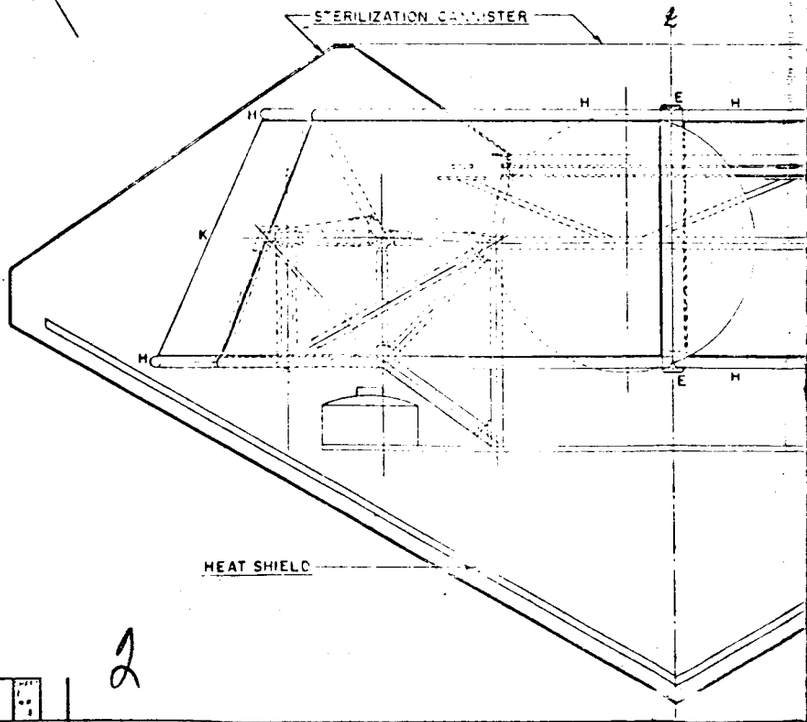

7254-110

2

REVISIONS				
ZONE	LTR	DESCRIPTION	DATE	APPROVED

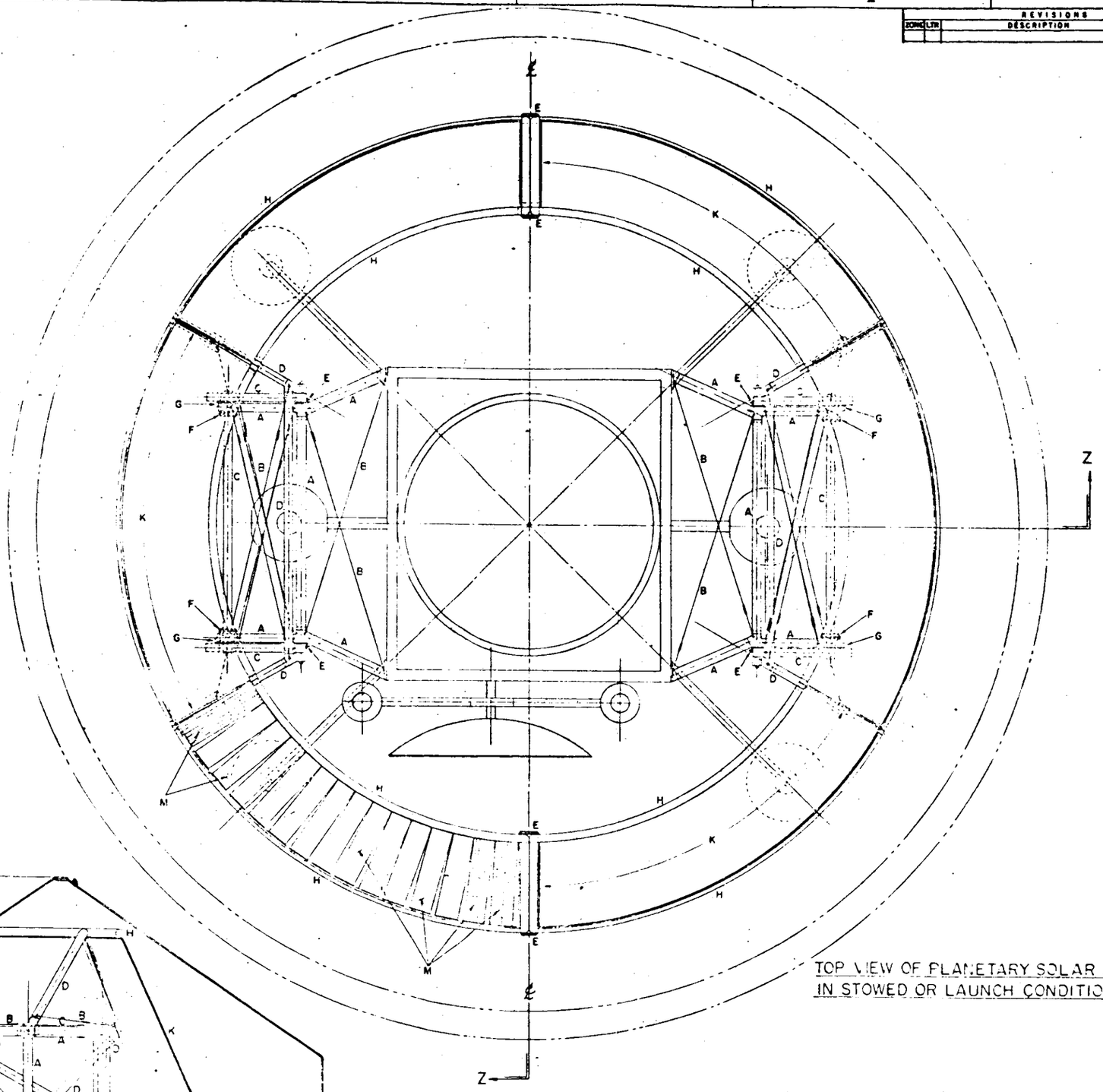

TOP VIEW OF PLANETARY SOLAR ARRAY IN STOWED OR LAUNCH CONDITION.

QUARTER SECTION Z-Z

SIDE VIEW OF PLANETARY SOLAR ARRAY IN STOWED OR LAUNCH CONDITION.

0 10 20 30 40 50 60 70 80 90 100

SCALE IN INCHES

QTY REQD	SYM	CODE IDENT	PART OR IDENTIFYING NO	NOMENCLATURE OR DESCRIPTION	MATERIAL	SPECIFICATION	UNIT WT	ZONE	ITEM NO

LIST OF MATERIALS

UNLESS OTHERWISE NOTED LINEAR DIMS IN INCHES. TOLERANCES DECIMAL .XX ± .XXX ± FINISH ANGULAR ± MMS DO NOT SCALE

MATERIAL

TREATMENT

CONTRACT NO

DRAWN P. L. [illegible] DATE 9-6-65

CHECK [illegible] DATE 9/6/65

DESIGN

APPD

DESIGN ACTIVITY APPD

CUSTOMER

ELECTRO-OPTICAL SYSTEMS, INC.
A XEROX COMPANY
[illegible] NORTH HALSTED STREET · CHICAGO, CALIFORNIA 91107

TITLE
PLANETARY SOLAR ARRAY-
NON-TRACKING DEPLOYABLE SYSTEM

SIZE J | CODE IDENT NO 12705 | DWG NO [illegible]-10

SCALE 1/10 | RELEASE DATE | SHEET 1 OF 1

ON | THRU | EFFECTIVE SERIAL NO | USAGE DATA

NEXT ASSY | USED ON | APPLICATION | DRAWING LEVEL

3

FOLDOUT FRAME 2-6

2-5

beryllium tubing which is bonded to specially designed lightweight metal end fittings. The upper bearing point of each assembled pair of array trusses is located at the true center of gravity, or balance point, of that particular 180 degree conical half-section of the completely assembled photovoltaic array. The lower bearing points are located at the junction of a line through the corresponding upper bearing point and perpendicular to the centerline of the bottom beryllium beam of each array truss.

By the use of thrust bearings and interconnecting beams in the form of thin-wall beryllium tubing, each array main support structure, each pair of deployment yokes, and each pair of deployable array trusses take the form of "box structures" with no remaining open-ended mechanical linkages. Each of these mechanical "box structures" is further braced by crossed tension cables,(B), in both the launch and deployed modes.

During the launch mode, or stowed condition, the two 180 degree half sections of the completely assembled and tested solar power system will be mated at their ends and securely latched together to form a 360 degree fustrum of a right cone. In this condition each set of deployment yoke assemblies will be rotated, or folded, inward toward the body of the spacecraft. Latches, (E), will be installed eight places to completely lock the total power system in the stowed condition. These latches are located at both the top and bottom of the ends of each 180 degree half-section of the array, and also at the points where the folded-in arms of the deployment yokes meet the angular fittings of the main support structures. All latch devices will be pyrotechnically actuated and may be of either the "pin puller" or "cable cutter" type.

2.2 DEPLOYMENT

After landing, deployment of the two 180 degree half-sections of the solar array will be accomplished in a sequential manner from a preprogrammed system to unlatch from the stowed condition, and by completely automatic

and fully mechanical devices. First, the four latches located at the extreme ends of the two conical half-sections will be fired and the ends unlatched. Second, the inboard latches located at the ends of the arms of the upper deployment yokes will be fired, completely releasing both halves of the system. At this point the pre-loaded and set Torsion Springs, (G), which are located at both ends of each of the four deployment yoke shafts are free to exert upper and outward rotary motive force into the deployment yokes. The rotary motion of the upper and lower deployment yoke on each side of the array is kept in perfect parallel synchronization by means of the Cable and Drum Assemblies, (F). By means of the torsion spring force, the deployment yoke arms lift each half-section of the array in an upward and outward mode through 180 degrees of travel.

Torsion spring dampers, of either the "negator" or "dash pot" type will be brought into play after each half-section of the array has traveled through approximately 110 degrees of its total 180 degree arc. These dampers are located at each of the eight deployment torsion springs and will be pre-set to exert a braking force to slow the motion of the two array half-sections as they travel through the final degrees of their outward 180 degree arc. When the two half-sections reach the end of this arc the solar array will be fully deployed and the two opposite sides of the spacecraft will be completely unobstructed. When the ends of both sets of deployment yokes have reached the fully deployed condition, eight spring-loaded positive-setting latches; four for each half-section of the array, will permanently lock the solar array in the fully deployed mode.

SECTION 3

ELECTRICAL ANALYSIS

This section details the electrical analysis for the nontracking deployable, conical solar array.

3.1 SOLAR CELLS

The solar cells selected for this array are discussed in the 2nd quarterly report, No. 7254-Q-2. A solar cell of N/P type silicon with a bulk resistivity of 1-3 ohm-cm has been selected. Cells of this type are capable of producing more power in a relatively radiation-free environment than cells of a nominal 10 ohm-cm bulk resistivity range. The optimum cell thickness to minimize the solar array area and allow the maximum specific wt/sq ft to the substrate was determined in the 15 December report, and is 0.010 inch thick. EOS has chosen a solar cell of a top contact configuration. The advantage of a cell of this type is that it can be readily adapted to a series-parallel matrix submodule array. In addition, all the solder joints are visible on the top surface after bonding to the panel substrate, and the design allows close packaging of the individual cells yielding a smaller overall circuit configuration. The replacement of an individual cell, in the event of accidental damage, can be readily accomplished, and the back surface of the solar cell submodules are flat, and unencumbered with a connector and solder joints. This allows a minimum adhesive thickness to bond the cells to the substrate. EOS has elected to stay with the 2 x 2 cm cell size, even though the cover glass has been eliminated, for reliability considerations and to obtain more flexibility in the circuit to conform to the truncated cone design. The cell specifications are:

a. Type - N/P silicon
b. Contacts - sintered silver-titanium
c. Size - 2 x 2 cm
d. Thickness - 0.010 ± 0.001 inch
e. Configuration - front contact (solderless)
f. Resistivity - 1-3 ohm-cm
g. Electrical output - 58 mW at 485 mV (28°C, AMO)

The cell is shown in EOS Drawing No. 7254-105, Fig. 3-1. A typical I-V curve of a cell of this type is shown in Fig. 3-2.

3.2 SOLAR CELL COVERING

Solar cell covers, or filters, of glass or fused silica have been used to enhance the emittance properties of solar arrays for many years. It has been empirically determined that 0.001 inch of either material is sufficient to yield the properties of the bulk materials. The filters also act as a shield to protect the cells from radiation degradation. The thickness of the filter is varied to suit the anticipated needs of the particular array. The radiation environment on the Martian surface is very low when compared to near earth environments, and this, coupled with the weight requirements of this mission, dictate the use of as thin a filter as practical. An 0.003 inch filter was first considered for the mission requirements.

However, a solar cell circuit operating on the Martian surface has a problem which is unique and not found in space applications. Mars has a dust condition which is considered severe; the dust is assumed to be iron oxide and electrically conductive. The electrical shorting caused by the dust would be catastrophic to the solar array. A study of the dust conditions on the Martian surface was made and reported in the first quarterly report. For reference, the electrical resistivity of iron oxide, in comparison with other known insulators, is as shown below:

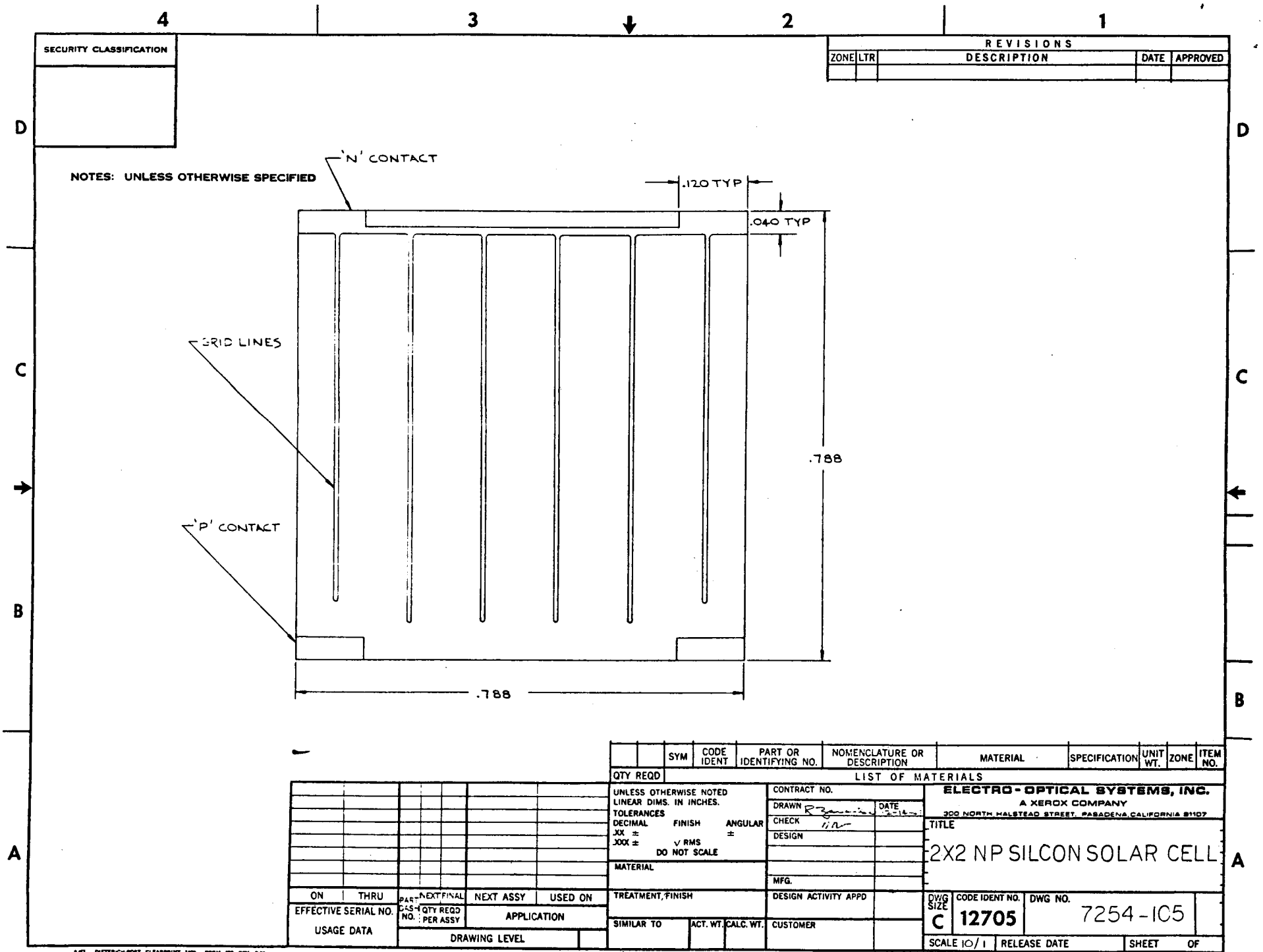

Figure 3-1. 2 x 2 NP Silicon Solar Cell

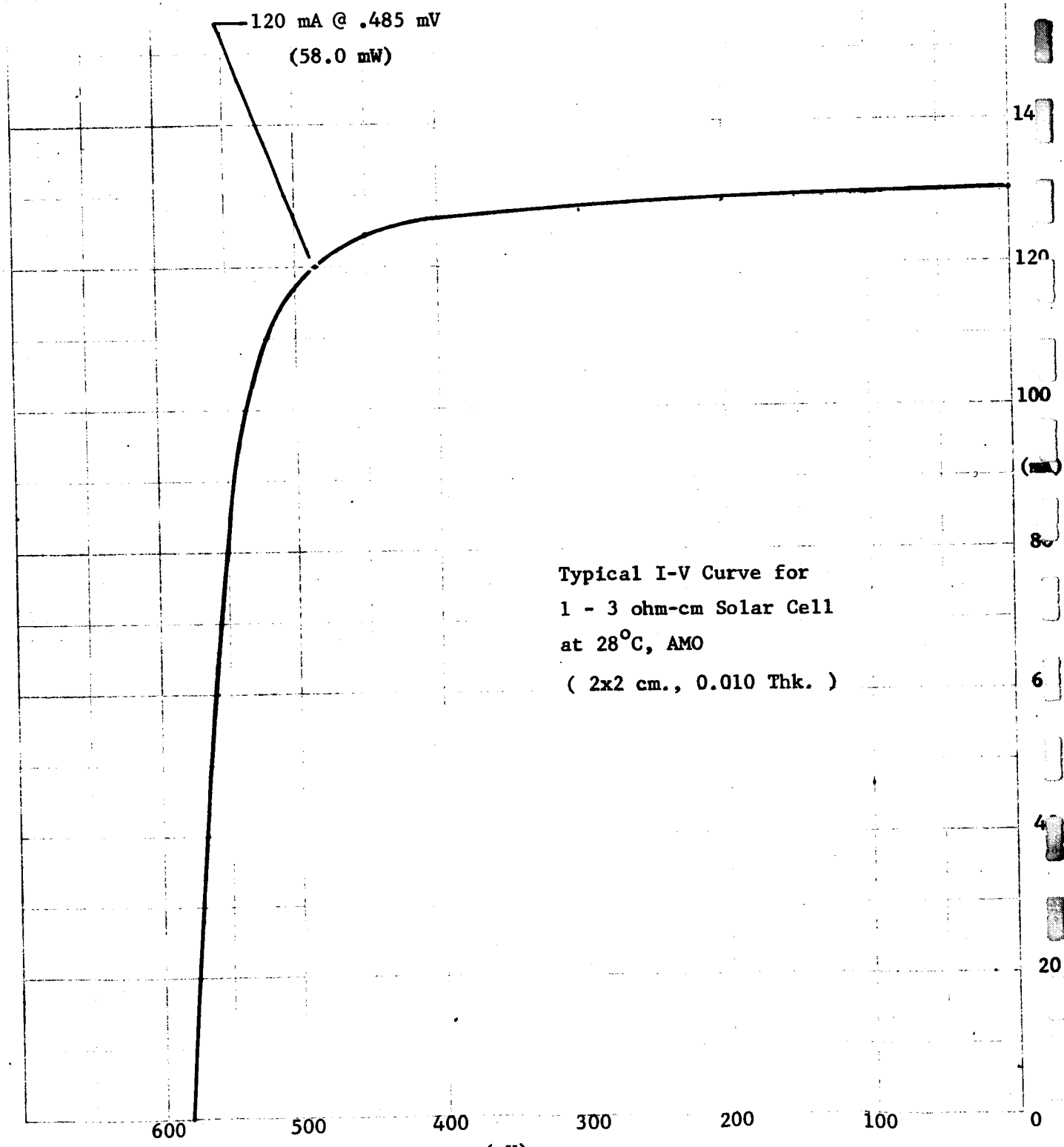

7254-9-3 Figure 3-2.

Material	Electrical Resistance (ohm-cm) at 300°K
1. 99.24 Fe_2O_3 and 0.76 Ti_1O_2	2
2. 99.85 Fe_2O_3 and 0.15 TiO_2	60
3. BeO	10^{11}
4. Al_2O_3	$> 10^{13}$
5. H-film (Kapton)	10^{14}

These data indicate that no electrical connections should be exposed.

One approach to this problem, which was considered, was to coat all electrically exposed areas of the solar cell circuit with filter adhesive. This approach has been used on solar panels for earth terrestrial applications. This method is tedious, virtually impossible to guarantee complete protection, and will add considerable weight to the solar array.

A second consideration was discussed in the 2nd quarterly report, that is, eliminating the cover glass and using a semiorganic resin developed by Dr. Burnn Marks of Lockheed Missiles and Space Company, Palo Alto, California. This coating has been developed specifically as a solar cell coating and can be applied by spraying techniques. This coating has been tested on solar cells for emissivity and light transmission, as well as for environmental space effects including ultraviolet, vacuum, electron irradiation, and temperature extremes. The principal drawback to this coating technique is the inability to completely insulate all electrically conducting surfaces. Spray application of the coating would not insulate the back side of connector tab, and dipping the total array is highly impractical. A heavy brush coating could be applied and techniques developed to remove the excess before curing. However, the material is not suited for this type of application.

EOS would like to propose a method for insulating the solar array by encapsulating the cells with a continuous sheet of DuPont Tedlar PVF film. Tedlar film is essentially transparent to, and unaffected by, solar radiation in the near ultraviolet, visible and near infrared regions of the spectrum. The transmission characteristics of transparent Tedlar film are shown in Figs. 3-3 and 3-4. One of the outstanding characteristics of Tedlar film is its resistance to solar degradation. Test samples of transparent film have not discolored and still retain 50% of their initial tensile strength after 10 years of outdoor weathering in Florida, facing south at 45° to the horizontal. Typical properties of Tedlar film Type 30 are:

a.	Tensile strength	- 13,000 psi
b.	Yield point	- 5,000 psi
c.	Density	- 1.38 g/cc
d.	Refractive index	- 1.467
e.	Melting point	- $> 300^{\circ}C$
f.	Service temperature	- $70^{\circ}C$ to $+105^{\circ}C$
g.	Coefficient thermal expansion	- 2.8×10^{-5} ($^{\circ}F$)
h.	Dielectric strength	- 3,500 V/mil
i.	Volume resistivity	- 10^{14} ohm-cm

No previous data are available for the a/e properties of a solar cell covered with Tedlar film and filter adhesive. These measurements should be made under the Phase II portion of the program. The a/e value will probably lie somewhere between that of a bare cell and a filtered cell.

Electrical measurements of a solar cell, "filtered" with 1 mil type 30 transparent Tedlar film, and Dow Corning type XR-6-3489 silicone adhesive, and the I-V curve of a coated cell are shown in Fig. 3-5. The degradation percent at the maximum power point is:

OPTICAL PROPERTIES

SPECTRAL TRANSMISSION

Transparent types of "Tedlar"* are essentially transparent to, and unaffected by, solar radiation in the near ultraviolet, visible and near infrared regions of the spectrum.

Transmission spectra for "Tedlar" are shown in Fig. 3-4.

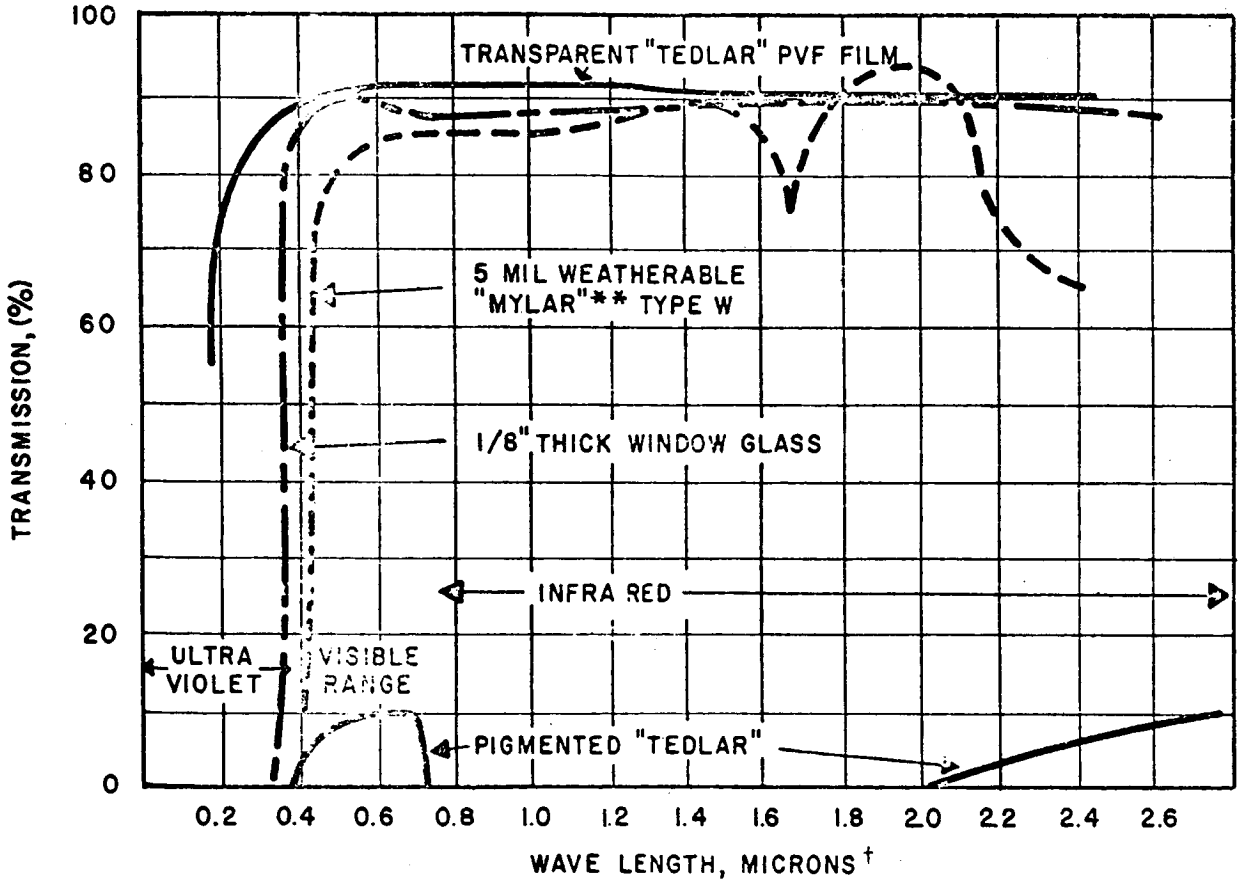

*Du Pont registered trademark for its PVF film

**Du Pont registered trademark for its polyester film

NOTE (†) 10,000 Angstroms = 1 Micron = 0.001 mm

Figure 3-3.

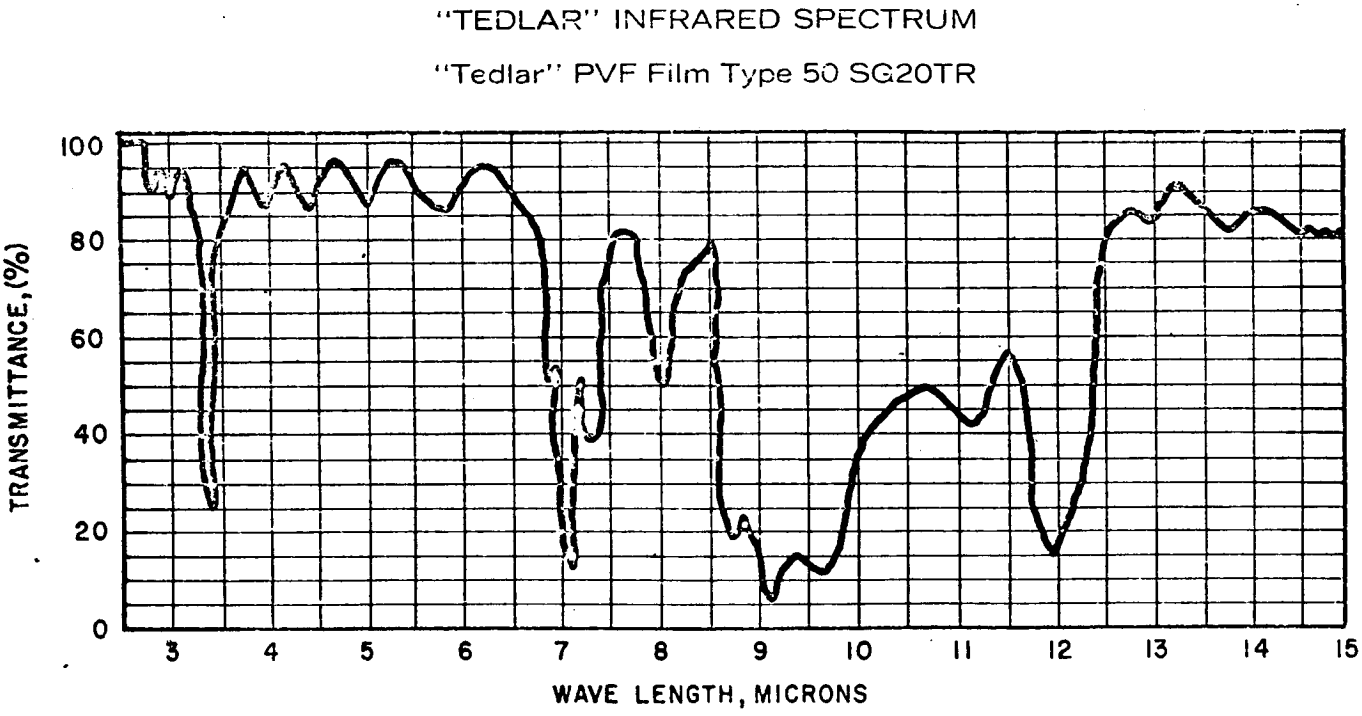
"TEDLAR" INFRARED SPECTRUM
"Tedlar" PVF Film Type 50 SG20TR
TRANSMITTANCE, (%)
100
80
60
40
20
0
3
4
5
6
7
8
9
10
11
12
13
14
15
WAVE LENGTH, MICRONS

Figure 3-4.

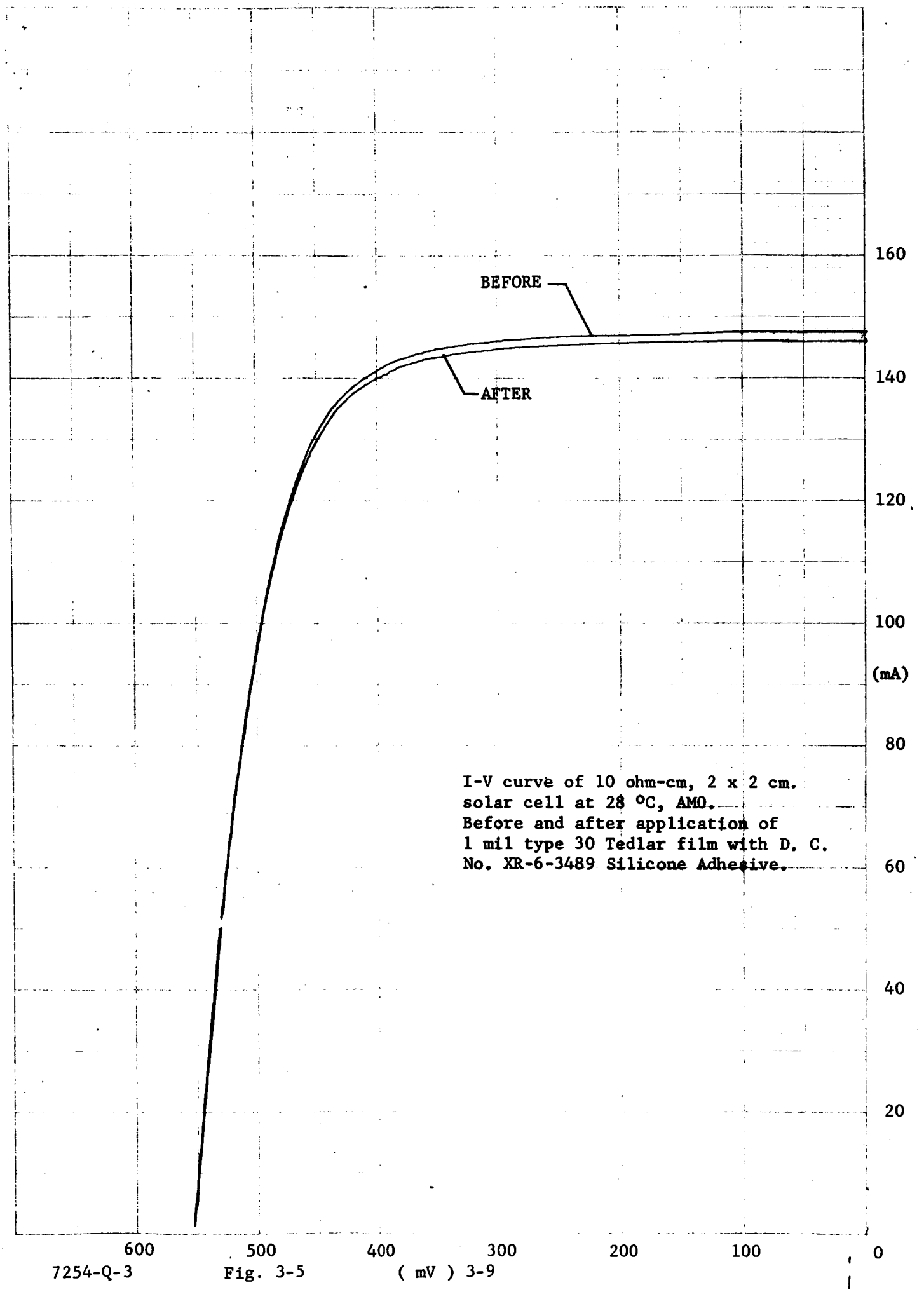

7254-Q-3 Fig. 3-5 3-9

$$\% = \frac{(136.5 - 135.5)}{136.5} \times 100$$

$$= 0.73\%$$

The degradation of less than 1% is comparable to losses experienced with quartz filters and significantly better than that experienced with microsheet filters.

The advantages of the film coating for the solar cell circuit are:

a. Total insulation of all electrical conducting surfaces

b. Low electrical loss due to coating

c. Material is readily available

d. Installation is easily accomplished using a space proven adhesive system

e. Finished coating eliminates gaps between cells, which would form a trap for dust accumulation

f. The coating will provide protection for the cells from low energy proton radiation, as the cells will have no exposed areas common to typically filtered cells

g. The film is low in weight

h. The flexible film, bonded with a resiliant adhesive should have better abrasion resistance to the 'sandblasting effect' of the dust than the hard surface of glass or quartz filters

3.3 SOLAR CELL RADIATION DEGRADATION

The radiation that the solar array will be exposed to while operating on the Martian surface will be ultraviolet radiation from the sun spectrum, and proton radiation as a result of solar flares.

The ultraviolet radiation will not affect the Tedlar film or the silicone adhesive used to bond the film to the cell.

The intensity of the solar flare radiation for the planetary array mission in 1973 is based on the information provided in the JPL Voyager Environmental Predictions Document SE-003BB01-1B28, Paragraph III, D.4 Table 13 as shown below:

MAXIMUM TIME-INTEGRATED SOLAR FLARE FLUXES

	Energy (MeV)	Flux (protons/cm^2) (11 gm/cm^2)
Maximum time-integrated proton flux/flare	E > 10	1.2×10^8
	E > 30	9.8×10^7
	E > 100	6.7×10^7
Maximum time-integrated proton flux/year	E > 10	1.6×10^8
	E > 30	1.3×10^8
	E > 100	9.3×10^7

Quantitative data for proton damage to silicon solar cells is relatively scarce compared to available electron damage data. Also, the mechanisms are not well understood. It has been found most convenient to refer proton damage to an equivalent of 1 MeV electrons and then proceed to use the available data for electron damage. A curve for 1 ohm-cm and 10 ohm-cm N/P solar cells plotting the equivalent 1 MeV electron damage rate as a function of proton energy is shown in Fig. 3-6. The most important feature of this curve is the reciprocal dependence of damage upon proton energy for energies greater than 1 MeV. The curve has been drawn from available data, which definitely indicates a change in slope between 40 and 100 MeV. There appears to be a change in defect production mechanism in this range causing the change in slope.

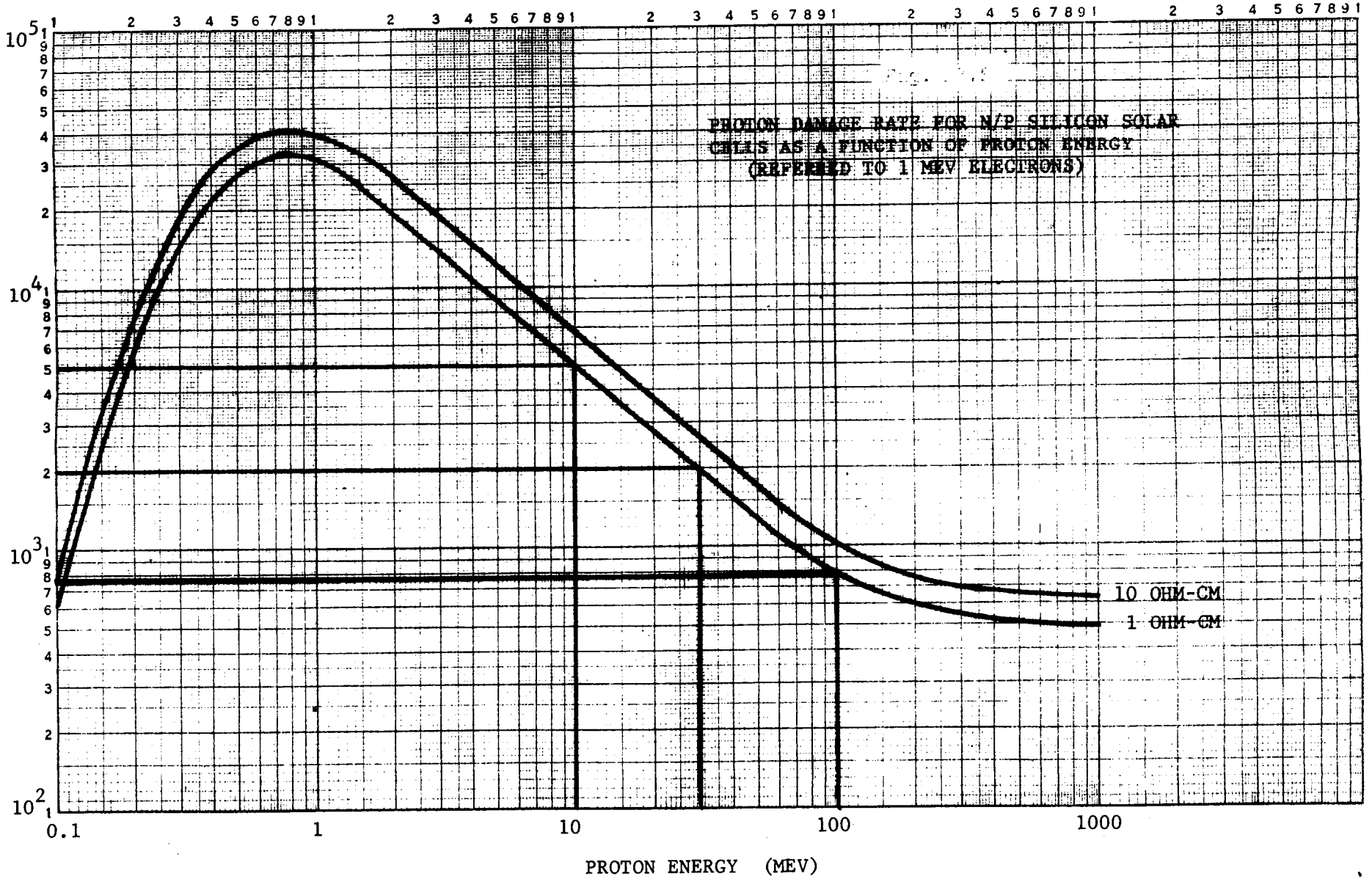

Figure 3-6.

In use, the proton flux is analyzed as a function of proton energy, and the equivalents for each energy are taken. The degradation may be found by referring to the electron damage curves for the flux obtained from the product of the proton flux and the damage equivalents.

The following curves, Figs. 3-6, 3-7, 3-8, and 3-9, used to represent the radiation damage effects, were taken from the space power manual, published by Hoffman Electronics Corporation.

Referring to Fig. 3-6, the following values of 1 MeV electron requirements are obtained for the flux/year data from JPL Document SE-003BB01-1-1B28.

	Proton Flux	(Eq 1 MeV E/P)	1 MeV E Flux
> 10	1.6×10^8	(5×10^3)	8.0×10^{11}
> 30	1.3×10^8	(2×10^3)	2.6×10^{11}
> 100	9.3×10^7	(7.6×10^2)	7.1×10^{10}

Reference to the curves, Figs. 3-7, 3-8, and 3-9, for degradation of short circuit current, maximum power point, and open circuit voltage indicates that no degradation should be expected for a bare unprotected solar cell at the radiation anticipated.

The complete covering of the solar panel by the Tedlar film will form a protective barrier against low energy protons, in the range from 0.1 to 1.0 MeV. Low energy protons can cause solar cell degradation if they are allowed to impinge on the bare cell.

Cells filtered in the normal manner, with glass or quartz coverslides, usually have exposed active area due to the tolerances of the cell and filter. These bare areas can result in excessive power degradations. However, these bare areas are eliminated by using the proposed Tedlar film protective covering.

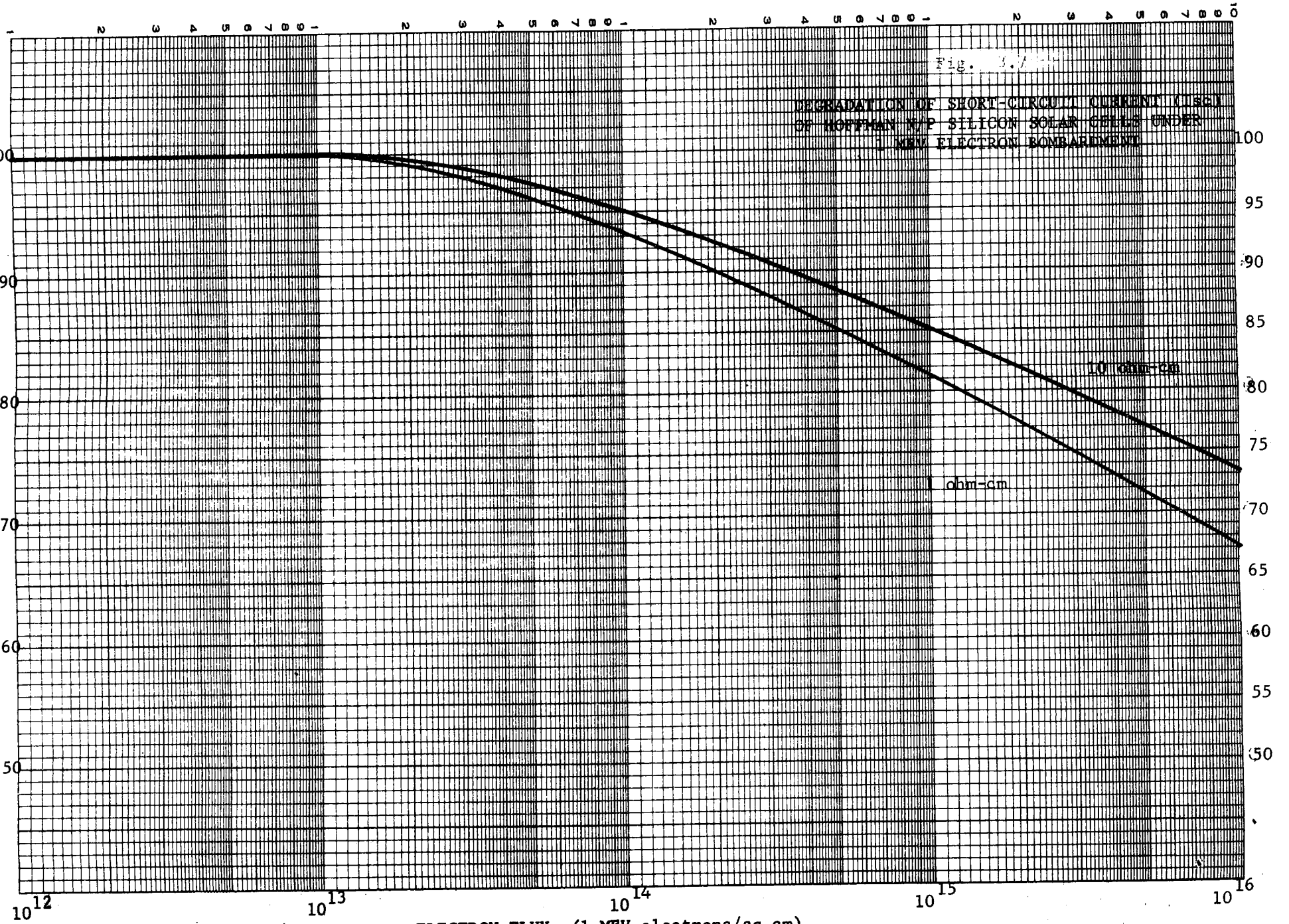

Figure 3-7.

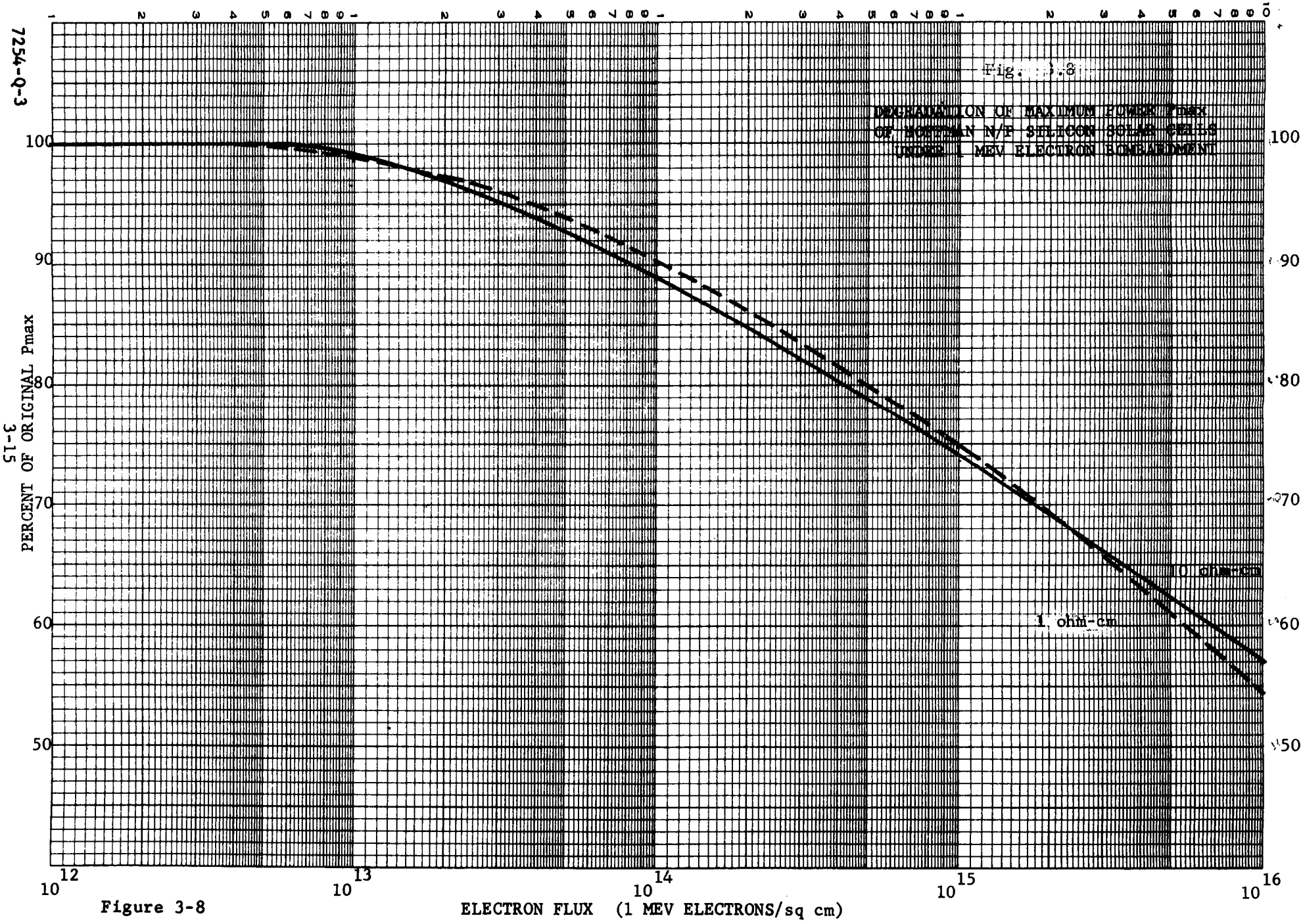

Figure 3-8

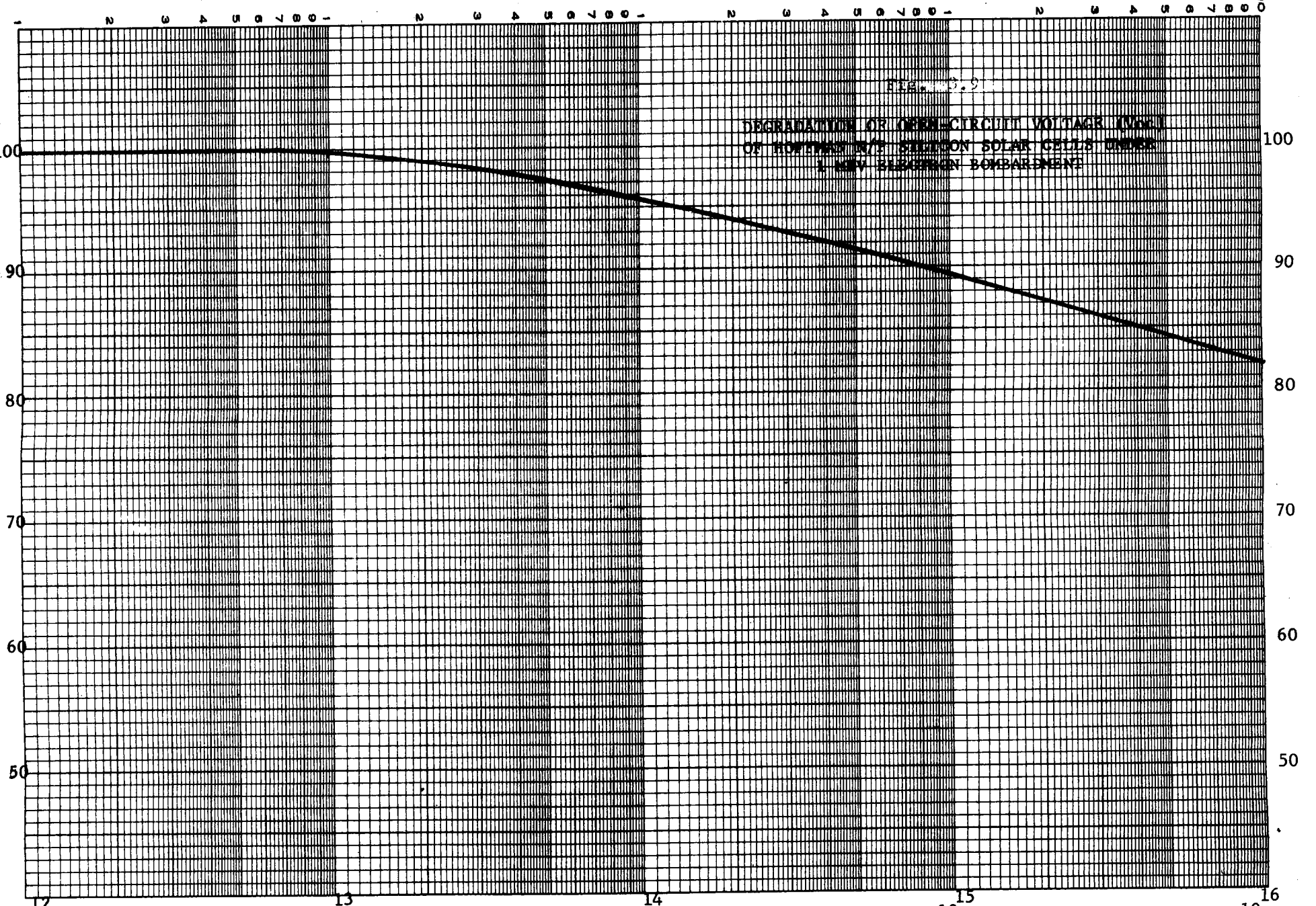

Figure 3-9

3.4 CIRCUIT DESIGN

The electrical circuit shall be a flat mounted array of series-parallel solar cells of 6P x 57S. The dimensions of the circuit are shown in Fig. 3-10. The electrical connector configurations are shown in Figs. 3-11 and 3-12. The reasons for preferring this type of circuit configuration were discussed in the 2nd quarterly report.

A drawing of a panel is shown in EOS Drawing No. 7254-111, Fig. 3-13. Each panel contains 15 solar cell circuits of 6P x 57S, and the circuits are alternated in direction to minimize the magnetic field effects. Each circuit is wired to a terminal board on the back side of the panel with two stranded wire leads for redundancy. Two isolation diodes are placed on the positive terminal board for each circuit, in series with the output leads. The circuits are wired in parallel with twisted stranded wire to an outlet plug on each panel.

7254-Q-3

3-18

SECURITY CLASSIFICATION

REVISIONS				
ZONE	LTR	DESCRIPTION	DATE	APPROVED

NOTES: UNLESS OTHERWISE SPECIFIED

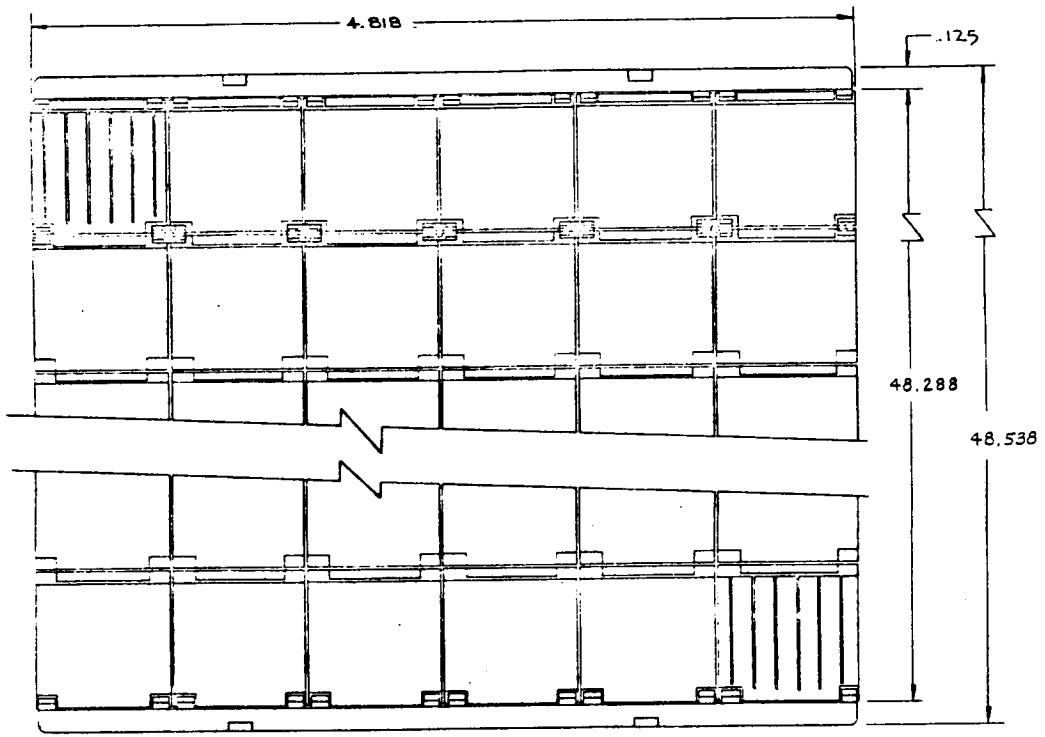

ITEM NO.	ZONE	UNIT WT.	SPECIFICATION	MATERIAL	NOMENCLATURE OR DESCRIPTION	PART OR IDENTIFYING NO.	CODE IDENT	SYM	QTY REQD

LIST OF MATERIALS

ON	THRU	PART DASH NO.	NEXT FINAL QTY REQD PER ASSY	NEXT ASSY	USED ON
EFFECTIVE SERIAL NO.				APPLICATION	
USAGE DATA			DRAWING LEVEL		

UNLESS OTHERWISE NOTED
LINEAR DIMS. IN INCHES.
TOLERANCES
DECIMAL XX ± XXX ±
FINISH √ RMS
ANGULAR ±
DO NOT SCALE

MATERIAL

TREATMENT/FINISH

SIMILAR TO | ACT. WT. | CALC. WT.

CONTRACT NO.

DRAWN R Bowman DATE 12-15-67

CHECK

DESIGN

MFG.

DESIGN ACTIVITY APPD

CUSTOMER

ELECTRO-OPTICAL SYSTEMS, INC.
A XEROX COMPANY
300 NORTH HALSTEAD STREET, PASADENA, CALIFORNIA 91107

TITLE
TYPICAL 6P x 60
SOLAR CELL CIRCUIT

DWG SIZE	CODE IDENT NO.	DWG NO.
C	12705	7254-120

SCALE 2/1 | RELEASE DATE | SHEET OF

9/67 DIETERICH-POST CLEARPRINT 3020 FORM 372 REV. 7-68

Figure 3-10 Typical 6P x 60 Solar Cell Circuit

REVISIONS				
ZONE	LTR	DESCRIPTION	DATE	APPROVED

CLASSIFICATION

NOTES: UNLESS OTHERWISE SPECIFIED

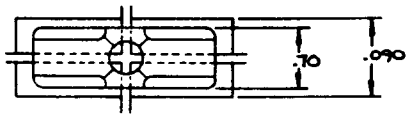

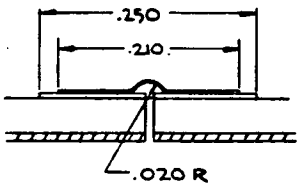

		SYM	CODE IDENT	PART OR IDENTIFYING NO.	NOMENCLATURE OR DESCRIPTION	MATERIAL	SPECIFICATION	UNIT WT.	ZONE	ITEM NO.
QTY REQD				LIST OF MATERIALS						

UNLESS OTHERWISE NOTED LINEAR DIMS. IN INCHES. TOLERANCES DECIMAL XX ± XXX ± FINISH √ RMS DO NOT SCALE ANGULAR ±

MATERIAL

TREATMENT/FINISH

SIMILAR TO | ACT. WT. | CALC. WT.

CONTRACT NO.

DRAWN R3 DATE 12-14-67

CHECK mw

DESIGN

MFG.

DESIGN ACTIVITY APPD

CUSTOMER

ELECTRO-OPTICAL SYSTEMS, INC.
A XEROX COMPANY
300 NORTH HALSTEAD STREET, PASADENA, CALIFORNIA 91107

TITLE
TOP CONTACT
TYPE CONNECTOR

ON	THRU
EFFECTIVE SERIAL NO.	
USAGE DATA	

PART DASH NO.	NEXT ASSY QTY REQD PER ASSY	FINAL NEXT ASSY	USED ON
APPLICATION			
DRAWING LEVEL			

DWG SIZE	CODE IDENT NO.	DWG NO.
C	12705	7254-106

SCALE 10/1 | RELEASE DATE | SHEET OF

Figure 3-11. Top Contact Type Connector

REVISIONS				
ZONE	LTR	DESCRIPTION	DATE	APPROVED

SECURITY CLASSIFICATION

NOTES: UNLESS OTHERWISE SPECIFIED

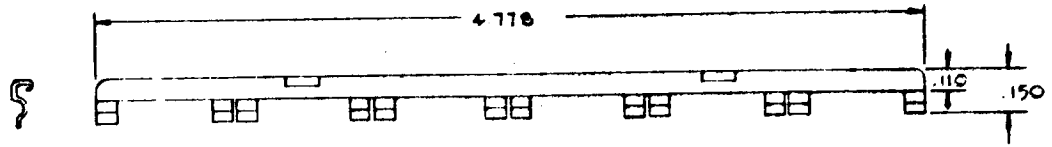

QTY REQD	SYM	CODE IDENT	PART OR IDENTIFYING NO.	NOMENCLATURE OR DESCRIPTION	MATERIAL	SPECIFICATION	UNIT WT.	ZONE	ITEM NO.

LIST OF MATERIALS

UNLESS OTHERWISE NOTED LINEAR DIMS. IN INCHES. TOLERANCES DECIMAL XX ± XXX ± FINISH √ RMS ANGULAR ± DO NOT SCALE

MATERIAL

TREATMENT/FINISH

SIMILAR TO | ACT. WT. | CALC. WT.

CONTRACT NO.

DRAWN | DATE 12-15-67

CHECK

DESIGN

MFG.

DESIGN ACTIVITY APPD

CUSTOMER

ELECTRO-OPTICAL SYSTEMS, INC.
A XEROX COMPANY
300 NORTH HALSTEAD STREET, PASADENA, CALIFORNIA 91107

TITLE: BUS BAR

DWG SIZE	CODE IDENT NO.	DWG NO.
C	12705	7254-107

SCALE 2/1 | RELEASE DATE | SHEET OF

ON	THRU
EFFECTIVE SERIAL NO.	
USAGE DATA	

PART DASH NO.	NEXT FINAL	NEXT ASSY	USED ON
	QTY REQD PER ASSY	APPLICATION	
DRAWING LEVEL			

9/69 DIETERICH-POST CLEARPRINT U.V. FORM 370 REV. 7-66

Figure 3-12. Bus Bar

SECURITY CLASSIFICATION

NOTES: UNLESS OTHERWISE SPECIFIED

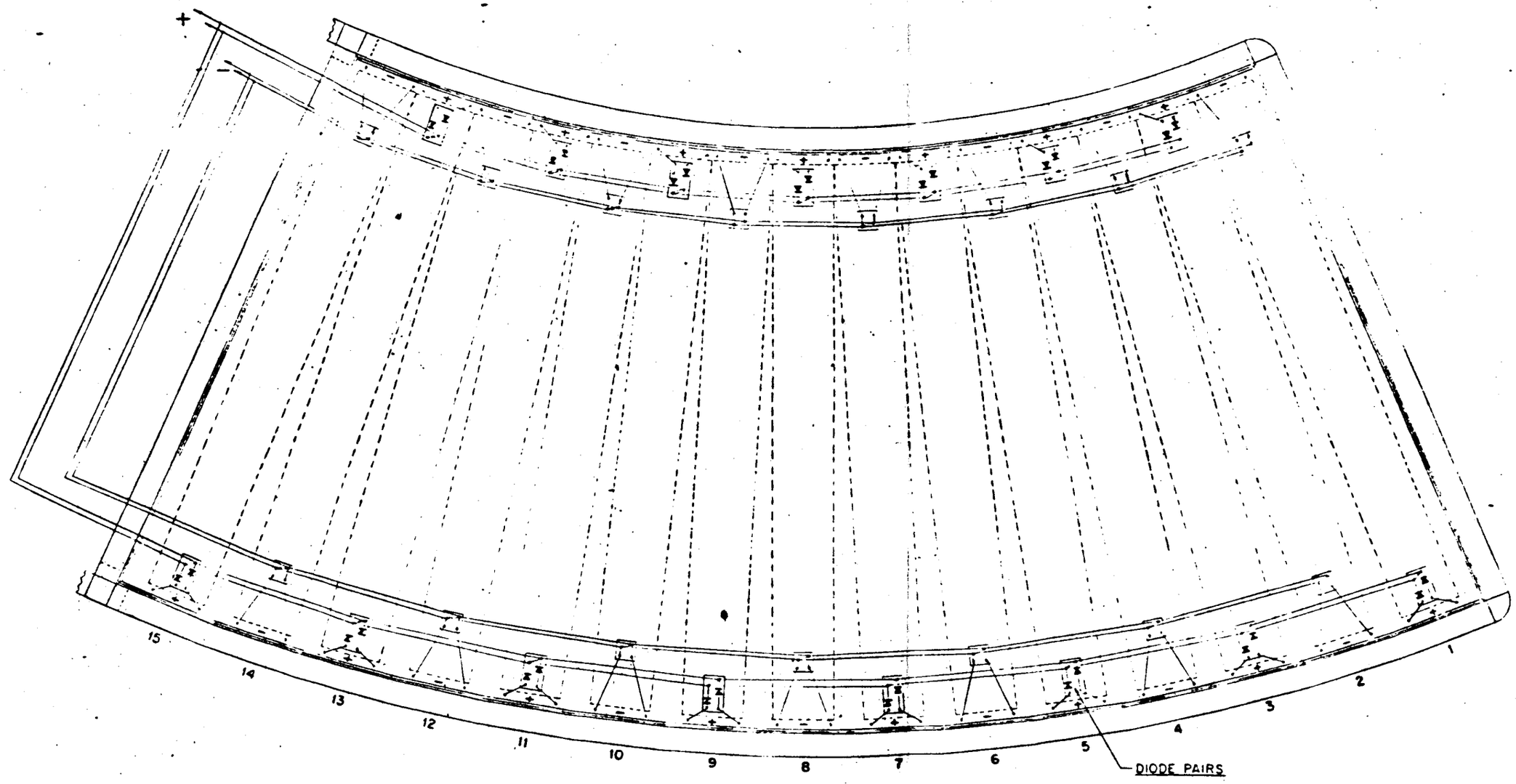

DEVELOPED VIEW OF INNER SURFACE OF ONE WIRED SOLAR PANEL

(WIRING SHOWN IN SEMI-SCHEMATIC FORM)

7254-111

3-21

FOLDOUT FRAME 1

FOLDOUT FRAME 2

REVISIONS				
ZONE	LTR	DESCRIPTION	DATE	APPROVED

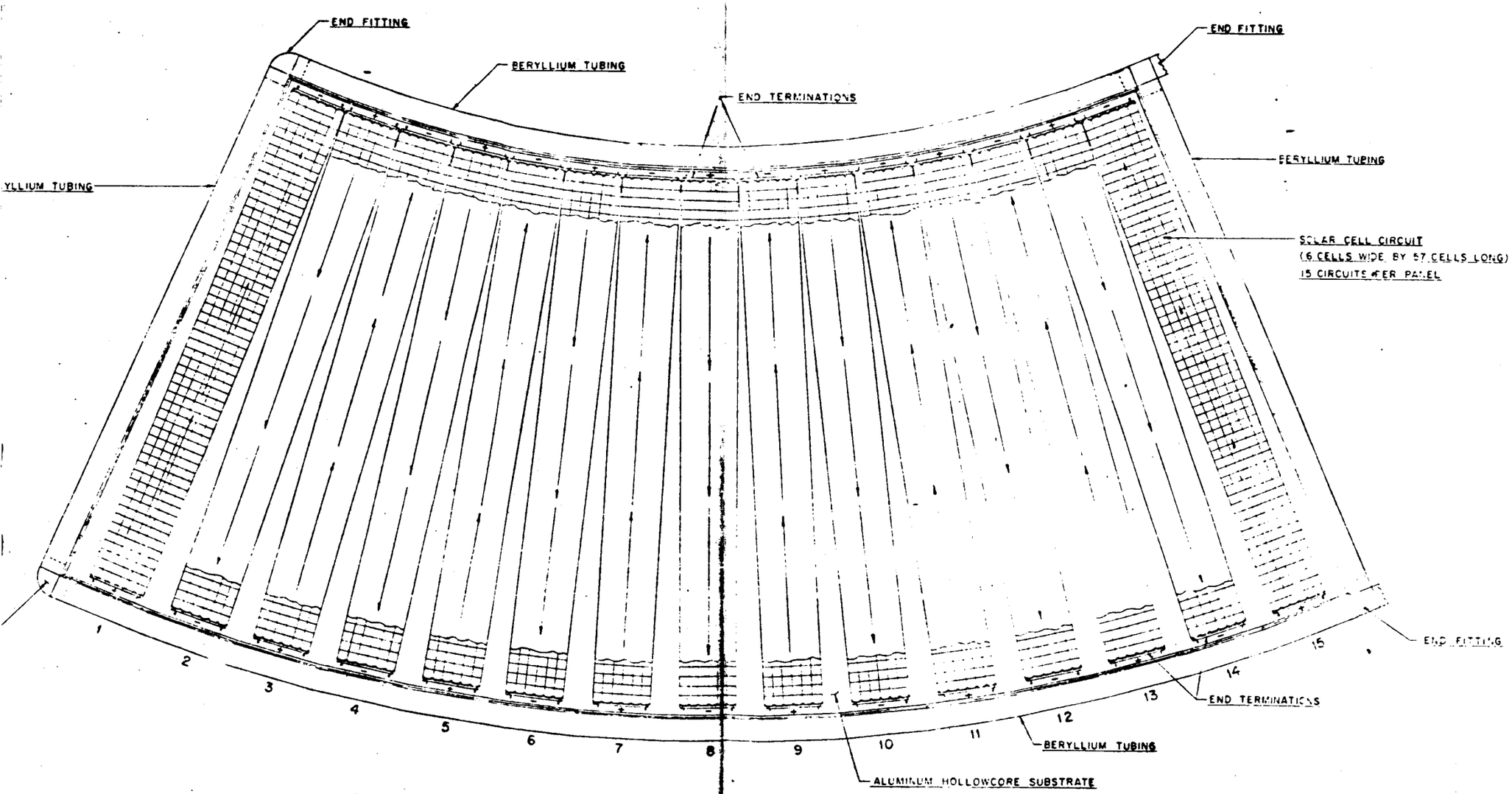

DEVELOPED OUTER VIEW OF ONE COMPLETE SOLAR PANEL
THREE REQUIRED PER ARRAY HALF-SECTION

2

SYM	CODE IDENT	PART OR IDENTIFYING NO.	NOMENCLATURE OR DESCRIPTION	MATERIAL	SPECIFICATION	UNIT WT	ZONE	ITEM NO.
QTY REQ:			LIST OF MATERIALS					

ELECTRO-OPTICAL SYSTEMS, INC.
A PERKIN COMPANY

TITLE
SOLAR PANEL ASSEMBLY-
DEPLOYABLE CONE CONCEPT
PLANETARY ARRAY

SIZE	CODE IDENT NO	DWG NO
J	12705	7254-111

SCALE — SHEET — OF

FOLDOUT FRAME 3

FOLDOUT FRAME

FOLDOUT FRAME 4

3.5 ELECTRICAL POWER ANALYSIS

The preferred circuit was detailed in the 2nd Quarterly Report as being 6P x 66S. A closer look at the I-V characteristics of a 1-3 ohm-cm cell revealed that the operating point could be taken as 0.485V instead of 0.450V as originally assumed. In addition, an estimate of the temperature of the array for noon sun conditions revealed that the average array temperature would be $8^{\circ}C$, near ambient.

The open circuit voltage of a solar cell changes rapidly with a change in temperature. Typical value for a sintered N/P solderless cell is -2.4 mV/$^{\circ}C$.

The new open circuit voltage of the cell would be:

$$580 \text{ mV} + (28^{\circ}C - 8^{\circ}C)\ (2.4 \text{ mV}/^{\circ}C)$$
$$580 \text{ mV} + 48 \text{ mV} = 628 \text{ mV}$$

The short circuit current decreases with respect to a decrease in temperature, but the change is much smaller than the voltage shift. A value of $+0.05\%/^{\circ}C$ is typical for the rate of change in short circuit current. The new short circuit current would be:

$$130 \text{ mA} - (28^{\circ}C - 8^{\circ}C)\ (0.0005)\ (130)$$
$$130 \text{ mA} - 1.3 \text{ mA} = 128.7 \text{ mA}$$

A typical I-V curve of a cell at $28^{\circ}C$ and $8^{\circ}C$ is shown in Fig. 3-14.

A new string length of 57 cells in series was selected. The operating point of the cell would be 28.0V plus 1 volt for diode and wiring losses:

$$29.0V/57 = 508 \text{ mV/cell}$$

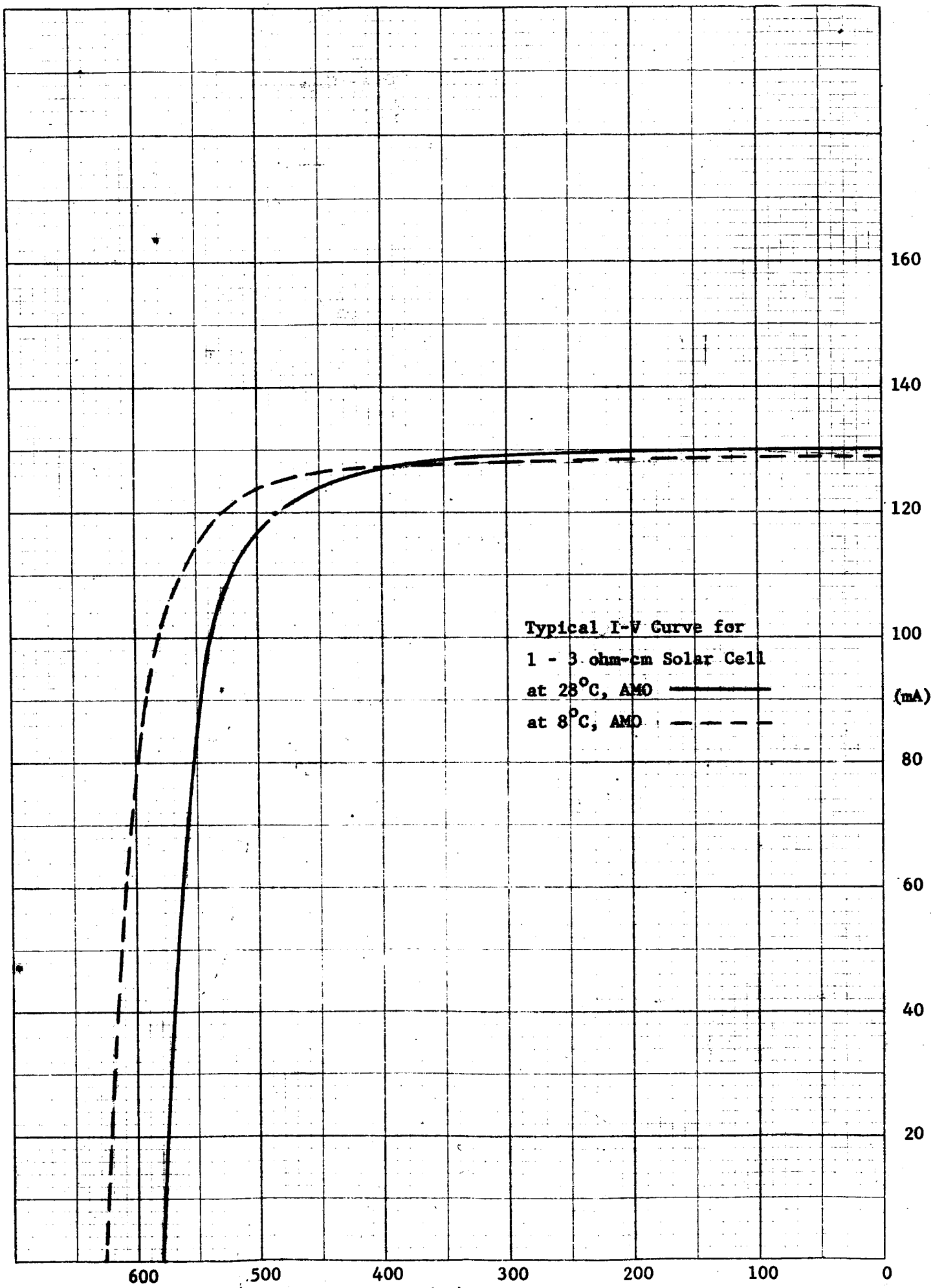

7254-Q-3 Figure 3-14.

As discussed in the 2nd Quarterly Report, the shift in voltage due to the intensity change from 140 mW/cm^2 to 50 mW/cm^2 is 8 mV, ref. Fig. 3-15. Therefore, referring to Fig. 3-14, of a typical cell at 28°C and 8°C, the current output at 508 mV plus 8 mV (the 8 mV is added instead of subtracted to simulate shifting the curve) is 122 mA.

The submodule output would be:

6 (122 mA) = 732 mA @ 508 mV

The submodule output corrected for the Tedlar film coating and fabrication allowance:

Tedlar film coating	- 1%
Fabrication allowance	- 2%
Total	- 3%

Submodule output:

732 (0.97) = 710 mA @ 508 mV

Circuit output = 710 mA @ 28.0V
(at 1 AU, 8°C)

The Martian mission has been established as 1 earth year, approximately equivalent to the time period from Martian spring through fall, as defined by the northern hemisphere. Figure 3-16 shows the seasonal position of Mars, and Figs. 3-17 and 3-18 show the inclination of Mars with respect to the Sun.

The attenuation of the Mars atmosphere was assumed to be a logarithmic function of pressure. By analogy with earth conditions, we assigned

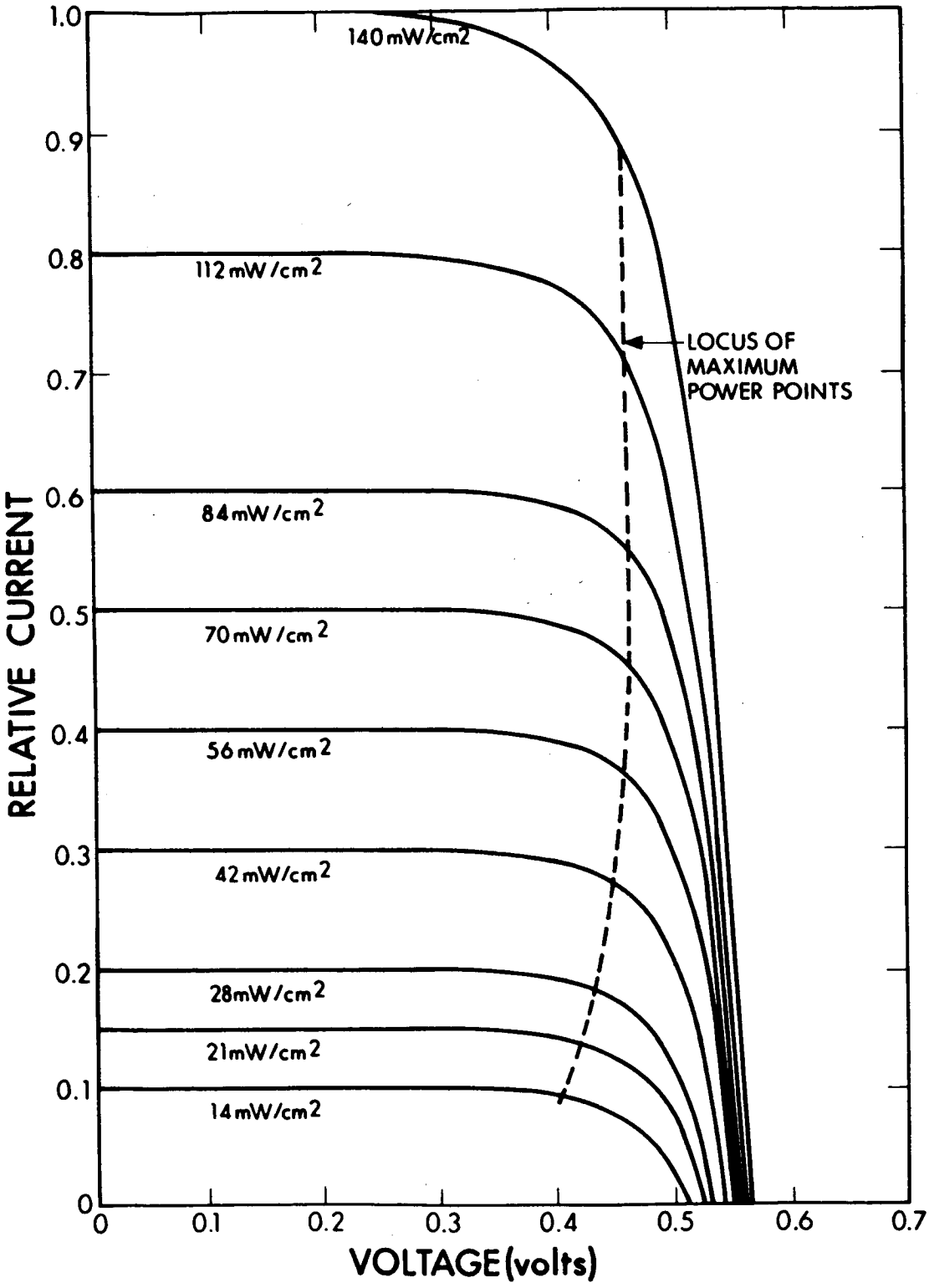

Figure 3-15. Typical I-V Characteristics as a Function of Solar Irradiation at Constant Temperature

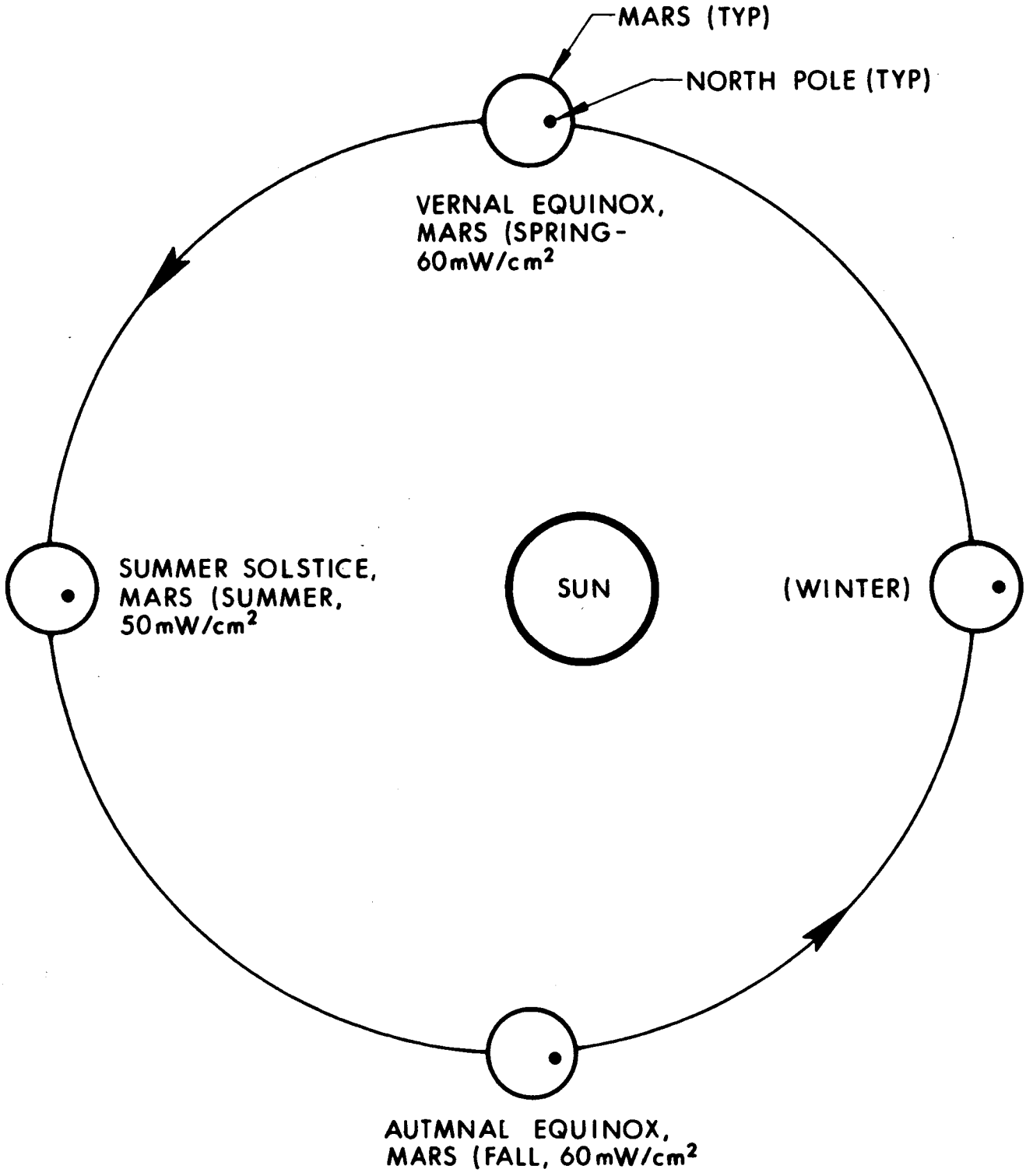

Figure 3-16. Positions of Mars During 1 Earth Year of Planetary Array Operation

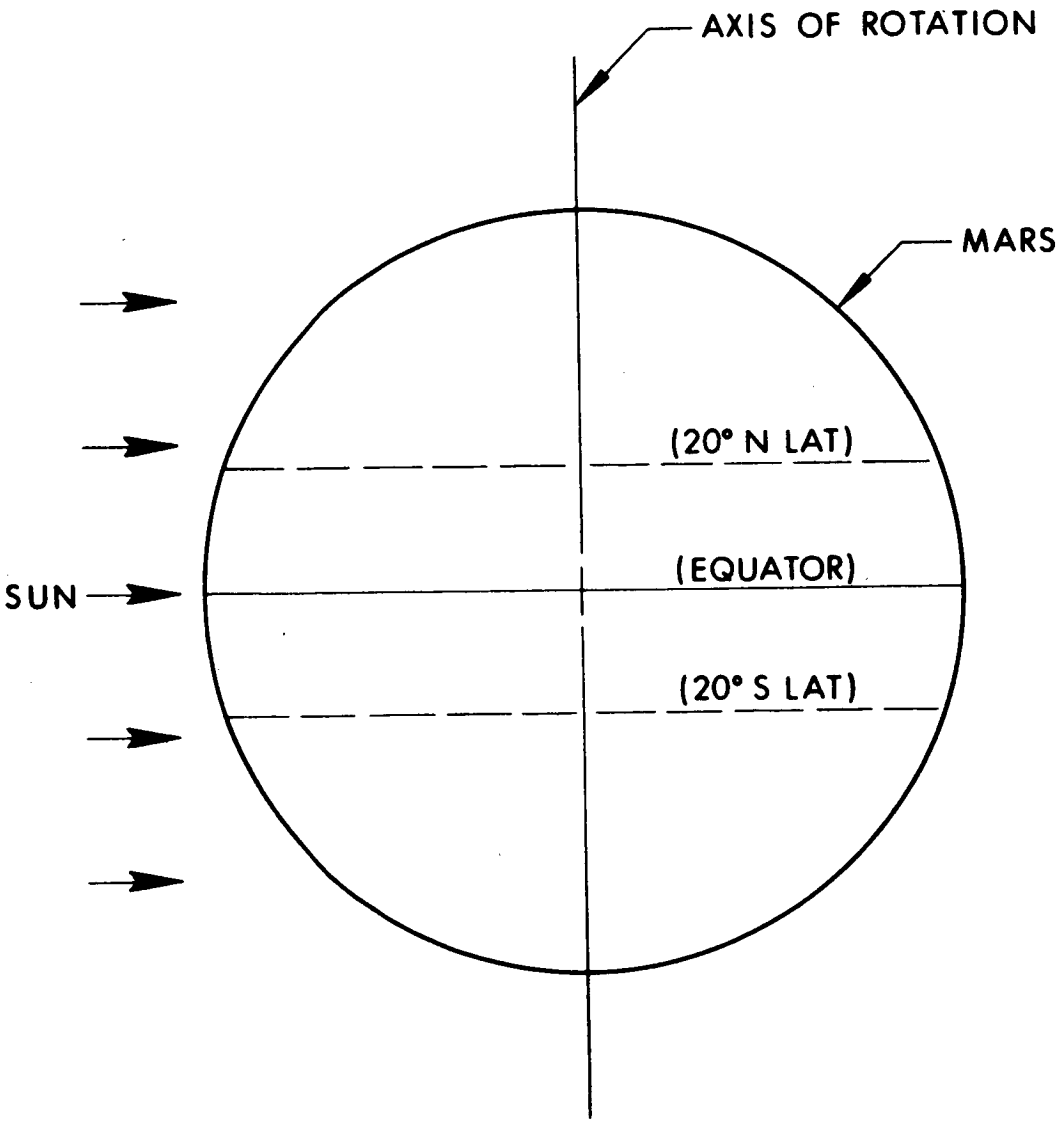

Figure 3-17. Position of Mars with Respect to the Sun at Noon for Spring and Fall

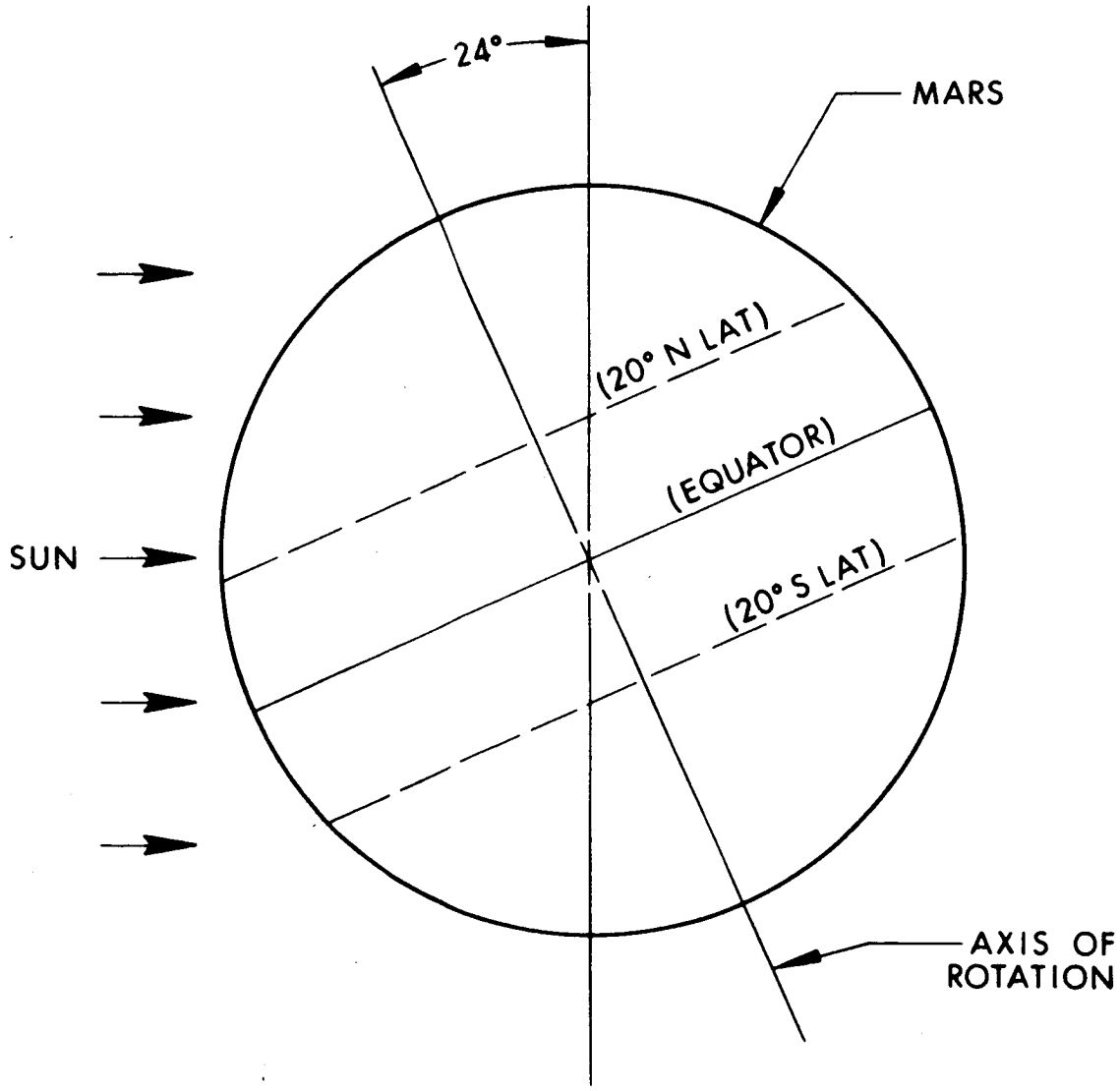

Figure 3-18. Position of Mars with Respect to the Sun at Noon for Summer

a transmission factor of 0.7 at a pressure of 1000 mb (earth AMI). The transmission factor at 1 mb was assumed at 1.0. By logarithmic extrapolation, the transmission factor at Mars surface (7 mb) was found to be 0.92. Reference Fig. 3-19 and the first Quarterly Report, para 2.1.4. We believe this transmission factor to be conservative; however, it has been established as a base line for the program.

The Mars surface solar intensities are:

spring and fall;
(60 mW/cm^2) (0.92) = 55.2 mW/cm^2
Ratio to AM0 = 55.2/140 = 0.394

summer;
(50 mW/cm^2) (0.92) = 46.0 mW/cm^2
Ratio to AM0 = 46.0/140 = 0.329

Current output per circuit at Mars AMI, 8°C normal to the sun:

spring and fall;
(710 mA) (0.394) = 279.7 mA

summer;
(710 mA) (0.329) = 233.6 mA

Power output:

spring and fall;
279.7 mA @ 28.0V = 7.83W

summer;
233.6 mA @ 28.0V = 6.54W

- NEAR MARS SPACE: 50 TO 74 mW/cm^2
- AT MARS SURFACE:
  RECOMENDED TRANSMISSION FACTOR AT AIR MASS ONE = 0.92
- RATIONALE:

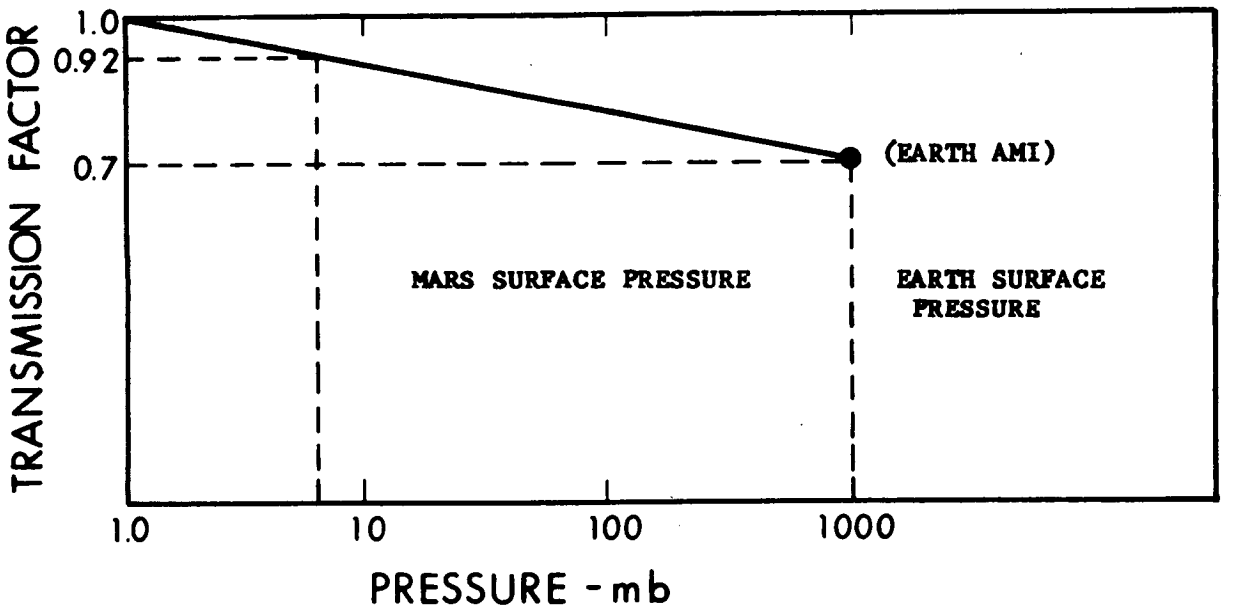

- JUSTIFICATION:
  a) ONLY GAS MOLECULE SCATTERING CAN BE COMPUTED
  b) WATER VAPOR SCATTERING - UNKNOWN
  c) DUST SCATTERING - UNKNOWN
  d) WATER VAPOR ABSORPTION - UNKNOWN
  e) CO_2 ABSORPTION CAN BE CALCULATED, BUT IT MAY BE NEGLECTED AS IT OCCURS AT LONG WAVELENGTHS ($> 2.5 \mu$)

Figure 3-19. Mars Solar Intensity

The actual power output of the nonoriented deployed conical array is a function of many variables:

a. Martian season;
   (1) Inclinations of Mars axis with respect to the Sun
   (2) Solar intensity as a function of the Mars-Sun distance
b. Position of the landed spacecraft within a location of ±20 latitude of the Mars equator
c. Position of the landed spacecraft with respect to the local horizon within a hill slope angle of up to 34^{o} in any direction
d. Time of the day, from sunrise to sunset, and particularly at solar noon
e. Temperature of the solar array

It is not the intent of this study to analyze all possible power outputs. As a function of the variables listed above, however, certain limiting conditions will be reviewed in detail, and it will be possible by extrapolation to estimate the power output for any set of conditions.

The objective of the conical nontracking array is to produce power with a minimum of deployment mechanisms. The goal is to avoid complex mechanisms for latitude, slope and position corrections and eliminate the need for a continuous tracking capability.

The power output is primarily a function of the sun angle, ϕ, with respect to the conical array for any set of spacecraft positions. The Sun will illuminate different areas of the arrays for the various possible positions of the array at solar noon, and during the Sun's travel from sunrise to sunset.

The projected area of the conical array as a function of Sun angle ϕ can be expressed as:

(a) For $0 \leq \varphi \leq \theta$; $\theta = \tan^{-1} \dfrac{H}{r_2 - r_1}$

$$A_p = \left(r_2^2 - r_1^2\right) \sin\varphi \left\{\pi - \sin^{-1} \left[1 - \frac{\tan^2\varphi}{\tan^2\theta}\right]^{1/2}\right\} \qquad (1)$$

$$+ H\,(r_1 + r_2) \cos\varphi \left[1 - \frac{\tan^2\varphi}{\tan^2\theta}\right]^{3/2}$$

(b) For $\theta \leq \varphi \leq \dfrac{\pi}{2}$

$$A_p = \pi\left(r^2 - r_1^2\right) \sin\varphi \qquad (2)$$

The nomenclature is self-explanatory from Fig. 3-20. The validity of Eqs. 1 and 2 can be tested from two limiting cases.

When $\varphi = 0$, Eq. 1 is reduced to

$$A_p\Big\}_{\varphi = 0} = H\,(r_1 + r_2)$$

which is an area of a trapezoid, as would be the projected area of the frustum cone looking from a horizontal position.

When $\varphi = \dfrac{\pi}{2}$, Eq. 2 is reduced to

$$A_p\Big\}_{\varphi = \frac{\pi}{2}} = \pi\left(r_2^2 - r_1^2\right)$$

which is an area of two concentric circles, as would be the projected area of the frustum cone looking from the top.

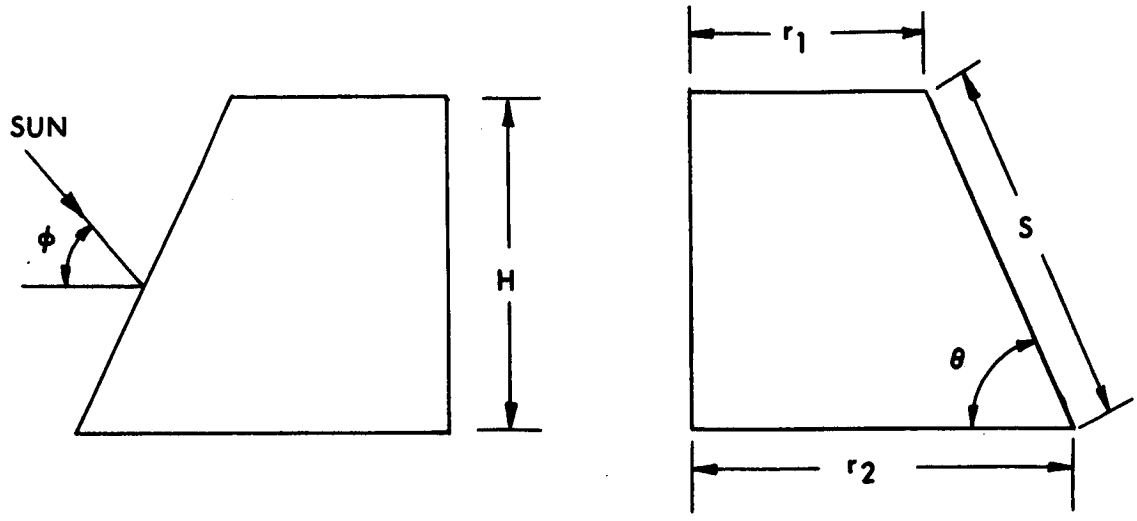

A_p = Projected Area

A_s = Surface Area

r_1 = Upper Radius (74.5")

r_2 = Lower Radius (93.8")

H = Height (43.9")

S = Slant Length (48.0")

θ = Cone Angle (66.2^{o})

ϕ = Sun Vector Angle ($0\text{-}90^{o}$)

Figure 3-20. Cone Nomenclature and Dimensions

The maximum power of the array occurs when the Suns vector ϕ is 90^{o}, directly overhead, and the angle of Sun with respect to the cells is $90-66.2 = 23.8^{o}$:

a. For spring and fall;

Corrected power/circuit = n.83W (sin 23.8^{o})

n.83W (0.4035) = 3.16 W/circuit

Array power = 3.16 W/circ (90 circ) = 284.4W

b. For summer;

Corrected power/circuit = 6.54W (0.4035) = 2/64 W/circuit

Array power = 2.64 W/circ (90 circ) = 237.6W

The power output of the array for the Sun vector angles $0-90^{o}$ as obtained by the general equation at spring-fall and summer are shown in Figs. 3-21 and 3-22.

The Sun vector angles, with respect to the array, for the conditions of the first day of spring, fall, and summer at 20^{o}N, 20^{o}S, and the equator, and for hill slopes of $\pm 34^{o}$ N.S. and E.W. have been derived. The calculation for these conditions, as well as a general equation for any condition, are included as Appendix A. The curves are shown in Figs. 3-23 through 3-26. The curves illustrate the Sun vector angle at noon, at dawn, and at sunset. It can be seen that for certain hill conditions the Sun vector angle can be less than 0^{o}. The solar array should be neglected for these negative angle conditions as the array is assumed shadowed by the horizon.

The temperature of the array affects the power output and will vary during the day for any one given location and season. For the specific condition of noon, the temperature will vary depending upon the latitude, position of the array, and the season. Figure 3-27 indicates the average temperature extremes of the array with respect to latitude position for the spring, fall and summer seasons. A detailed thermal analysis of the array is given in Section 5.

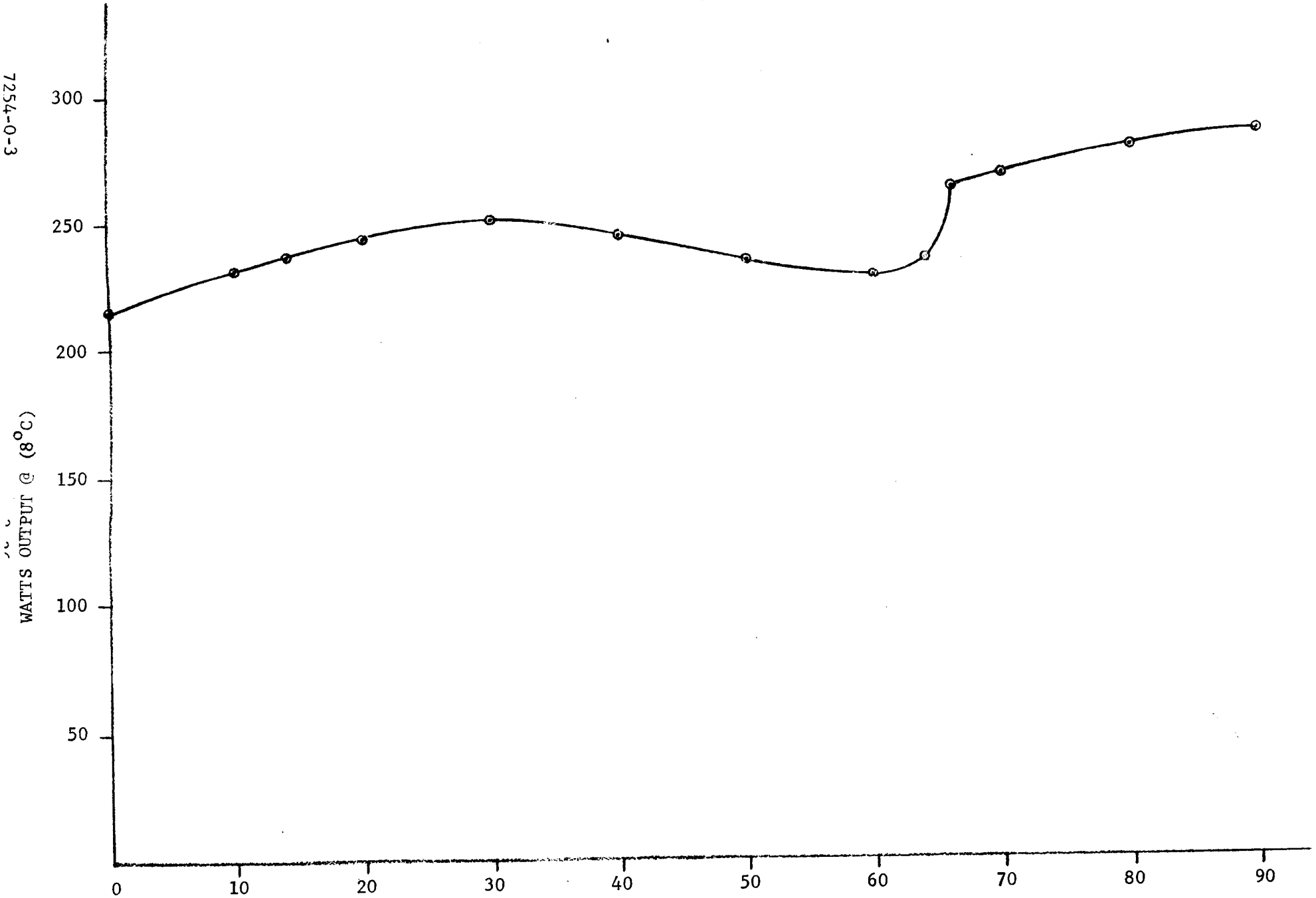
300
250
200
150
100
50
WATTS OUTPUT @ (8°C)
0
10
20
30
40
50
60
70
80
90
SUN VECTOR ANGLE (DEGREES)
SPRING AND FALL

Figure 3-21.

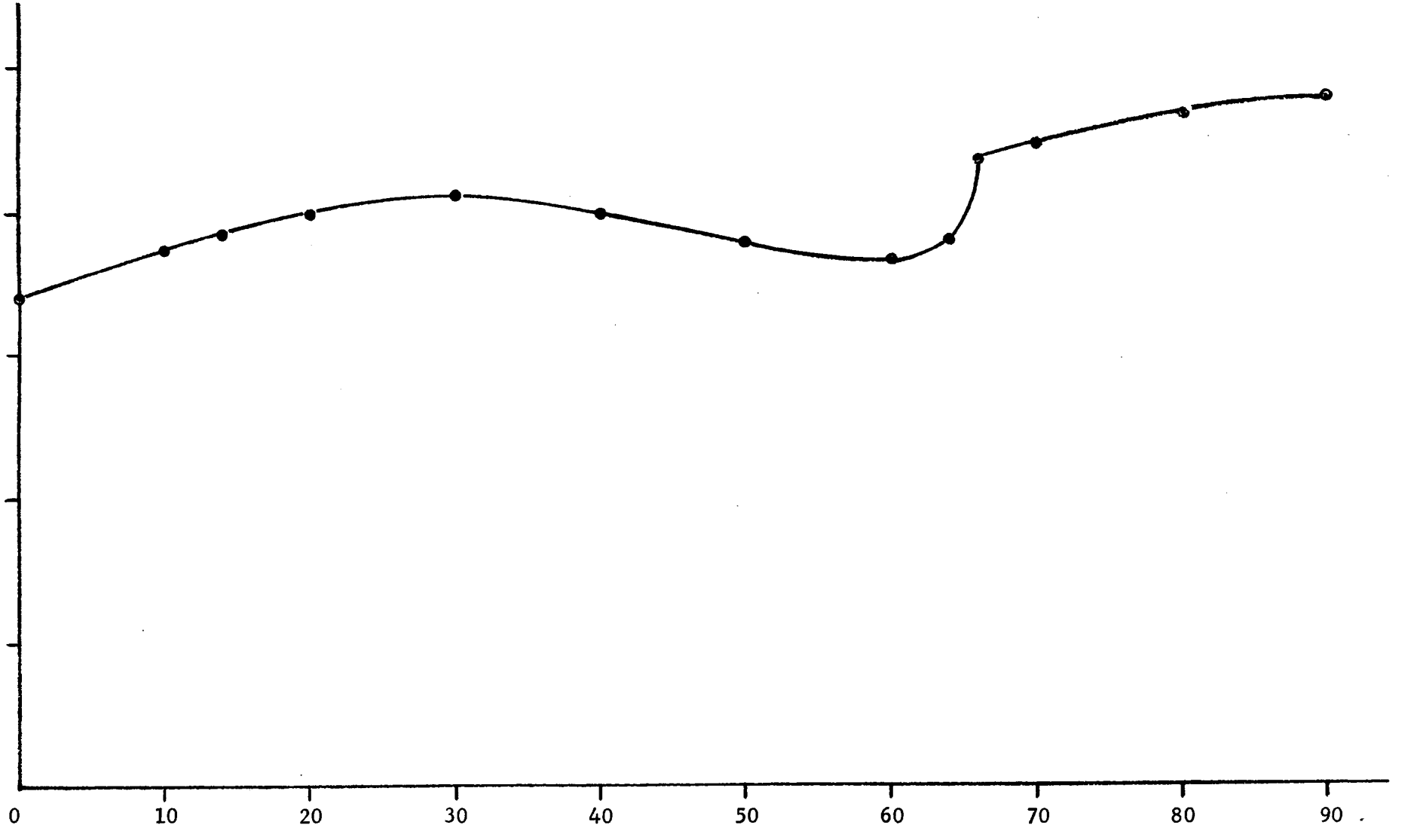
250
200
150
100
50
WATTS OUTPUT @ (8°C)
0
10
20
30
40
50
60
70
80
90
SUN VECTOR ANGLE (DEGREES)
SUMMER

Figure 3-22.

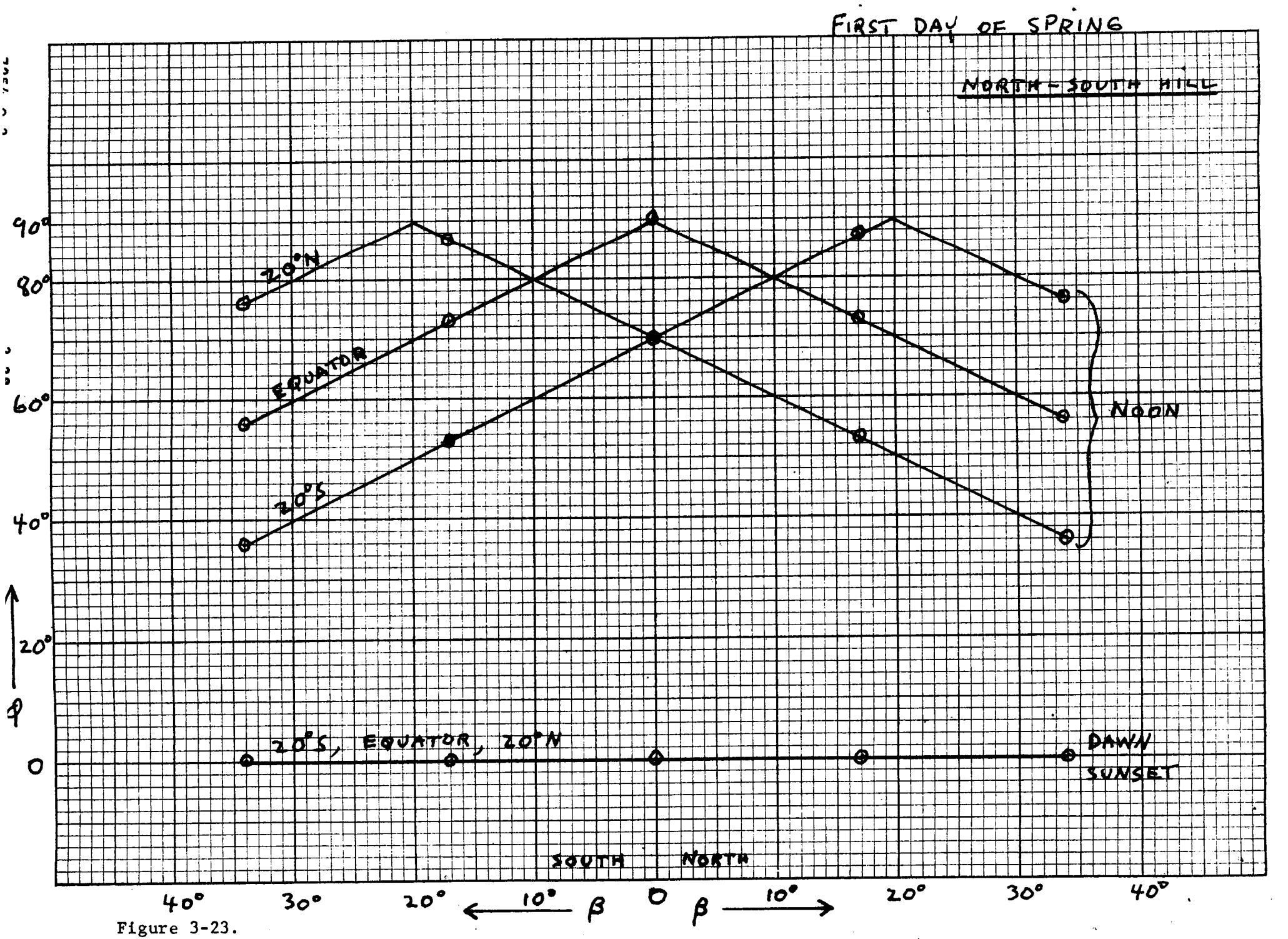
FIRST DAY OF SPRING
NORTH - SOUTH HILL
90°
80°
60°
40°
20°
0
φ
20°N
EQUATOR
20°S
NOON
20°S, EQUATOR, 20°N
DAWN
SUNSET
SOUTH
NORTH
40°
30°
20°
10°
β
0
β
10°
20°
30°
40°

Figure 3-23.

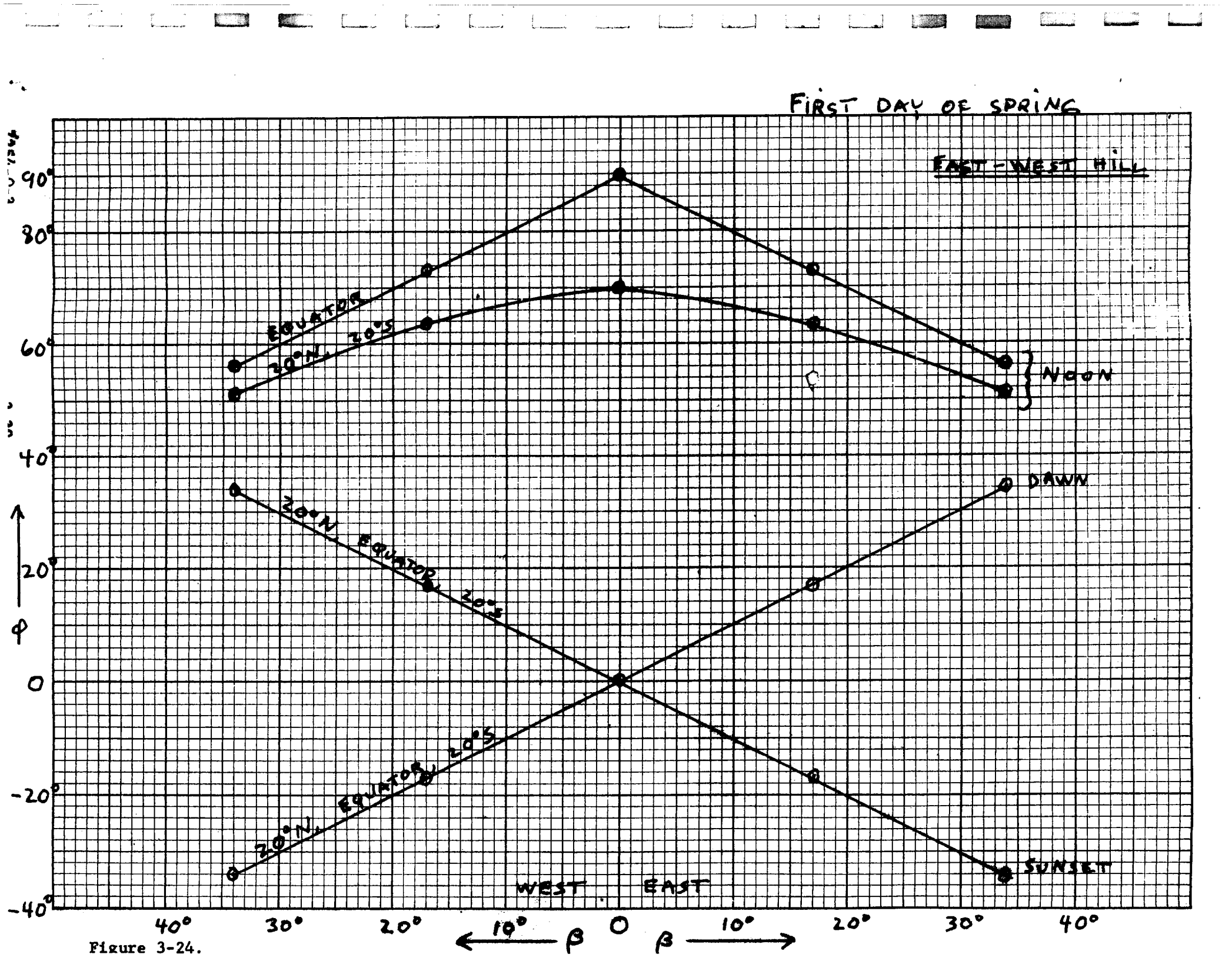
FIRST DAY OF SPRING
EAST-WEST HILL
90°
80°
60°
40°
20°
0
-20°
-40°
φ
EQUATOR
20°N, 20°S
NOON
DAWN
20°N
EQUATOR
20°S
20°N, EQUATOR, 20°S
SUNSET
WEST
EAST
40°
30°
20°
10°
β
O
β
10°
20°
30°
40°

Figure 3-24.

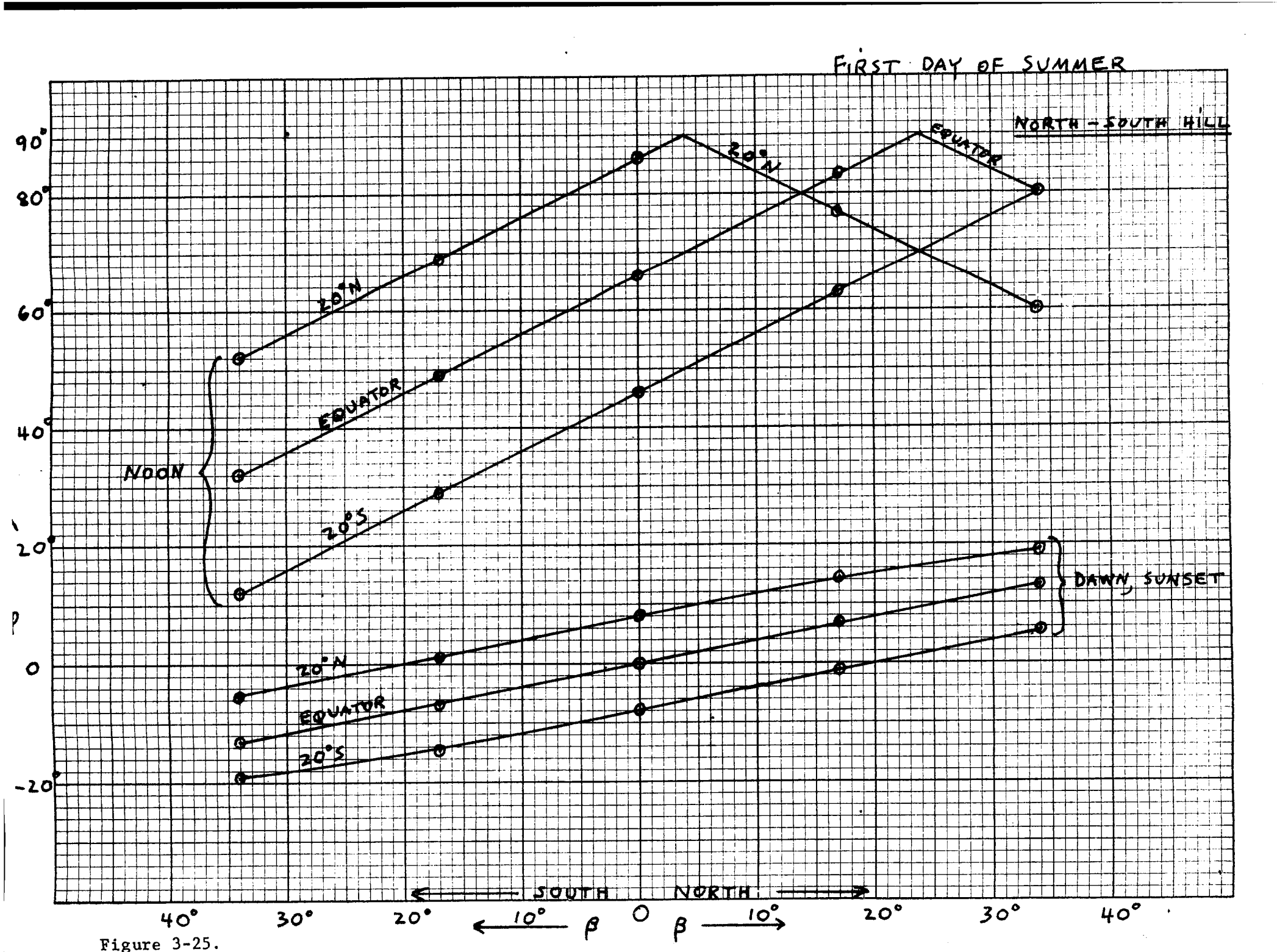
FIRST DAY OF SUMMER
NORTH - SOUTH HILL
90°
80°
60°
40°
20°
0
-20°
20°N
EQUATOR
20°S
NOON
20°N
EQUATOR
20°S
DAWN, SUNSET
SOUTH
NORTH
40°
30°
20°
10°
β
O
β
10°
20°
30°
40°

Figure 3-25.

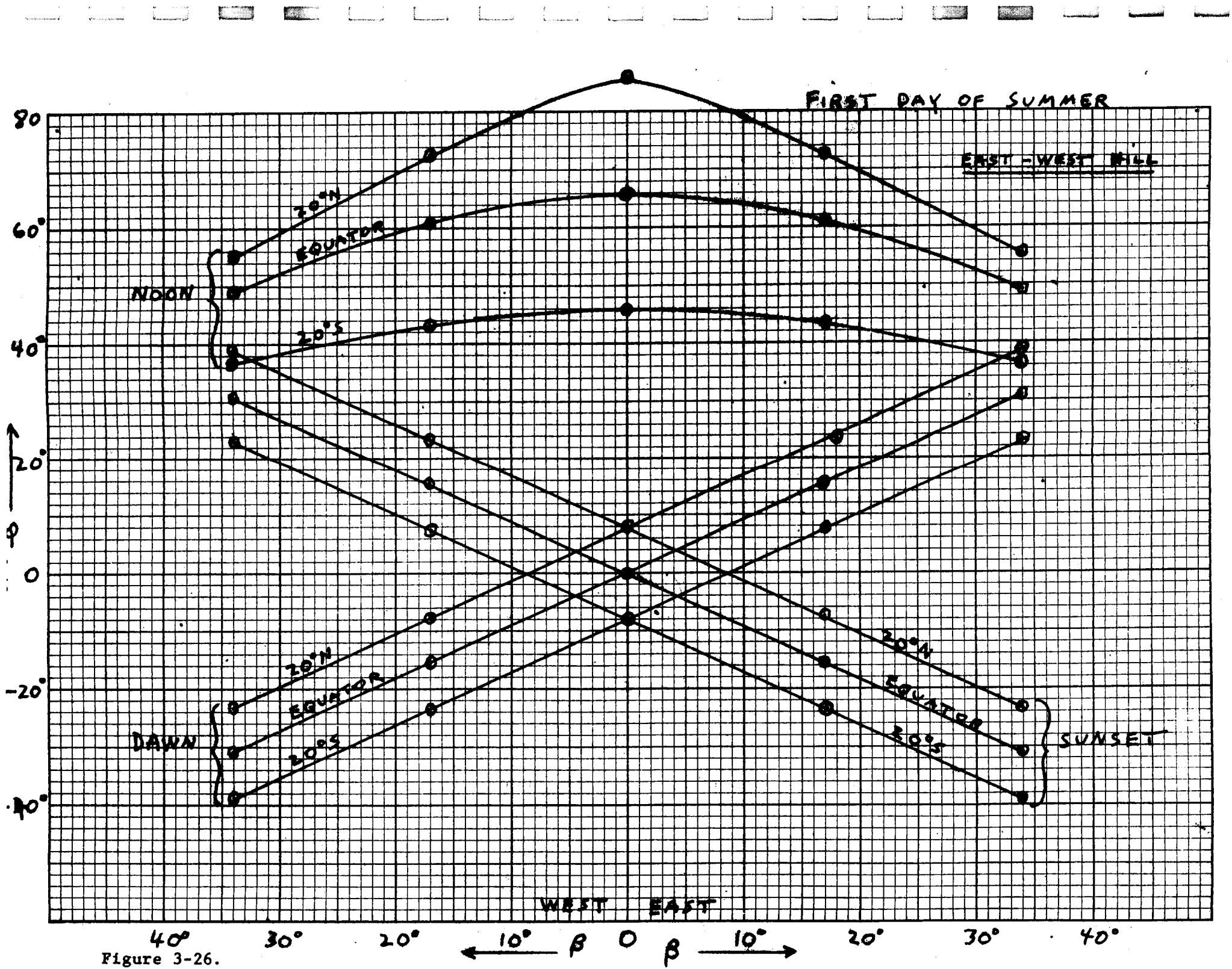
FIRST DAY OF SUMMER
EAST - WEST HILL
80
60°
40°
20°
0
-20°
-40°
φ
20°N
EQUATOR
20°S
NOON
DAWN
SUNSET
WEST
EAST
40°
30°
20°
10°
β
0
β
10°
20°
30°
40°

Figure 3-26.

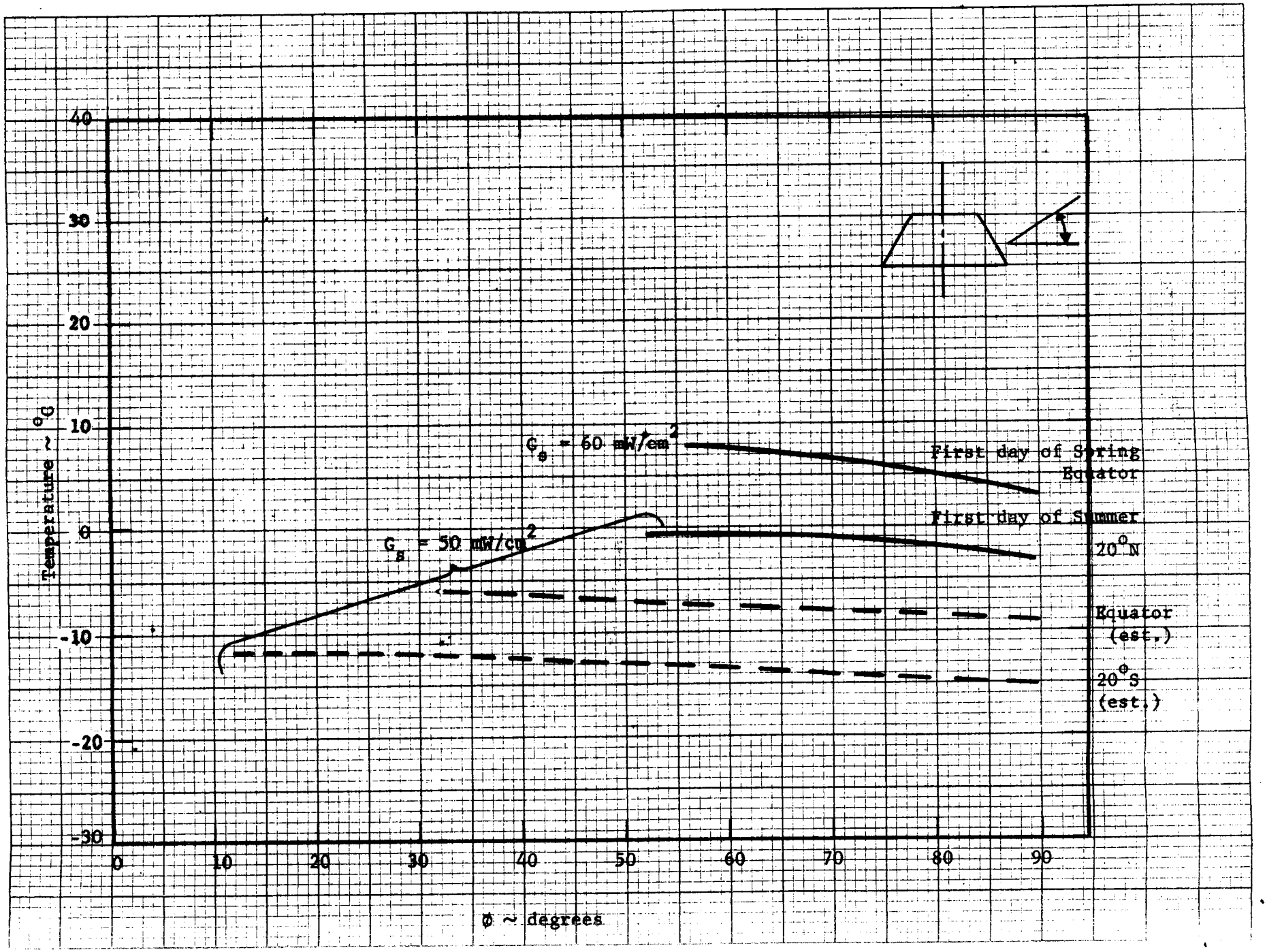

Figure 3-27. Average Temperature at Noon versus Sun Angle

The power of the array can be corrected for the average temperature for any condition at noon by estimating the temperature for the latitude position as shown in Fig. 3-27. The temperature correction factor is plotted in Fig. 3-28, based on $8^{o}C$ as 1.0.

The minimum and maximum power of the array at noon for spring, fall and summer seasons are shown in Table 3-I.

3.6 MAGNETIC FIELD ANALYSIS

An analysis was made to estimate the magnitude of the magnetic field created by the current carrying circuits of the solar array. The field resulting from magnetization of the materials is absent since all the array materials are nonmagnetic.

For the fixed deployable array which has a cone angle of 66.2^{o}, there are 90 circuits; each consists of 57 6-cell submodules in series. The voltage output of the circuit is 28 volts. The circuit current varies as a function of the sun angle.

Figure 3-29 shows a typical bus and circuit arrangement which minimizes the magnetic field. The bus bars can be made from twisted wires or conductor strips as shown. A calculation of the magnetic field can be effected by considering a pair of adjacent circuits as a current loop whose dipole moment is given by:

$$m = IA \qquad (1)$$

where m is dipole moment directed from the center of the loop and perpendicular to the plane of the loop; I is the circulating current; A is the area of the loop. In the rationalized MKS units, the dipole moment is in amp-meters^2; the current in amperes; and the area in meters^2.

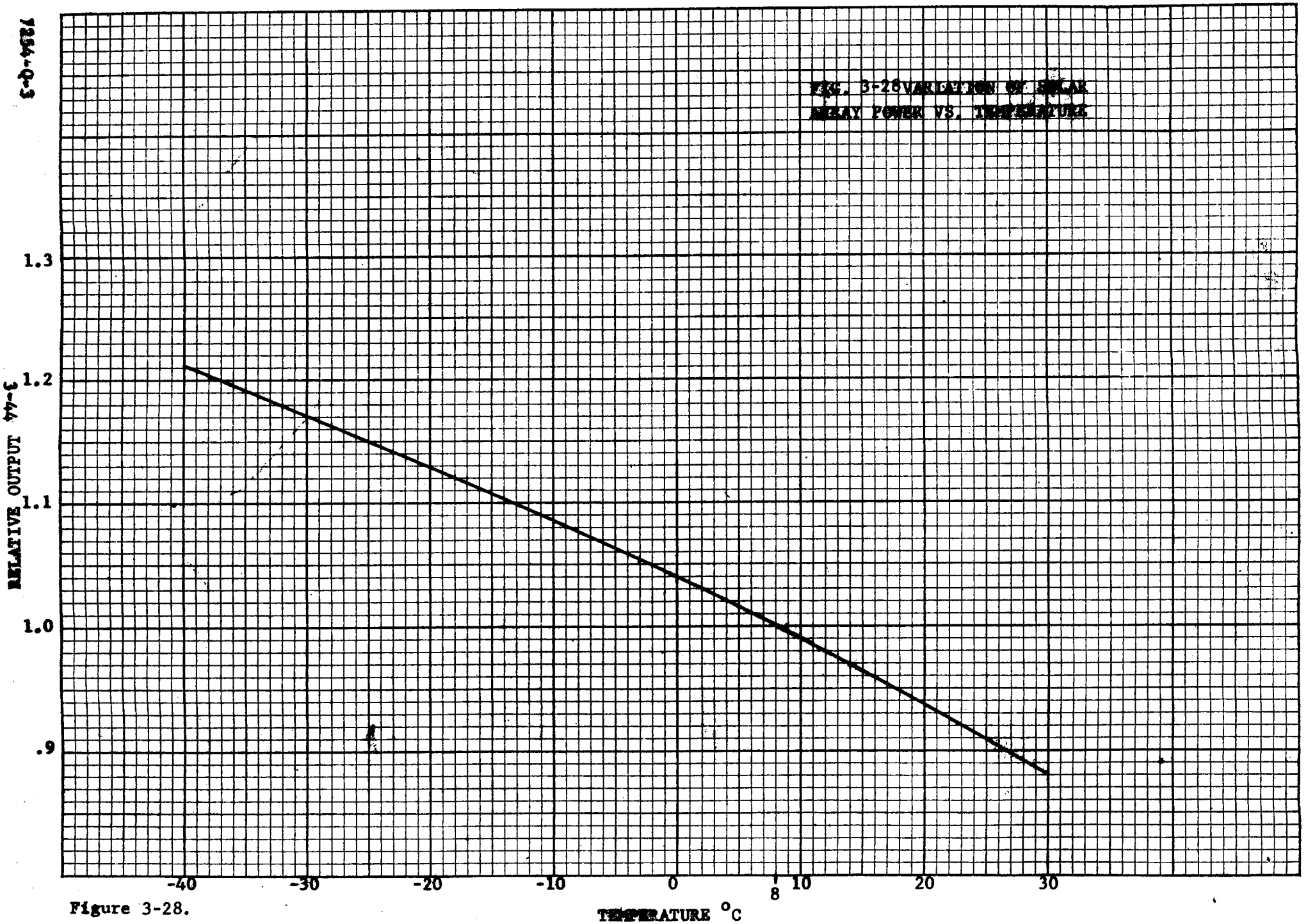
FIG. 3-28 VARIATION OF SOLAR ARRAY POWER VS. TEMPERATURE
RELATIVE OUTPUT
1.3
1.2
1.1
1.0
.9
-40
-30
-20
-10
0
8
10
20
30
TEMPERATURE °C

Figure 3-28.

TABLE 3-I

MIN AND MAX POWER AVAILABLE FROM THE SOLAR ARRAY
AT NOON FOR THE FIRST DAY OF SPRING, FALL AND SUMMER

	Hill Angle and Direction	Lat.	Sun Vector Angle	Power (watts) @ 8°C	Estimated Avg. Temperature	Correct. Factor	Correct Power (watts)
Spring (max)	20°N,S	20°N,S	90°	284	-3°C	1.053	299
Spring (min)	30°N,S 30°E,W	EQ.	60°	228	+7.5°C	0	228
Summer (max)	24°N	EQ.	90°	237	-9°C	1.08	256
Summer (min)	26°S 29°E,W	20°N	60°	182	-1.0°C	1.04	190

The magnetic field due to the dipole at a point P can be divided into two components, i.e.:

$$B_r = \frac{\mu_o}{4\pi}\left(\frac{2m\cos\theta}{r^3}\right) \quad (2)$$

$$B_\theta = \frac{\mu_o}{4\pi}\left(\frac{m\sin\theta}{r^3}\right) \quad (3)$$

The r and θ coordinates are defined in Fig. 3-30. Equations 2 and 3 are good approximations where the characteristic dimension of the loop (the equivalent radius in this case) is small compared to the distance r.

The magnetic field at any point can be calculated by applying the three equations to the current loop formed by two adjacent circuits. The resultant field is the vector summation of the contribution of every individual loop. We shall assume that the instruments which are sensitive to the magnetic field are mounted near the spacecraft structure. Because the exact locations of these instruments have not been specified we shall pick the spots in the vicinity of the spacecraft to illustrate the order of magnitude of the field.

3.6.1 SUN AT ZENITH OF SPACECRAFT

For this case, all currents in each circuits are equal. The circuit current corresponding to the maximum power output of 284 watts is 0.113 ampere. Consider the spacecraft center (P_o) as the point to compute the field. It can be seen from Fig. 3-31 that the field will be zero by virtue of its symmetry. This is because, for a given dipole field, we can select another dipole which is directly opposite to cancel the field. The resultant field is therefore zero.

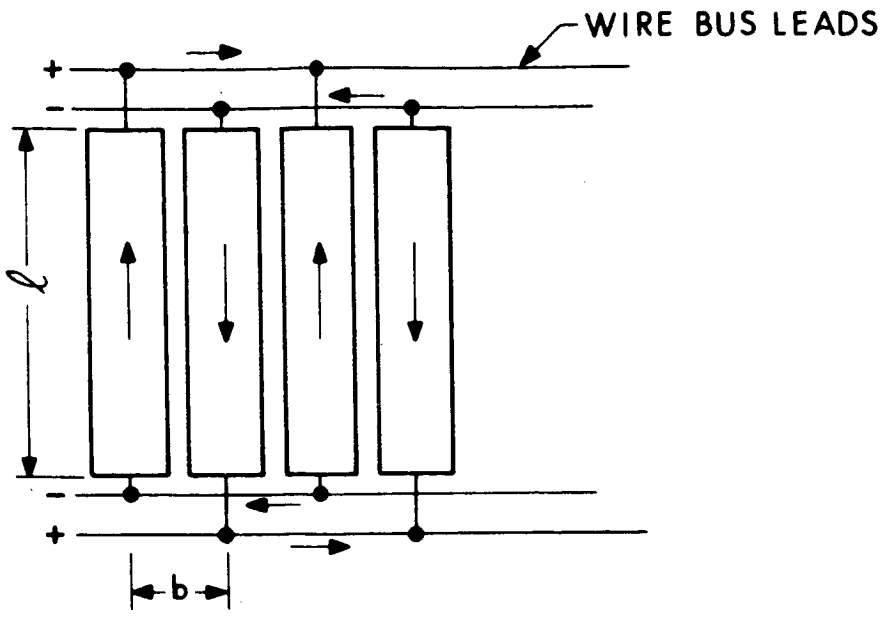

Figure 3-29. Bus and Circuit Arrangement

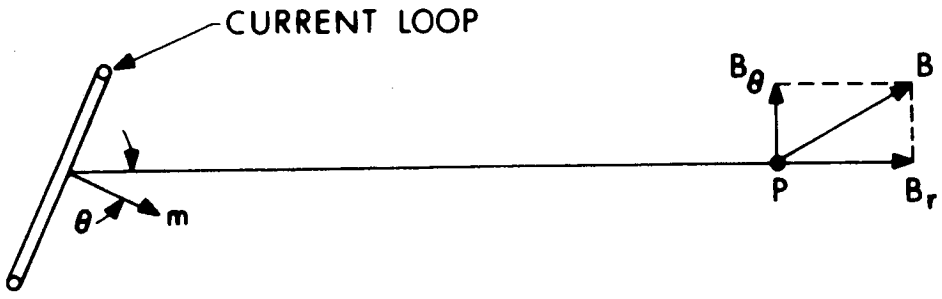

Figure 3-30. Coordinates of Dipole Field

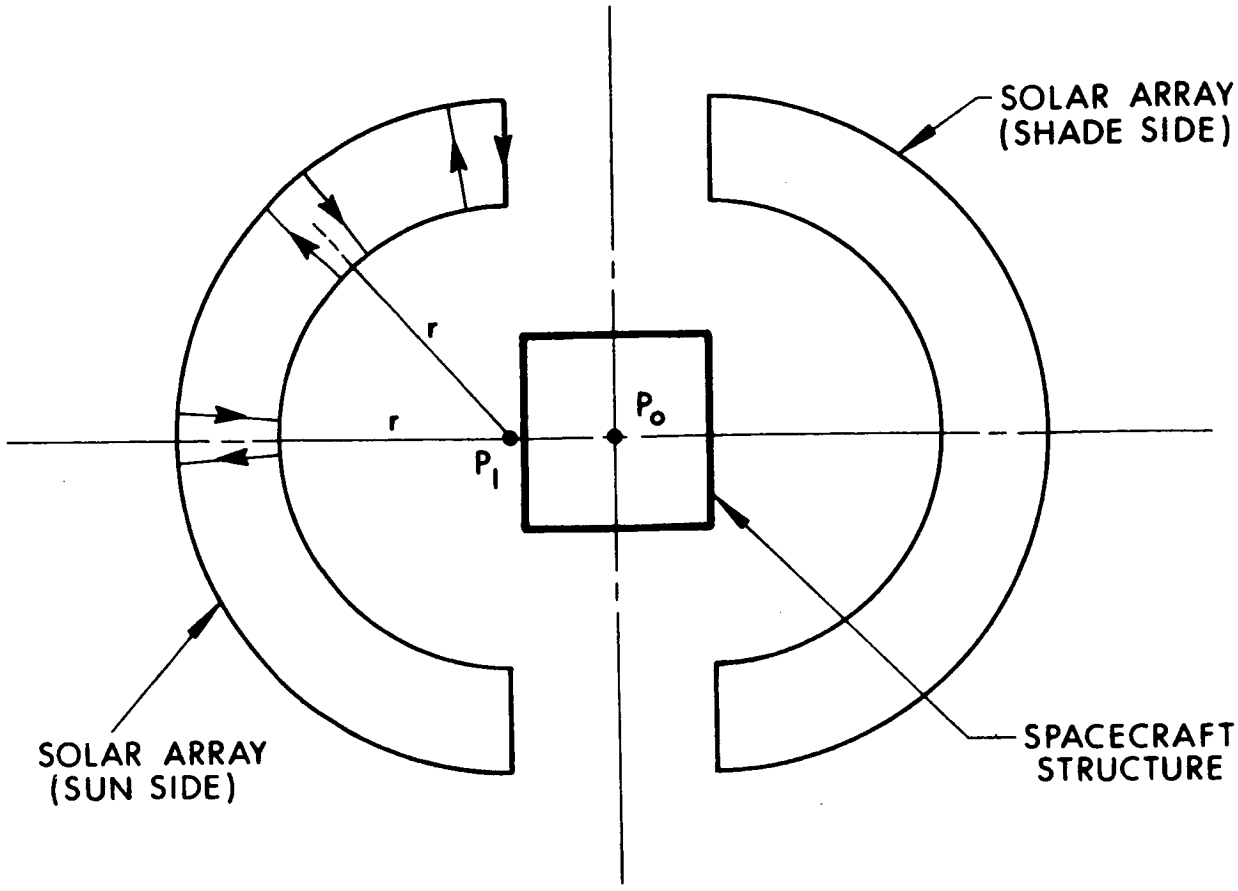

Figure 3-31. Geometrical Relationship of Current Loops with Respect to Spacecraft

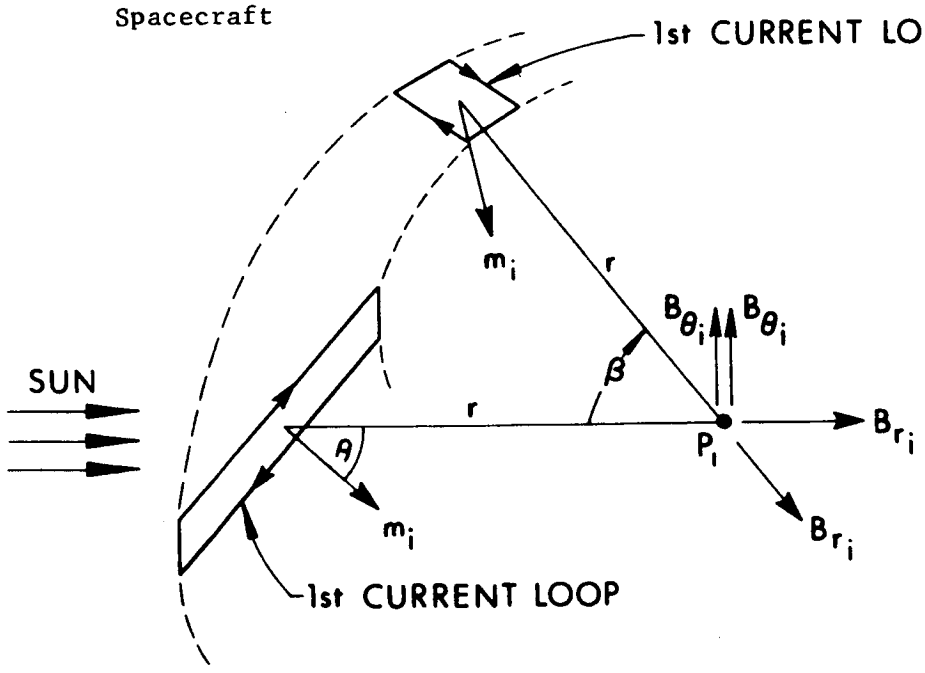

Figure 3-32. Field Vectors Due to Two Dipole Fields

807

At P_1, a point next to the spacecraft structure, the field will be non-zero but relatively weak. We shall not compute the field for this case since it is not the worst case.

3.6.2 SUN-SHADE CONDITION

When the Sun angle with respect to the local horizontal plane is less than 66.2^{o}, one half of the array will be in the shade, and the other half in the Sun. The maximum power point occurs when the angle is about 30^{o}. If we assume that the Sun traverses in the prolonged axis of the solar array, the current in the first loop will be maximum. See Fig. 3-32. The current in the adjacent loop will be decreased according to the cosine law. That is,

$$\text{First Loop: } I_1 = I_o$$

$$\text{ith Loop: } = I_o (\cos\beta_i)$$

The dipole moments corresponding to these loop currents are:

$$\text{First Loop: } = m_1 = I_o A$$

$$\text{ith Loop: } = m_i = I_o A (\cos\beta_i)$$

We are now in a position to compute the field at P_1 which is the center point of the sunlit array. Referring to Figs. 3-30 and 3-32, we can see immediately that the B_o fields can be added algebraically. However, the B_r fields must be added vectorially. Each B_r field can be resolved into the sine and cosine components. Fortunately, because of the symmetry made possible by the choice of P_1, the sine components cancel out. All the cosine components can be added directly and all are in the direction of Br_1.

The expressions for the resultant B_o and B_r fields are:

$$B_o = 2 \sum_{i=1}^{''} B_{oi} \tag{4}$$

$$B_r = 2 \sum_{i=1}^{''} Br_i \ (\cos\beta i) \tag{5}$$

where

$$B_{o_i} = \frac{\mu_o I_o A \sin\theta}{4\pi r^3} \ (\cos\beta i) \tag{6}$$

$$B_{ri} = \frac{\mu_o I_o A \cos\theta}{2\pi r^3} \ (\cos\beta i) \tag{7}$$

Combining Eqs. 4 and 6 and Eqs. 5 and 7 we have:

$$B_o = \frac{\mu_o I_o A \sin\theta}{2\pi r^3} \sum_{i=1}^{''} \cos\beta i \tag{8}$$

$$B_r = \frac{\mu_o I_o A \cos\theta}{\pi r^3} \sum_{i=1}^{''} \cos^2\beta i \tag{9}$$

The angle βi varies from 0 to 90 degrees at an increment of 8.2 degrees. The following are the appropriate constants which will be used.

μ_o = $4\pi \times 10^{-7}$ henries/meter
I_o = 0.280 amp
A = b x 1 = 0.122 x 1.20 = 0.146 meter^2
θ = 23.8^o
r = 85 inches = 2.16 meters

$$\frac{\mu_o I_o A}{\pi r^3} = \frac{4\pi \times 10^{-7} \times 0.280 \times 0.146}{\pi (2.16)^3}$$

$$= 1.63 \times 10^{-9} \text{ weber/meter}^2$$

The cosine functions in Eqs. 8 and 9 were computed:

$$\sum_{i=1}^{11} \cos\beta_i = 6.998$$

$$\sum_{i=1}^{11} \cos^2\beta_i = 5.499$$

The B_r and B_o fields are then:

$$B_o = \frac{1.63 \times 10^{-9} \sin 23.8^o}{2} \times 6.998 = 2.3 \times 10^{-9} \text{ weber/meter}^2$$

$$B_r = 1.63 \times 10^{-9} \cos 23.8^o \times 5.499 = 8.2 \times 10^{-9} \text{ weber/meter}^2$$

The total resultant field B_T is:

$$B_T = (B_r^2 + B_o^2)^{1/2} = 8.5 \times 10^{-9} \text{ weber/meter}^2 = 8.5 \text{ gamma}$$

3.6.3 CONCLUSION

In the vicinity of the spacecraft, point P_1 receives the maximum field intensity. The magnetic field at this point was computed to be 8.5 gamma. Placement of the instrument at some other locations will insure a lower magnetic effect.

SECTION 4

STRUCTURAL DESIGN AND ANALYSIS

This section contains the following information:

a. A functional description of each of the major mechanical components of the conical solar array baseline configuration

b. A discussion of the criteria used to select the material for each component

c. A description of the mathematical model(s) used to analyze each component

d. The loads analysis performed to establish the critical loading condition for each component

e. The stress analysis for each component and a summary of the respective margins of safety

f. Conclusions and recommendations

The mechanical components of the array are:

a. Substrate

b. Peripheral frame of the substrate

c. Substrate support truss

d. Pivotal deployment structure

e. Space frame support from spacecraft

f. Mechanisms

4.1 SUBSTRATE

4.1.1 DESCRIPTION

The substrate sections of the conical array are six identical 60° sectors of the frustum of a right circular cone. The radii of the base and top of the frustum are 91.75 inches and 72.4 inches respectively. The height of the frustum is 43.9 inches. The nominal thickness of the substrate is 0.10 inches.

4.1.2 MATERIAL SELECTION

The substrate material chosen for this configuration is electroformed aluminum hollowcore. This material was chosen for this application based on the following considerations:

a. Fabrication: The electroforming fabrication technique eliminates in-process handling of foil gage materials and difficult bonding operations required to produce comparable types of sandwich shell structures.

b. Weight: The one-piece structure which results from the electroforming process is lighter than laid-up sandwich structures of equivalent stiffness.

4.1.3 MATHEMATICAL MODEL

The substrate dynamic analysis is based on the model shown in Fig. 4-1. This lumped parameter model simulates one of the 60° sectors of the conical frustum and the peripheral frame for that section. The joint coordinates for the nodes of the model are shown in Table 4-I. The weights assigned to each node are listed in Table 4-II. The stiffness parameters were calculated as follows:

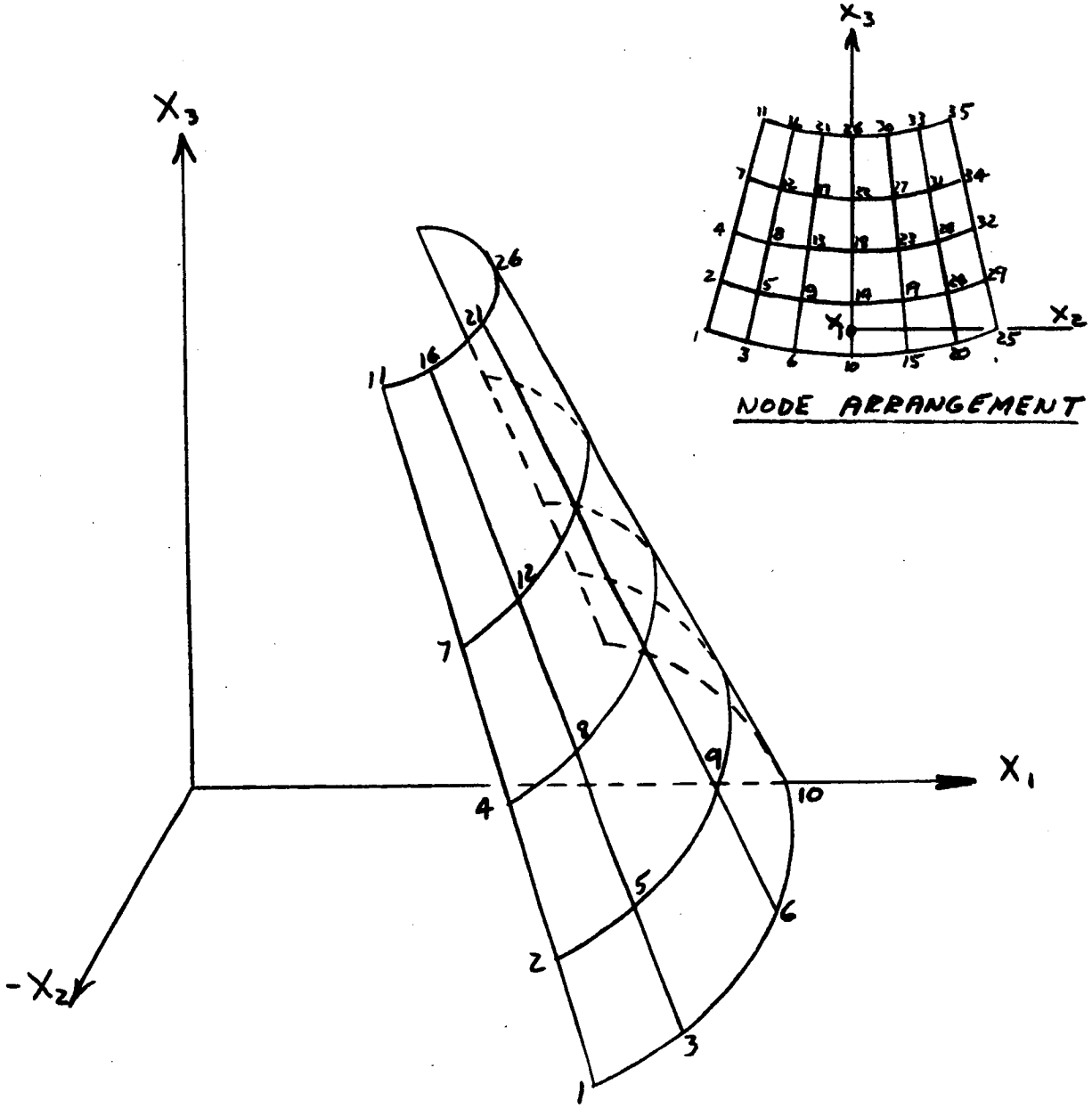

Figure 4-1. Substrate Computer Model

TABLE 4-I

JOINT COORDINATES

Joint	X(1)	X(2)	X(3)
1	81.23000	-46.90000	0.00000
2	76.42000	-44.13000	12.57500
3	88.14000	-32.08000	0.00000
4	71.63000	-41.36000	25.15000
5	82.93000	-30.18000	12.57500
6	92.37000	-16.28000	0.00000
7	66.82000	-38.58000	37.72500
8	77.72000	-28.29000	25.15000
9	86.91000	-15.32000	12.57500
10	93.80000	0.00000	0.00000
11	62.00000	-35.80000	50.30000
12	72.51000	-26.39000	37.72500
13	81.45000	-14.36000	25.15000
14	88.25000	0.00000	12.57500
15	92.37000	16.28000	0.00000
16	67.28000	-24.49000	50.30000
17	75.99000	-13.39000	37.72500
18	82.71000	0.00000	25.15000
19	86.91000	15.32000	12.57500
20	88.14000	32.08000	0.00000
21	70.51000	-12.43000	50.30000
22	77.16000	0.00000	37.72500
23	81.45000	14.36000	25.15000
24	82.93000	30.18000	12.57500
25	81.23000	46.90000	0.00000
26	71.60000	0.00000	50.30000
27	75.99000	13.39000	37.72500
28	77.72000	28.29000	25.15000
29	76.42000	44.13000	12.57500
30	70.51000	12.43000	50.30000
31	72.51000	26.39000	37.72500
32	71.63000	41.36000	25.15000
33	67.28000	24.49000	50.30000
34	66.82000	38.58000	37.72500
35	62.00000	35.80000	50.30000

TABLE 4-II

WEIGHT DISTRIBUTION

Joint	Weight (lb)
1	1.470000E-01
2	2.040000E-01
3	2.240000E-01
4	1.960000E-01
5	2.680000E-01
6	2.240000E-01
7	1.870000E-01
8	2.510000E-01
9	2.680000E-01
10	2.240000E-01
11	1.200000E-01
12	2.340000E-01
13	2.510000E-01
14	2.680000E-01
15	2.240000E-01
16	1.720000E-01
17	2.340000E-01
18	2.510000E-01
19	2.680000E-01
20	2.240000E-01
21	1.720000E-01
22	2.340000E-01
23	2.510000E-01
24	2.680000E-01
25	1.470000E-01
26	1.720000E-01
27	2.340000E-01
28	2.510000E-01
29	2.040000E-01
30	1.720000E-01
31	2.340000E-01
32	1.960000E-01
33	1.720000E-01
34	1.870000E-01
35	1.200000E-01

4.1.3.1 Calculation of Stiffness Parameters for Aluminum Hollowcore

The bending stiffness for the minimum section of the aluminum hollowcore is given by the following equation:

$$D = \frac{Et}{2a}\left[2\left\{(2a-d)(h/2)^2 + \frac{h^3}{12}\right\}\right]$$

where the parameters are defined by the sketch below.

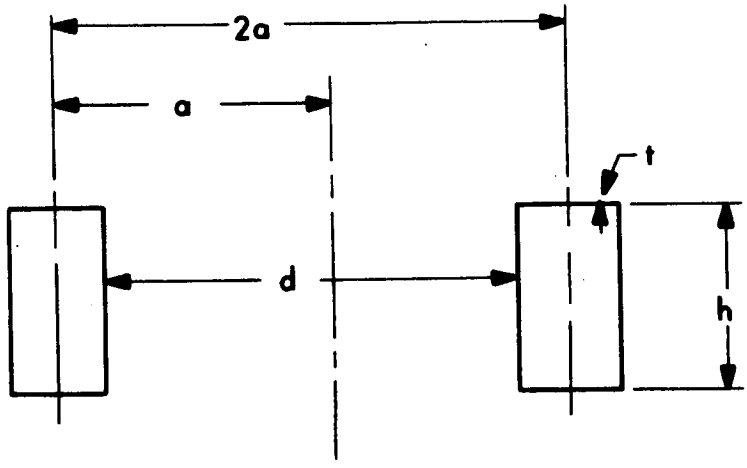

and

D = EI = Bending Stiffness lb-in^2/in

E = Young's modulus of electroformed aluminum = 7.8×10^6 psi

The mathematical model was constructed based on the following values.

h = 0.10 inch
d = 1.00 inch
t = 0.004 inch
a = 0.525 inch

So that,

$$I = t/2a\ [2\{(2a-d)(h^2/2) + h^3/12\}]$$

$$I = 1.58 \times 10^{-6}\ \text{lb-in}^2/\text{in.}$$

The shear stiffness for the hollowcore is calculated from the following relation:

$$GA_s = \frac{Et}{2(1+\upsilon)}\ [2 + h/a - \sqrt{3/2}\ (d/a)]$$

where G = shear modulus

υ = Poisson's ratio = 0.33

A_s = shear area

Using the values for E, t, h, a, and d as before,

$$A_s = 2.16 \times 10^{-3}\ \text{in}^2/\text{in}$$

4.1.3.2 Calculation of Stiffness Parameters for Beryllium Beams

The frame stiffness for this model is based on a two inch diameter beryllium tube with a 0.012 inch wall.

$$I = \pi R^3 t = 0.012\pi = 0.0377\ \text{in}^4$$

$$A = 2\pi Rt = 0.024\pi = 0.0754\ \text{in}^2$$

$$E = 44 \times 10^6\ \text{psi}$$

$$\upsilon = 0.1$$

$$G = E/2(1+\upsilon) = 20 \times 10^6\ \text{psi}$$

4.1.3.3 Restraints

The panel section is assumed to be restrained from rotation or translation at each of the four corners (joints 1, 11, 25, and 35).

4.1.4 LOADS AND DEFLECTION ANALYSIS (Launch Vibration)

The computer analysis of the mathematical model described in Subsection 4.1.3 predicts substrate resonant frequencies at 3.19 Hz, 4.45 Hz, 5.84 Hz, 6.56 Hz, 6.67 Hz and 8.32 Hz. The design loads in this frequency range are the decaying sinusoidal low frequency transients. The steady state sinusoidal equivalent of the transients is 0.49 g's (0-peak) (see EOS Report 7254-Q-1).

The frequency response solution for this model indicates that the largest deflections and stresses occur at the second natural frequency, 4.45 Hz, which is the first symmetric mode. This response was computed using a modal damping coefficient, c/cc, of 0.01 for each of the six modes included in the modal summation. This modal damping coefficient produced Q = 50 i.e., Q = 1/2 c/cc = 50.

For a input of 1.25 x 0.49 g's (ultimate design load) in the x_1 direction at 4.45 Hz. The maximum deflection of the substrate occurs at joint 18 and has a magnitude of 0.55 inches. The maximum internal loads associated with this loading are shown in Table 4-III.

TABLE 4-III

TABULATION OF ULTIMATE DESIGN LOADS

Member from A to B		P (lb) Axial Load	M (in-lb) Bending Moment	T (in-lb) Torsional Moment	V (lb) Shear Load
A	B				
8	12	0.58	0.34	0.0245	0.025
10	14	0.44	1.23	0.010	0.012
15	19	0.04	0.16	0.325	0.025
4	8	0.43	1.20	0.037	0.153

4.1.5 SUBSTRATE STRESS ANALYSIS

4.1.5.1 Stresses Due to Launch Loads

4.1.5.1.1 Maximum Bending Stress

The maximum bending stress occurs at the minimum cross section of the hollowcore. The maximum bending moment predicted by the loads analysis is 1.23 in-lb in member 10 to 14. The total cross sectional moment of inertia for this member is 2.135×10^{-5} in^4. The bending stress is:

$$S = \frac{Mc}{I} = \frac{1.23\ (0.05)}{2.135 \times 10^{-5}}$$

$$S = 2890 \text{ psi}$$

The margin of safety:

$$M\,S = \frac{\text{Allowable Stress}}{\text{Ultimate Stress}} - 1$$

The yield strength of electroformed aluminum is 20,500 psi, therefore

$$MS = \frac{20{,}500}{2890} - 1 = 6.1$$

The parameters for the baseline design are:

$K = 12$ (TN 3781)
$E = 7.8 \times 10^6$ psi
$\upsilon = 0.33$
$t = 0.004$
$S = 4a - \sqrt{3d}$
$a = 0.525$
$d = 1.00$

Therefore,

$$\sigma_{cc} = \frac{12\pi^2 (7.8)(10^6)}{12 (0.89)} \left(\frac{0.004}{0.368}\right)^2$$

$$\sigma_{cc} = 8650 \text{ psi}$$

The design ultimate stress for the local crippling of the triangular plate is the summation of the bending stress and the axial compressive stress. Assuming the maximum bending stress as calculated above and the maximum compressive stress are applied simultaneously, a conservative assumption, the ultimate stress is

$$\sigma_c = S_{bending} + \frac{P}{A}$$

$$\sigma_c = 2890 + \frac{0.58}{0.03} = 2910 \text{ psi}$$

4.1.5.1.2 Maximum Shear Stress

The maximum shear stress occurs in member 4 to 8 and is 0.153 lb. The shear area for this member is 0.03 in^2.

$$S_S = \frac{V}{A_S}$$

$$S_S = \frac{0.153}{0.03} = 5.1 \text{ psi}$$

The margin of safety is high.

4.1.5.1.3 Local Crippling Stress

The local crippling stress for the hollowcore is based on the crippling of the triangular plate included between three adjacent holes

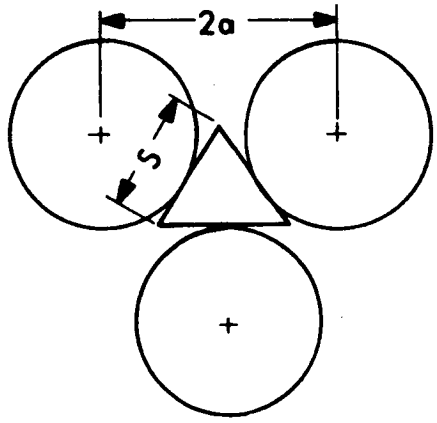

The allowable stress is given by

$$\sigma_{cc} = K \frac{\pi^2 E}{12 (1 - \nu^2)} (t/s)^2$$

from NASA TN 3781.

The margin of safety on crippling is

$$MS = \frac{8650}{2910} - 1 = 1.98$$

4.1.6 CONCLUSIONS AND RECOMMENDATIONS

The analysis of baseline configuration that the substrate parameters assumed for the first iteration of the analysis provide positive margins of safety for the launch vibration environment. Further analysis of the aerodynamic loads for the deployed configuration and of the dynamic coupling with the space frame structure should be conducted.

4.2 PERIPHERAL FRAME OF THE SUBSTRATE

4.2.1 FUNCTIONAL DESCRIPTION

The substrate frame lies along the periphery of each of the two, half-truncated cone sections making up the planetary array. The peripheral frame in the baseline design is tubular beryllium, 2 inches O.D. with a 0.010 inch wall. The peripheral frame maintains the shape and strengthens the truncated cone by clamping the substrate about its edges.

4.2.2 MATERIAL SELECTION CRITERIA

Beryllium was selected because of its high stiffness-to-weight ratio.

4.2.3 MATHEMATICAL MODEL(S)

a. Dynamic Launch Load. The model used for the dynamic launch loads is described in Subsection 4.1.3.

b. Wind Load. The model used for the Martian wind load assumed that the two outboard 60° segments of the half-truncated cone are cantilevered off the center 60° segment.

4.2.4 CRITICAL LOADS ANALYSIS

a. Launch Loads. The maximum moment and shears loads during launch as determined by the LESAR Structural Computer Program are 9.17 in.-lb and 0.8 lb respectively.

b. Wind Load. The following equations were used to determine the maximum moment and the deflections in the vertical and horizontal directions. (The equations are for a circular cantilever of radius R and uniform radial pressure p lb per linear in.)

$$M = pR^2(1 - \cos\theta)$$

$$y = \frac{pR^4}{EI} (\sin\theta + \sin\theta \cos\theta - 3/2\ \theta \cos\theta - 1/2 \sin^3\theta - 1/2 \cos^2\theta \sin\theta)$$

$$x = \frac{pR^4}{EI} (1 - 3/2\ \theta \sin\theta + \sin^2\theta - \cos\theta)$$

Based on these equations, the maximum moment, vertical deflection and horizontal deflection are 163 ft-lb, 0.585 in., and -0.795 in. respectively.

4.2.5 STRESS ANALYSIS

Environment	Load Condition	Allowable Stress (psi)	Actual Stress (psi)	Margin of Safety
Launch	Buckling	196,500*	292	336.0
	Yield	62,000		169.0
	Shear	70,000	12.75	2744.0
Wind	Buckling	196,500*	49,500	2.18
	Yield	62,000		0.02

*North American Aviation Structures Manual, "Critical Buckling Stress Coefficients for Circular Cylinders Subjected to Pure Bending," pg. 9.23.02.

4.2.6 CONCLUSION

Based on the foregoing analysis, the critical environment for the substrate frame is the wind load in the deployed configuration. Further optimization of the peripheral frame will require a more detailed analysis of the aerodynamics of the overhanging structure.

SECTION 5

SYSTEM ANALYSIS

5.1 ENVIRONMENTAL INTERACTION

5.1.1 EARTH ENVIRONMENTAL INTERACTION

5.1.1.1 Assembly and Handling

This environment is governed by manufacturing techniques and is discussed in Section 6.

5.1.1.2 Sterilization

5.1.1.2.1 ETO Phase

"Type Acceptance" levels are most extreme and for ETO, are as follows:

a. Temperature: 50°C
b. ETO Concentration: 600 mg/liter
c. Freon Ratio: 88 parts Freon 12/12 parts ETO
d. Relative Humidity: 50%
e. Time of Exposure: yet to be determined

ETO may interact with spacecraft components in two ways: by direct attack on organic materials and by contamination of surfaces with reaction products. Inorganic materials sensitive to moisture also may be affected by this hot, humid environment.

An extensive study performed for JPL (JPL Contract No. 951003) revealed only two out of several hundred polymers tested which were significantly

degraded by exposure to the ETO sterilization environment. These two materials were "Kapton" and "Tedlar" films, both of which are scheduled for use in the JPL/SPA.

Mr. Donald Kohorst of JPL reports that subsequent studies of these two materials by General Electric and by Autonetics found no adverse reaction to this environment. The Autonetics study, on the contrary, found properties of "Kapton" improved by the full sterilization cycle (ETO followed by heat). Degradation levels reported in the study would still leave these materials more than qualified for their intended uses. Confirming tests of organic materials should nevertheless be included in this program.

ETO is polymerized by many metallic and oxide surfaces, which act as a catalyst and assist in its recomposition. While the exposed surface area is too small to create an explosive hazard (the presence of Freon and water vapor also guards against violent reaction), the products of decomposition may collect as a film or residue and may or may not be driven off during the heat sterilization. Tests will be required to evaluate this effect and, if it is found to be significant, protective coatings will be required for reactive surfaces. All metallic components, in any case, are scheduled for corrosion resistant surface treatment.

5.1.1.2.2 Heat Phase

All potentially temperature-sensitive materials should be required to withstand 300°F for 100 hours. This requirement should be made to ensure that the materials are capable of withstanding 135°C (275°F) for 24 hours in a system test, where exterior components may have to be overheated to ensure an adequate interior temperature level.

The following information is referenced from JPL Technical Report No. 32-973, "Effects of the Thermal Sterilization Procedure on Polymeric Products."

The following values were obtained before and after a thermal exposure of 3 cycles of 40 hr each at 300°F in a nitrogen atmosphere.

Sylgard 182 (XR-6-3489)

	Before	After
Mech. Hardness (A)	50	52
Vol. Resis. (Ω-cm)	1.15×10^{14}	1.65×10^{15}
Wt Loss (%)	–	0.855
Vol. Change (%)	–	3.08

Compatibility Rating - Compatible

'H' Film (Kapton)

	Before	After
Tensile Stg (psi)	24,153	19,811
Elongation (%)	70	31
Tear Stg (lb/in)	3259	3118
Vol. Resis. (Ω-cm)	1.20×10^{16}	8.59×10^{16}
Wt Loss (%)	–	0.624

Compatibility Rating - Marginal

Tedlar Film (PVF)

	Before	After
Tensile Stg (psi)	8022	10,744
Elongation (%)	82	104
Tear Stg (lb/in)	1907	1928
Vol. Resis. (Ω-cm)	1.01×10^{15}	1.64×10^{15}
Wt Loss (%)	–	0.106

Compatibility Rating - Compatible

The above materials are considered usable in their specific application based on the test data presented.

5.1.1.3 Shipment and Storage

This environment is well defined in previous practice and appropriate packaging and shipping methods will be established.

5.1.2 LAUNCH, FLIGHT, AND LANDING

5.1.2.1 Launch

The accelerations, vibration, and shock present in launching compose the severest environment to be experienced by this spacecraft. The structural design is governed by the requirements of this phase. This presentation is contained in Section 4.

5.1.2.2 Flight

Except for relatively moderate forces which may be imposed by course correction maneuvers, the environment of flight is entirely passive. The spacecraft is enclosed in a canister which totally shields it from irradiation, and extended (6 month) exposure to hard vacuum imposes the severest parameter to be met during this phase. Materials and techniques responsive to this parameter are established state of the art.

5.1.2.3 Landing

Levels of acceleration, vibration, and shock during this phase are to be less than at launch. The most questionable condition occurs during entry into the atmosphere. As presently projected, the heat shield is contained within the canister which must therefore be jettisoned before entry is begun. During this critical maneuver, the spacecraft will be sheltered only by the heat shield and will otherwise be entirely exposed. It is to be expected that some ablated material will migrate into the

sheltered region and that contamination by this material may occur. A study of turbulence to be expected in the sheltered region is indicated for Phase II planning.

5.1.3 MARS ENVIRONMENTAL INTERACTION

A detailed discussion of this environment is contained in the first quarterly report (7254-Q-1). Parameters of the selected model are reproduced in Table 5-I.

Analysis of the radiative and thermal environments has shown them to be insignificant in their interaction with the spacecraft.

The presence of H_2O in the Martian atmosphere has not been firmly established. The evidence is that, if present, the quantity is very small. Nighttime temperatures on Mars fall to -30 to -35°C. Warming rate of the environment after sunrise is 7 to 8°C/hr. Portions of the spacecraft receiving direct sunlight will warm much more rapidly. Saturation pressure for H_2O at 0°C is six milibars. The model adopted for the Martian atmosphere assumes a pressure of seven milibars. Any condensation of H_2O will occur as frost at night and should dissipate by sublimation immediately after sunrise. Effects of moisture (and of the resulting carbonic acid) should be negligible under these conditions.

Maximum wind speed is predicted to be 325 feet per second. Energy of this wind is equivalent to a 18.5 mph wind at one Earth atmosphere. "Free stream continuous surface wind speed" is placed at 186 feet per second, and the attenuation factor of 0.67 to correct for the conditions near the Martian surface gives a wind speed of 125 feet per second, and gusts may reach 200 feet per second. The solar array structure has been analyzed and found competent to resist steady-state wind forces and nonresonant gusts, but Phase II should contain a more detailed aerodynamic analysis to determine whether any oscillator or vibrating

TABLE 5-I

MARS ATMOSPHERIC CONSIDERATIONS

Property	Dimension	Model
Surface pressure	mb	7.0
Surface density	$(gm/cm^3)10^5$	1.85
Surface temperature	^oK	200
Stratospheric temperature	^oK	100
CO_2 (by mass)	%	100
N_2 (by mass)	%	0.0
A (by mass)	%	0.0
Molecular weight	mol^{-1}	44.0
Specific heat ratio	cal/gm^oC	0.166
Specific heat ratio	-	1.37
Adiabatic lapse rate	$^oK/km$	-5.39
Tropopause altitude	km	18.6
Free stream continuous surface wind speed	ft/sec	186
Maximum hour surface wind speed	ft/sec	125
Design gust speed	ft/sec	200
Maximum combined wind speed	ft/sec	325

response to wind is to be expected and to evaluate the cumulative effect of such oscillation or vibration upon the array structure during its projected life.

Dust is assumed to be an oxide of iron, a conductive and abrasive material. Dust particles having a size range of 1 to 1000μ can be made airborne when wind speed exceeds 300 feet per second. The first quarterly report (7254-Q-1) cites studies which show that abrasion by dust may be a serious problem in its effect on protective coatings, both of solar cells and of structure. Thermal control coatings are not contemplated and the anticorrosive coatings to be provided for protection of metallic components in Earth environment will be superfluous in the non-reactive Martian atmosphere.

The threat of abrasion of cell coatings, however, presents a serious threat to extended performance of this array and more examination of this interaction will be required. Tests have shown that an exposure of 60 minutes is sufficient to pit or to frost conventional coverglass under conditions of wind velocities of 300 to 520 ft/sec. The resistance of resilient materials to such abrasion is known to be much better than that of glass and the projected Tedlar film is resilient, but the maintenance of all performance for the period of a year may be difficult.

Accumulation of dust in a manner to cause shorting between cells will be prevented by enclosure in the Tedlar film and by filling of all spaces between cells with adhesive. Surface accumulation in a manner to degrade all performance is improbable on an array with steeply sloping surfaces in an environment characterized by high winds.

5.2 MATERIALS EVALUATION

A tabulation of the materials considered for critical areas is shown in Table 5-II.

TABLE 5-II

CRITICAL MATERIALS LIST

Material Function	Candidate Material	ETO Sterilization	Thermal Sterilization	Mars Atmosphere	Space Environment	Other Comments
1. Solar cells	N/P silicon		OK for 300°F less than 100 hr		Effects of radiation damage must be a parameter of system design	
2. Filter	Tedlar film	OK	Some shrinkage at 300°F	Possible dust erosion and/or surface contamination. Chosen for dust protection	OK	
3. Filter adhesive	Silgard	OK	OK	Must consider dust erosion to degree that it functions as encapsulant	OK	
4. Connectors	Moly, Kovar, copper	OK	OK	May need protection against iron oxide dust dust		Mechanical design must take thermal expansion, formability into account
5. Solder joints	Sn 63 solder	May polymerize ETO	Slight reliability drop must be accounted for	May need protection against iron oxide dust		
6. Wire insulation	Teflon, polyvinyl chloride	OK	OK			Irradiated polylefin will not take temperature
7. Bonding adhesive	RTV 41, 577, 3145	Same comments as item 3	Design must take loss of strength during immersion into account			
8. Dielectric	H-film, epoxy glass,	OK, but absorption and outgassing should be checked				Mylar will not take temperature
9. Substrate	Aluminum hollowcore, nickel hollowcore, stretched glass epoxy tape (Boeing System)	All OK; should be checked for possible ETO polymerization	OK	OK		Nickel hollowcore presents magnetization problems
10. Frame	Beryllium, aluminum alloy, Al/boron fiber composite	Same as item 9	OK	Must have protective		Al/boron fiber probably not state of the art, 1969. Structural considerations will dictate choice
11. Deployment structure	Beryllium, Al/boron composite	Same as item 9	OK	Same as item 10		Most critical stiffness/weight problems
12. Hinge and bearing lubricants	MoS_2, Teflon sleeves	OK	OK, Sealed bearings not suitable			
13. Thermal control coating						
14. White paint	Sodium silicate ZnO (Z-93)	Data not available	OK, slight optical degradation		Long term ultraviolet degradation	Best optically
	Dow Corning Methyl silicone ZnO	OK	Same as Z-93		Long term ultraviolet degradation	
15. Black paint	Cat-a-lac black	OK	OK			
	Laminar X-500	OK	OK			

Since the solar array is required to be 1969 state-of-the-art, most of the materials and processes must be well established and proved in a space environment. Those materials that are not established should be included only when the promise of improved performance outweighs the risks involved in using a material that does not have a substantial available backlog of properties information. One example of this is the use of Tedlar film in place of coverglass.

There are three potentially troublesome areas from the standpoint of materials selection:

a. The ETO and thermal sterilization tests create a severe environment for many of the commonly used organic substances making up the dielectric coatings, thermal control coating, adhesives and potting compounds.

b. The stiffness/weight requirements of the substrate and deployment structures have dictated a design based on a tubular beryllium frame supporting an aluminum hollowcore substrate.

c. Wind and dust environment on Mars imposes severe problems in the maintenance of solar panel performance over the scheduled spacecraft life.

It should be emphasized that the ETO/heat sterilization problem is more involved than merely obtaining assurance that all candidate materials are not degraded by the environment. ETO is polymerized by many metallic and oxide surfaces, which act as a catalyst and assist in its decomposition. While the exposed surface area is too small to create an explosive hazard (the presence of Freon and water vapor also guards against violent reaction), the products of decomposition may collect as a film or residue and may or may not be driven off during the heat sterilization.

All potentially temperature-sensitive materials should be required to withstand 300^{o}F for 100 hours. This requirement should be made to

ensure that the materials are capable of withstanding 135°C (275°F) for 24 hours in a system test, where exterior components may have to be overheated to ensure an adequate interior temperature level.

5.3 THERMAL ANALYSIS, NONTRACKING CONICAL ARRAY

Solar panel performance degrades with increasing temperature, and this degradation must be accounted for in the panel design. The design output power requirements for all solar panel configurations are a peak of 200 watts at noon with a minimum solar intensity of 50 mW/cm^2. Preliminary panel designs were sized for a nominal operating temperature of 300°K (27°C). The fixed deployable array will stabilize at a lower temperature, since the available heat rejection area from its curved surface is much greater than the area normal to the sun. In sizing estimates an average operating temperature of 281°K (8°C) has been assumed.

The fixed deployable array differs from the oriented arrays in that a considerable variation in temperature can be expected over the power producing surface. An oriented array will tend to stabilize at a uniform temperature unless there is shadowing.

Since the cell layout of a fixed array consists of strings of submodules running vertically along the sides of the truncated cone, each string sees a uniform vertical and horizontal sun angle and therefore tends to stabilize at a uniform temperature. Therefore, for this configuration, the lowest voltage will be determined by the temperature of the hottest string of submodules, and the lowest specific power by the solar intensity and the average panel temperature. For this reason, both the peak temperatures and average temperatures are of significance.

The results of an analysis to determine the amount of temperature variation are presented in Figs. 5-1 and 5-2. The angle ϕ is identical to

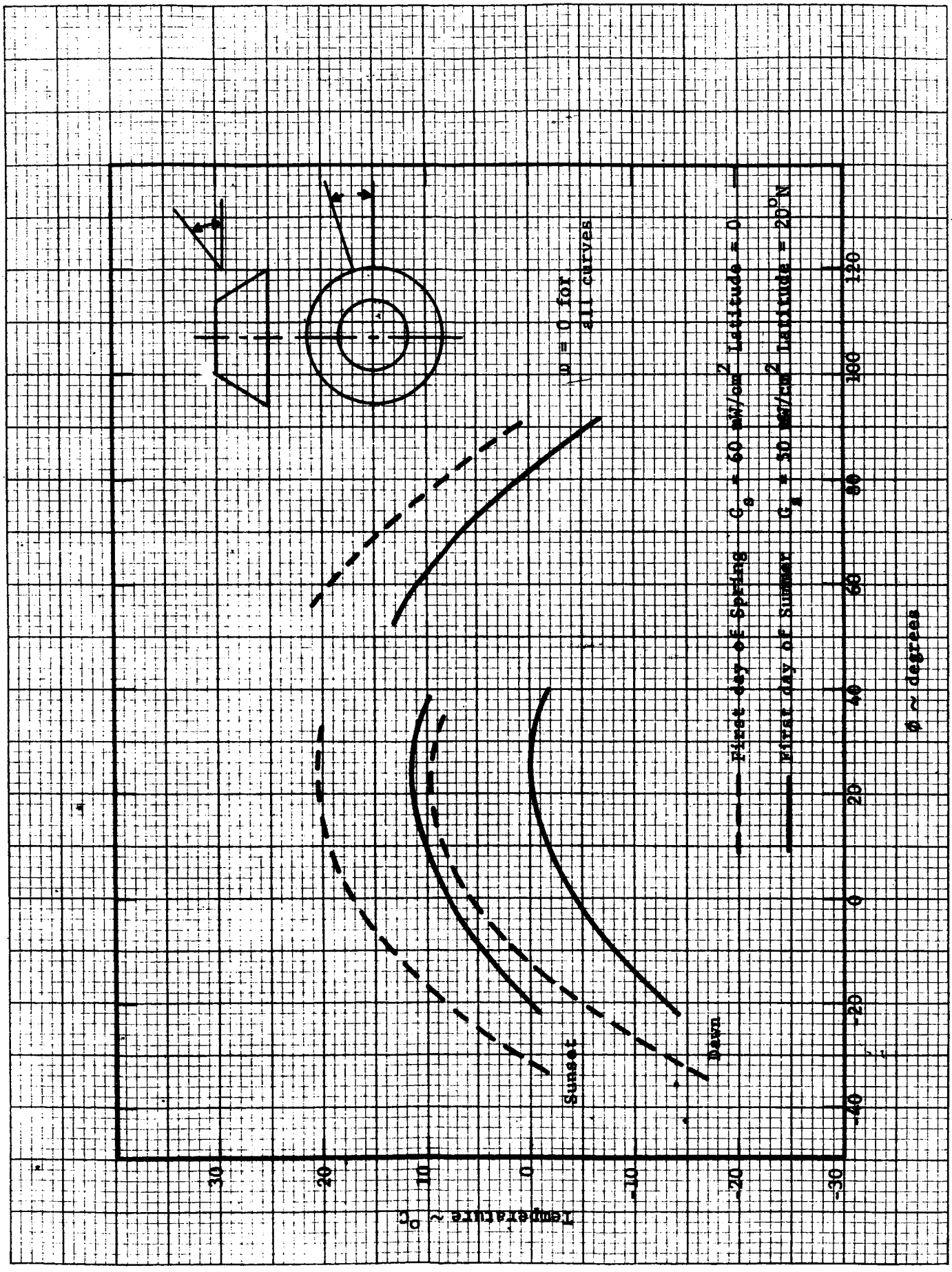

Figure 5-1. Maximum Panel Temperature versus Sun Angle

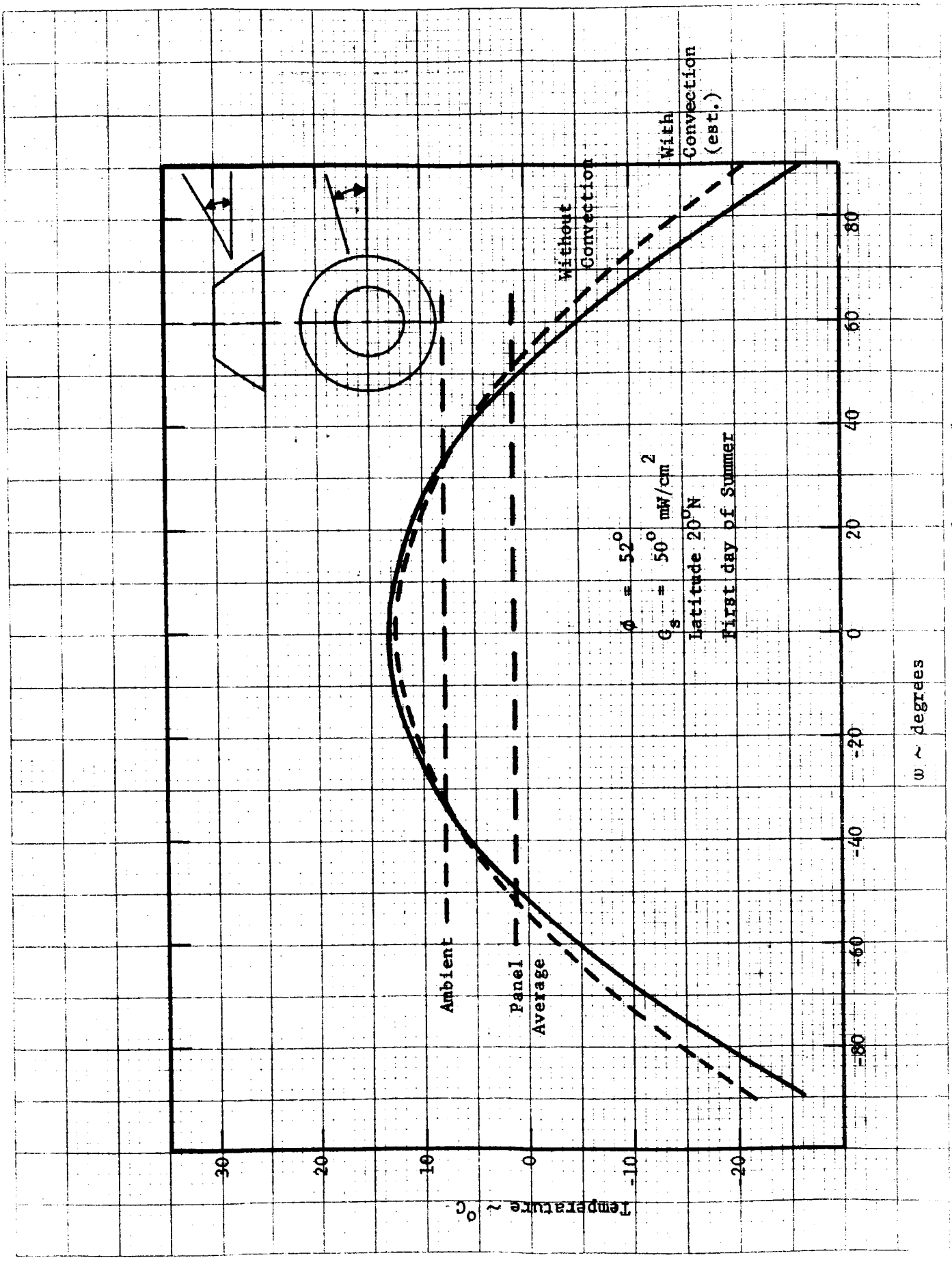

Figure 5-2. Panel Temperature Variation versus Horizontal Sun Angle

the angle ϕ of the geometrical analysis (see Appendix A) and the range of ϕ is taken from that analysis. The angle ω is defined as shown. The string at $\omega = o$ is the hottest string on the panel. The temperatures of these strings are shown in Figure 5-1 as a function of ϕ.

Two cases were considered: (1) The probable power minimum, which is a latitude of 20^{o} North and a heliocentric longitude of 180^{o} (first day of summer) this corresponds to the highest Martian surface temperatures likely to be encountered at the solar intensity minimum of 50 mW/cm^2. (2) The probable voltage minimum, which for this mission is a heliocentric longitude of 90^{o} (first day of spring) and a latitude of 0^{o} (equator). The corresponding solar intensity is 60 mW/cm^2.

Surface temperatures were estimated from Figure 12 of the Voyager Environmental Predictions Document reproduced here for reference as Figure 5-3. The temperatures are tabulated in Appendix B. The heat balance described in Appendix B of this report was reduced to a function of ϕ for sunrise, sunset, and noon for each of the two cases. View factors and surface property assumptions are discussed in Appendix B. Convection was assumed to be negligible to simplify the analysis. The effects of convection would be to flatten the curves by perhaps 5-10 percent of the total temperature range.

Variation around the power producing half of a panel at noon for the case $\phi = 52^{o}$, first day of summer (Gs = 50 mW/cm^2) are given in Figure 5-2. The dotted line represents an estimate of the warming effects of convection based on the results of earlier calculations. The average temperature for this curve is $1.3^{o}C$.

Average temperatures of the illuminated surface at noon as a function of sun angle are shown in Figure 5-4. The averages for the two lower cases are estimates.

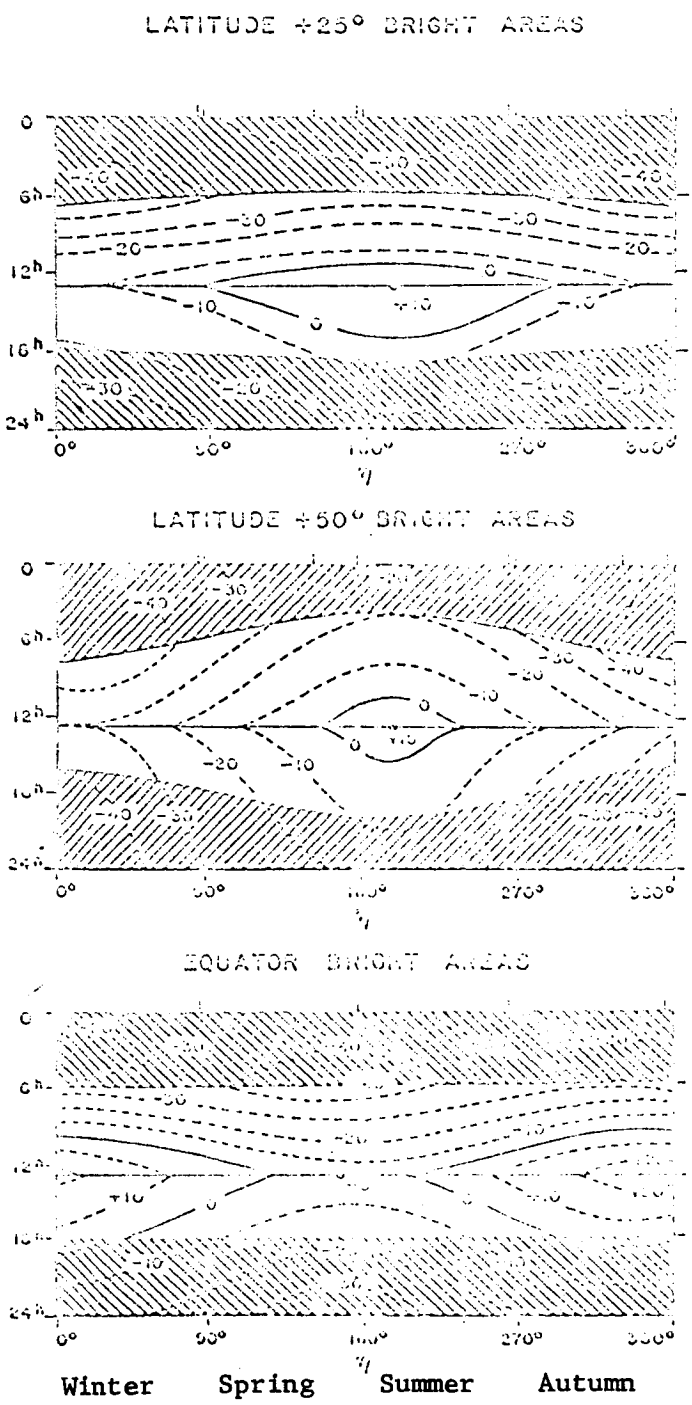

Figure 5-3. Mean Temperature of Bright Areas in ^{o}C for Several Latitudes as a Function of the Time of Day (Ordinate) and the Heliocentric Longitude, η (Abscissa)

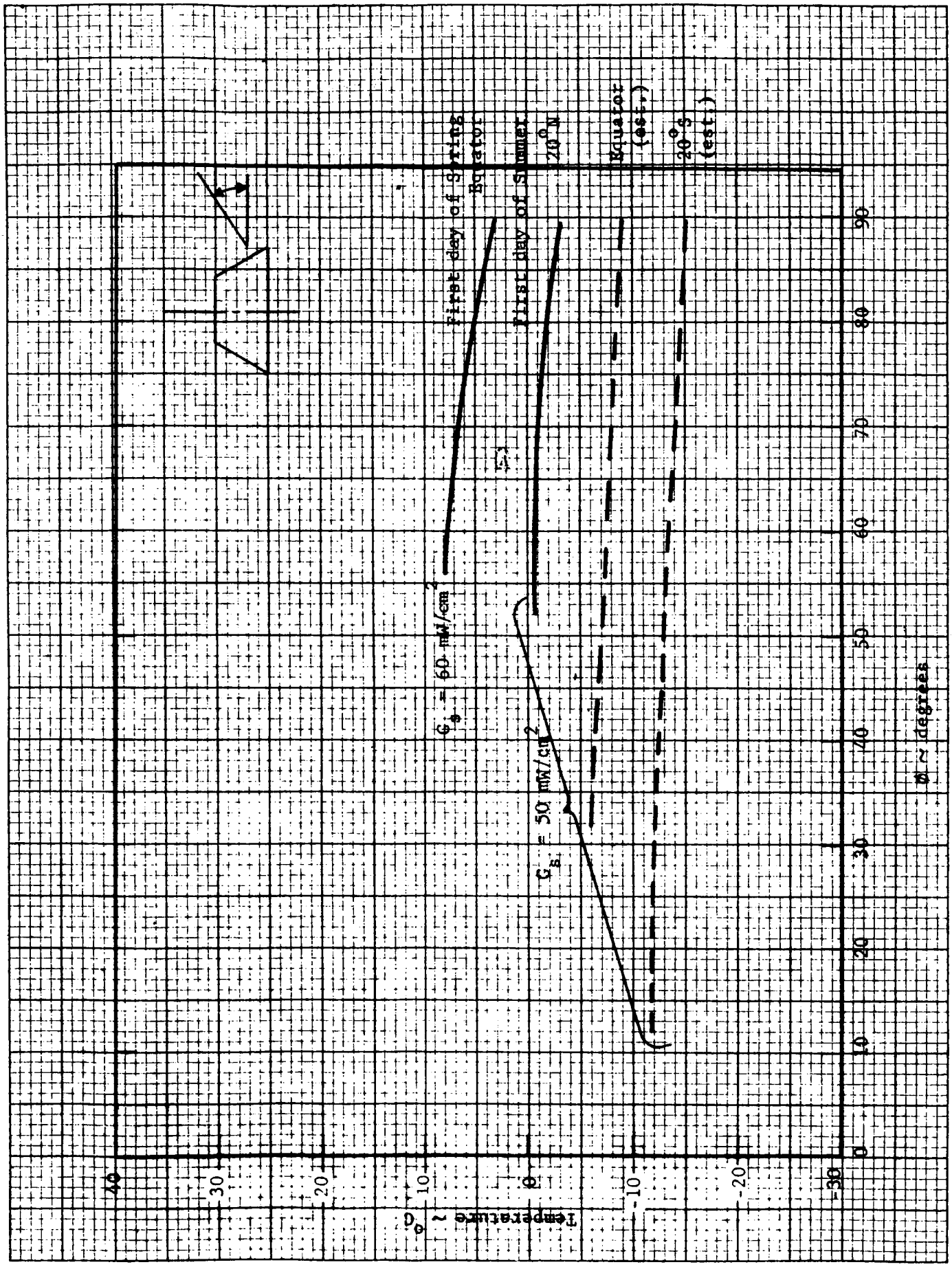

Figure 5-4. Average Temperature at Noon versus Sun Angle

These results show that the assumed average of 8°C was conservative for this panel configuration, and that shorter submodule strings can be used for fixed curved array compared to a flat oriented array.

5.4 WEIGHT ANALYSIS, NON TRACKING CONICAL ARRAY

The weight breakdown for the Planetary Array (truncated cone concept) is presented in Table 5-III.

5.5 RELIABILITY CONSIDERATIONS FOR THE NONTRACKING CONICAL ARRAY

The reliability considerations described in EOS Report 7254-Q-2 have been utilized in the following paragraphs to permit a preliminary evaluation of the "deployable nontracking array" electrical system reliability.

The electrical configuration, as shown in Fig. 5-5, has submodules consisting of six parallel cells each. A total of 57 submodules are connected in series to form one section and the overall array requires 90 sections to complete the electrical system. Electrical isolation of the cells from the load output is achieved by the use of parallel redundant diodes. A pair of diodes is connected in series with each of the 90 electrical sections.

5.5.1 RELIABILITY DEFINITION

The array electrical reliability is defined as the probability that the panel power output will meet the 200 watt minimum power output during the Martian summer season at a sun angle (ϕ) of 90° for a period of one Earth year as described in Section 3 of this report.

5.5.2 POWER CAPABILITY

From Section 2, the expected power output of the array, under the conditions stated in Subsection 1.2, will be 256 watts. Therefore, the allowable

TABLE 5-III

TRUNCATED CONE, PLANETARY ARRAY

WEIGHT SUMMARY

7254-Q-3

Item	Description	Weight/Unit Calculated	Weight/Unit Estimated	No. of Units	Total Weight Lb
I MECHANICAL					
A. Solar Panel					
1. Substrate	Aluminum Hollowcore-1.25 in. Holes 4 Mil skin	0.035 lb/ft^2		173.5 Ft^2	6.07
2. Beams	Beryllium - 2 in. Dia. 0.010 in wall	.05 lb/ft		103.7 Ft	5.19
3. Hinge Fittings	Titanium		.10 lb	8	.80
4. Attachment Clip	Aluminum Extrusion	0.012 lb/ft		111.6 Ft	1.34
5. Dielectric Film	Kapton H-Film 1 Mil	0.0072 lb/ft^2		173.5 Ft^2	1.25
B. Adhesives					
1. H-Film to Substrate	2 Mil Narmco 3135-18% area	0.0103 lb/ft^2		31.2 Ft^2	.322
2. Substrate to Clip	10 Mil	.04 lb/ft^2		2.12 Ft^2	.0848
3. Clip to Beam	10 Mil	.04 lb/ft^2		1.08 Ft^2	.0432
4. Beam to Fitting	10 Mil	.04 lb/ft^2		1.08 Ft^2	.0432
C. Substrate Support Brace					
1. Beams	Beryllium - 2 in. Dia. 0.010 in wall	.05 lb/ft		41.7 Ft	2.08

TABLE 5-III (Contd)

TRUNCATED CONE, PLANETARY ARRAY

WEIGHT SUMMARY

7254-Q-3

Item	Description	Weight/Unit Calculated	Weight/Unit Estimated	No. Of Units	Total Weight Lb
2. Bearings	Teflon Sleeve		2 Oz	8	1.00
D. Space Frame - Spacecraft Extension					
1. Beams	Beryllium - 2 in. Dia. 0.010 in wall	.05 Lb/Ft		28.3 Ft	2.91
2. Bearings	Thrust Bearing		2 Oz	8	1.00
3. S/C Attachment:					
a) Fittings	Titanium		2 Oz	8	1.00
b) Hardware	Nuts, Bolts, Etc.		.25 Lb	1	.25
E. Pivotal Deployment Mechanism					
1. Beams	Beryllium - 2 in. Dia. 0.010 in wall	.05 Lb/Ft		33.6 Ft	1.68
2. Torsion Springs			2 Oz	8	1.00
3. Dampers			2 Oz	4	.50

TABLE 5-III (Contd)

TRUNCATED CONE, PLANETARY ARRAY

WEIGHT SUMMARY

7254-Q-3

Item	Description	Weight/Unit Calculated	Weight/Unit Estimated	No. of Units	Total Weight Lb
F. Miscellaneous					
1. Latches	Stowed (8 Min.) Deployed (8 Min.)		2 Oz.	16	2.00
2. Rotating Drums	Titanium		.20 Lb	4	.80
3. Cable	1/4"	0.1 lb/ft		16.5 Ft	1.65
4. Tie - Wires			0.01121 $\frac{lb}{ft}$	184.0 Ft	2.06
II ELECTRICAL					
A. Solar Panel					
1. Solar Cell	10 Mil, 2x2 cm, n-p silicon	5.35×10^{-4} $\frac{lb}{cell}$		30,780 cells	16.380
2. Coverglass	Tedlar Film	5.0×10^{-5} $\frac{lb}{in^2}$		20,430 in^2	1.022
3. Interconnections		2.2×10^{-5} $\frac{lb}{unit}$		30,780 cells	.678
4. Terminals		7.7×10^{-4} $\frac{lb}{unit}$		180	.1388
5. Diodes	2/circuit	.0010 $\frac{lb}{unit}$		180	.180
6. Cabling	Raychem No. 44/0414-22-9 No. 22 AWG copper wire	.0029 $\frac{lb}{ft}$		80 Ft	.232

TABLE 5-III (Contd)

TRUNCATED CONE, PLANETARY ARRAY

WEIGHT SUMMARY

7254-Q-3

Item	Description	Weight/Unit Calculated	Weight/Unit Estimated	No. of Units	Total Weight Lb
B. Adhesives					
1. Solar Cells	4 Mil RTV 41	1.1×10^{-4} Lb/cell		30,780 cells	3.385
2. Coverglass	Dow Corning XR-63489	4.4×10^{-5} Lb/cell		30,780 cells	1.355
	Total Panel A = 173.5 $Ft.^2$				
	60^o Sector A = 28.9 $Ft.^2$				
				GRAND TOTAL	56.444 Lb

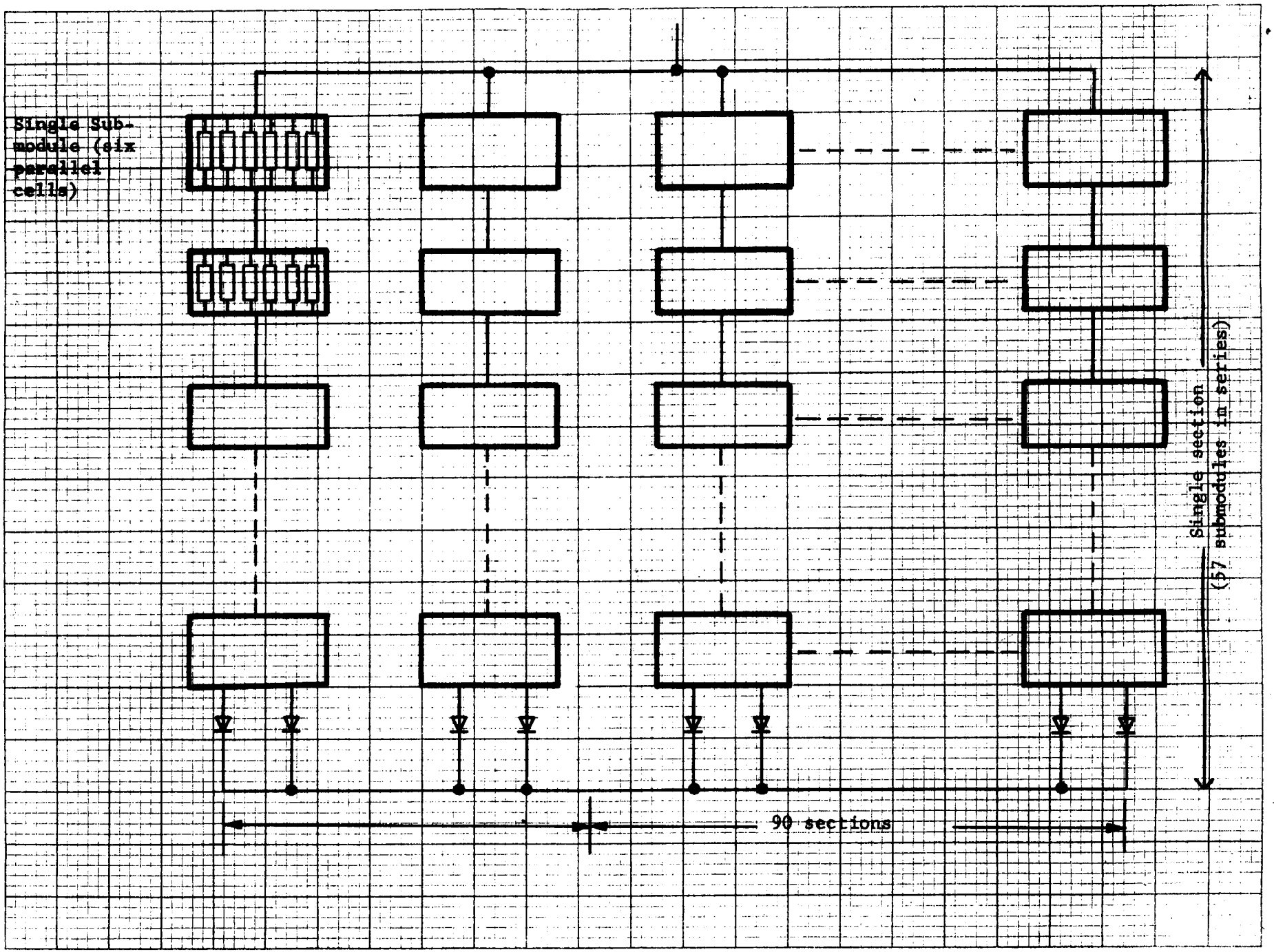

Figure 5-5. Electrical Configuration

power loss is 56 watts. The expected power output during the spring-fall season under the same operating conditions described above will be 299 watts, thus permitting a loss of 99 watts in array output. Since the summer season condition permits the least power loss, this environment will be used for the reliability calculations.

5.5.3 FAILURE MODE DISCUSSION

5.5.3.1 Diodes

The array will function with shorted diodes. Since parallel redundant units will be used in each section, and each diode is capable of handling a section load, the critical mode is the probability of more than one diode opening in each section during the mission.

5.5.3.2 Solar Cells

The critical mode for the cell array in terms of power loss is the open cell or cells due to current limiting in the section containing the open units.

Shorted cells have a smaller effect on the array power output than open cells. For the array under consideration, the loss (short) of one sub-module will result in a drop in array power output of 0.02 percent. Therefore, for the purpose of this analysis only, the effects due to open cells will be considered.

5.5.3.3 Failure Rates

The failure rates are:

Solar cell = $0.01/10^6$ hours

Diode = $0.02/10^6$ hours

The cell failure rate is based on the value used for the EOS 770 Program for a 2 x 2 cm cell. The diode failure is that used for the Surveyor solar panels built by EOS.

The operational mission time = 8760 hours.

5.5.3.4 Method of Analysis

The analysis is based on the maximum number of electrical sections that may be rendered inoperative and still permit the array to meet the minimum power requirements throughout the operating period.

5.5.4 CALCULATIONS

5.5.4.1 Logic Diagram

The electrical reliability of the array is expressed as the product of each of the panel functional elements used during the mission phase as shown below

$$R = R_D \times R_A$$

where:

R = Solar panel electrical reliability

R_D = Isolation diode reliability

R_A = Solar cell array reliability

5.5.4.2 Permissible Section Failures

- Maximum allowable power loss = 256 -200 = 56 watts
- Nominal section power = $\frac{256}{90}$ = 2.84 watts
- Allowable section failures = $\frac{56}{2.84}$ = 19 sections.

5.5.4.3 Diode Reliability

$$\text{Single diode } (R_C) = e^{-\lambda ct} = e^{-(.02 \times 10^{-6} \times 8760)} = R_C > 0.9998$$

$$\text{Redundant diodes } (R_{DS}) = 1 - (1 - R_D)^2$$

$$R_{DS} = 1 - (1-0.9998)^2 > 0.99999$$

5.5.4.4 Cell Section Reliability

Assuming worst case condition (no cell failures) the section reliability will be:

$$R_{SC} = e^{-n\lambda t} = e^{-(342 \times 0.01 \times 10^{-6} \times 8760)}$$

$$R_{SC} = 0.97044$$

5.5.4.5 Total Section Reliability (R_S)

$$R_S = R_{SC} \times R_{DS} = 0.97044 \times 0.99999$$

$$R_S = .97043$$

5.5.4.6 Total Array Reliability (R_A)

Array reliability is defined as the probability that no more than 19 of the 90 sections fail during the mission time. This value is determined by expansion of the first 20 terms of the binomial distribution.

$$R_A = R_S^{(M)} + MR_S^{(M-1)} q_S + \frac{M(M-1) \quad (M-18)}{19!} \times R_X^{(M-19)} q^{19}$$

$$R_A = (.97043)^{(90)} + 90\,(.97043)^{(89)}\,(.02957) + \frac{90(89) \quad (72)}{19!}\,(.97043)^{(71)}\,(.02957)^{(19)}$$

$$\therefore \quad R_A > 0.999999$$

5.5.5 CONCLUSIONS

The probability of the array meeting the minimum power requirements under the conditions imposed in the analysis is virtually unity.

SECTION 6

PRELIMINARY MANUFACTURING PLAN

EOS has been responsible for the fabrication and test of several types of solar cell panels for space use and terrestrial applications. Of particular importance to the proposed JPL/SPA program are the proven fabrication techniques and the extremely high quality workmanship used on solar panels presently being fabricated at EOS. This section briefly describes the preliminary flow plan for panel manufacture, describes several of the more significant process steps, and discusses controls to be exercised in EOS production. All processes and inspection steps will be generated and identified during the Phase 2 portion of the proposed contract.

Design features of the assembly have been discussed in Section 3.

6.1 FACILITIES

6.1.1 LOCATION

The hollow core will be produced and the substrates assembled at our Pomona facility. The production area for solar cell application to the panels is located at the 250 North Halstead Street, Pasadena, California, facility of EOS.

The entire solar panel manufacturing area will be air conditioned in a closed and limited access area. The area would have general-purpose lighting of a minimum of 100 foot candles which is further supplemented by special purpose lighting when needed. The SPA area will be separated from all other programs.

Program management and engineering functions will be located in a "project" area in the Pasadena facility. Other specialized facilities for all aspects of the program will be installed as required.

6.1.2 WHITEROOM FACILITIES

All of the assembly areas used on the proposed program will be whiterooms featuring:

a. Use of hats and coats which are lint-free.

b. Regular particle counts to verify dust requirements.

c. Controlled temperature of 72^{o} (±10)F.

d. Controlled humidity of 30 to 70%.

e. Construction features which enhance cleanliness.

f. Assembly benches located in such a way as to prevent traffic hazards to the panels being assembled.

g. Adequate lighting. At least 100 ft-candles at the level of assembly where required.

h. Adequate electrical outlets, water, and other utilities as required.

i. Specially designed hoods and vents to enable rapid elimination of fumes from cleaning agents.

6.1.3 STORAGE AREAS

Bonded store areas will be provided for all materials and assemblies. Stores will be provided in two general areas:

a. The first storeroom will feature less than 20% humidity and controlled temperature between 60 and 70^{o}F. The low-humidity storage area will contain solar cells and completed solar panel assemblies. The low-humidity storage area will be used to insure that solar cells are not exposed to long-term humidity conditions.

b. The second storage area, also a bonded area, will remain at the same atmospheric conditions as the assembly and test areas and will be used for storage of all other program components.

6.1.4 RESIDENT OFFICES

Ample office space and furniture will be provided to JPL residents in the 250 North Halstead Building, within the "project" area.

It is understood that monitoring of the program will be accomplished by JPL personnel. JPL personnel are welcome to witness any part of the operation at any time, without prior notice. Non-escort badge privileges will be extended to all resident personnel.

6.2 MANUFACTURING FLOW PLAN

The elements of the SPA solar panel assembly, inspection, and test, are shown in the manufacturing flow plan depicted in Fig. 6-1. A brief description of many of the operations will be given in the following subsections. A major innovation to accommodate the Mars environment will be the substitution of a transparent envelope covering the entire panel in place of individual coverglasses. Apart from this, the manufacturing plan for the SPA solar panels will be essentially identical to that used by EOS on other solar panel programs.

6.2.1 INCOMING CELL TEST AND MATCHING

Solar cells will be 100% physically and electrically tested and inspected prior to the receipt of the cells at EOS. Certification will be obtained for these tests and delivered with the cells. Sample tests include thermal shock, temperature cycling, contact strength and adherence, silicon strength, etc. Complete manufacturing, reliability, and quality control plans to be used by the selected solar cell vendor will be transmitted to JPL for approval within one week after program initiation.

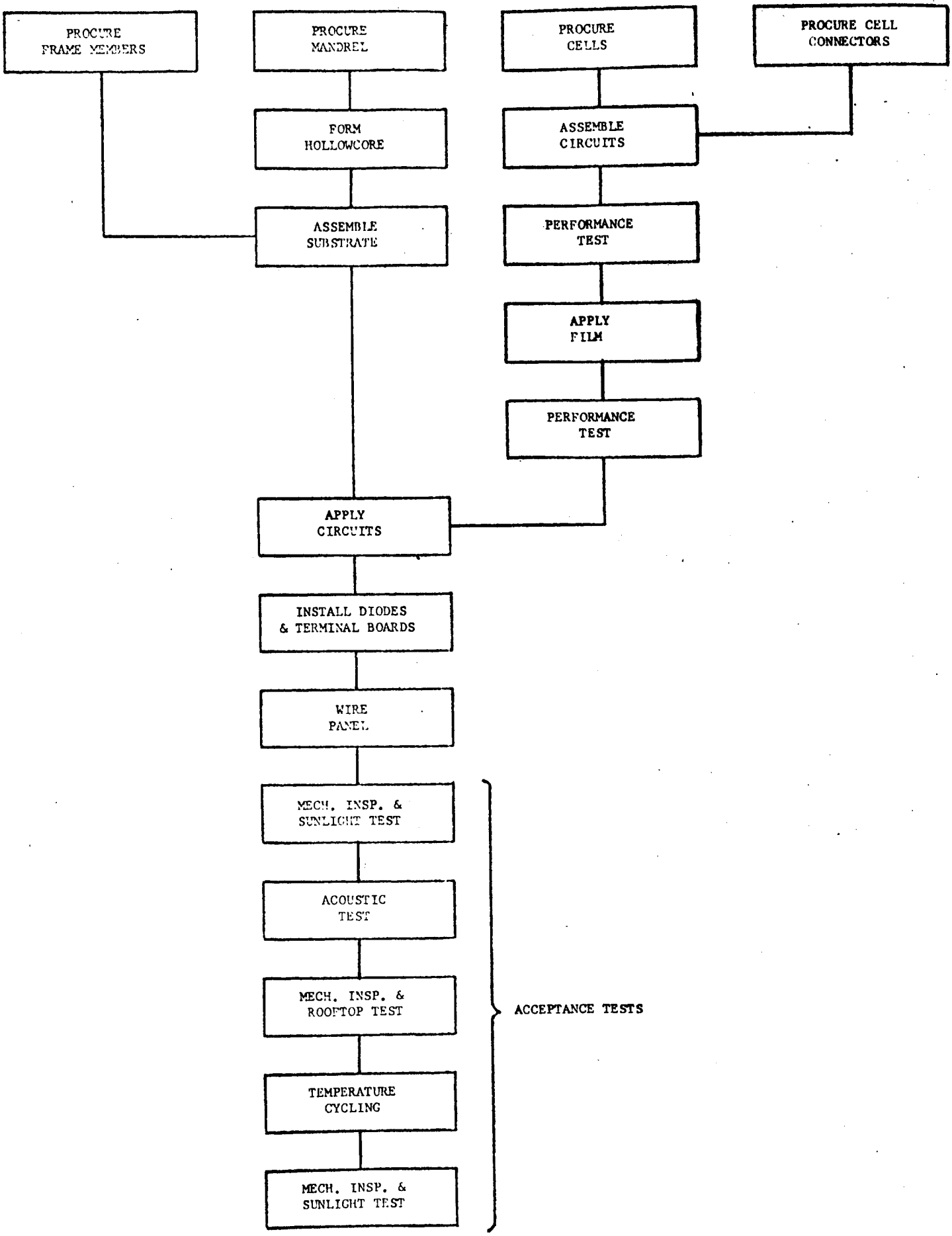

Figure 6-1. Manufacturing Flow Plan

The solar cells received from the lower tier subcontractors which have already been 100% mechanically and electrically inspected will receive a sample incoming physical and electrical inspection by the EOS quality control group. These cells will be visually inspected on a sample basis for chips, scratches, gridline continuity, physical dimensions, and other special items.

Throughout inspection and all subsequent operations, the submodules will be handled with gloves or fingercots, and in specially designed holding fixtures. Each submodule is connected by means of a flexible bus bar. Material for the bus bar consists of 2-mil molybdenum plated with a gold flash and then silver-plated per QQ-S-365A.

In the process of cell electrical testing, the cells are categorized, based on current output at a specified voltage. The cells are then matched to meet the parallel connection current requirements of the solar panel. The matching will enable good control of the panel output.

6.2.2 SUBMODULE FABRICATION

Matched solar cells per 6-cell submodules are mounted in a fixture for assembly to the cell connector strip. Solder flow and cell connector strip attachment is accomplished by controlled resistance soldering, a technique presently being utilized by EOS. This type of soldering is especially significant in minimizing cell degradation. EOS proposes to use the resistance soldering technique on the JPL/SPA program.

A 100% inspection of each solder connection will be performed.

6.2.3 MODULE SERIES STRINGS

The submodules will be assembled into series strings consisting of 57 submodules each. The metal tabs projecting from the positive surface of each submodule will be soldered to the ohmic strip, or negative

terminal, of the next adjacent submodule, two tabs per cell, or to the positive end termination bus at the positive end of the series string. Appropriate tooling and fixtures will be provided for these operations.

Specific criteria for inspection of tabs have been established and are currently used. It is also the practice of EOS to make a number of sample connections to provide specific examples. A prototype panel will be used for this purpose.

6.2.4 SUBSTRATE FABRICATION

Facilities for plating and etching hollow core are installed at our Pomona facility. Substrates will be assembled and dielectric applied there.

An electroformed, conical substrate will be used with a suitable framework support as a basic structural concept. Analysis and experiment have shown that aluminum electroformed substrates and beryllium frames can be used. Electroforming is used as a means of attaining a rigid thin-skinned method structure with the large open areas necessary to a high strength-to-weight ratio. EOS is now engaged in a program for development of large hardened aluminum (magnesium/aluminum) hollowcore substrates for NASA.

6.2.5 HANDLING PROCEDURES

During all assembly operations, the panel shall remain in a handling frame (with the exception of the weighing operation of the solar panel). When not in use, the solar panel is covered with a dust cover. When a solar panel is to be moved from one location to the next, it can be moved only by authorized personnel instructed in its handling. A solar panel dolly will also be available that accepts the handling frame.

This is used for certain assembly operations when the panel is moved from one room to the next. Process specification for handling and transportation requirements of the solar panel are presently in use describing the procedures and precautions necessary for moving solar panels.

6.2.6 MODULE BONDING TO SUBSTRATE

RTV adhesive will be used to bond the modules to the substrate. Tooling will be developed to insure proper thicknesses of adhesive and accurate placement of modules, and to provide required bonding pressure during cure.

6.3 MATERIAL STATUS CONTROL

Material status control shall perform the following functions for the JPL/SPA program:

a. Establish bill of materials list.

b. Establish critical parts list.

c. Establish minimum material levels predicted on lead times.

d. Prepare and maintain a status report depicting quantity levels of both direct and indirect materials. This status report will be updated weekly and distributed to the cognizant people concerned with the SPA program. This report includes the following:

   (1) Purchase request number

   (2) Purchase order number

   (3) Vendor

   (4) Description of item

   (5) Quantity ordered

   (6) Date ordered

   (7) Date due

   (8) Date received

(9) Unit cost

(10) Total cost

(11) Date required for program

All incoming material will be expedited through Receiving and Receiving Inspection and transferred directly to a bonded stockroom. No material will be accepted without proper paperwork; this includes certifications, inspections tags, etc. Once the material is accepted, it will be logged in and placed in the appropriate storage area, e.g., bins, shelves, cabinets, or special storage containments if necessary. The logging in and out of materials shall be recorded in a Kardex system. This system is presently used at EOS for solar panel programs and includes the following:

e. EOS Form No. 311 contains information pertaining to:

(1) Purchase request number

(2) Purchase order number

(3) Vendor

(4) Description of item

(5) Quantity ordered

(6) Date ordered

(7) Date received

(8) Unit cost

(9) WA number

(10) Serial number if applicable

f. EOS Form No. 298 contains information pertaining to:

(1) Date received

(2) Quantity received

(3) Balance on hand

g. When parts are issued the following is recorded:

(1) Quantity issued

(2) Balance left in stock

(3) Person parts issued to

(4) WA number

Records on Card No. 311 will be maintained from material status report until all purchase orders are placed, and as GFE parts are received in plant.

Records on Card No. 298 will be maintained on receipt of parts from Receiving Inspection.

All parts issued from the stockroom initially on a WA number will be recorded on Card No. 298, quantities, etc.

Replacement of any part damaged in fabrication or for any reason, requires a material requisition (EOS Form No. 7450) to be made out and signed by authorized person for the replacement part. This information will be noted on Card No. 298.

A shortage list will be originated and maintained from information furnished by material control with respect to parts returned by fabrication for replacement, and from delivery dates as reported from vendors. This list will be distributed as often as necessary. All items with delivery dates later than program required dates will be listed. Any materials rejected or scrapped shall be placed in special storage cabinets until resolution is made to disposition.

6.4 DOCUMENT PREPARATION AND ITS USE

One of the keys to fabricating solar panels successfully and consistently is the use of detailed plans and procedures to instruct and guide all cognizant personnel in the fabrication, assembly, inspection and in-process testing of the solar panels. One of the most important documents used in manufacturing hardware is the manufacturing flow plan. The flow plan provides the detailed step-for-step sequence of events to be followed by the assembly and inspection personnel during the fabrication operation. It refers to each applicable process specification, inspection instruction and drawing for each step.

A detailed flow plan for the SPA fabrication will be prepared as a part of the Phase II program.

Based on the flow plan, process specifications are prepared which list applicable documents, direct and indirect materials, detailed assembly procedures and instructions, cautions and data recording requirements for each assembly step.

Inspection instructions for each inspection step will be prepared for the SPA program. These instructions will be consistent with the manufacturing and inspection flow diagram and will cover all receiving, in-process and final inspection activities.

Prior to the start of fabrication of each panel, a manufacturing order (MO) is prepared that lists in sequence the step-for-step operations to be performed by the assemblers and inspectors. This document follows the sequence of the flow plan and is used to record the date each operation is completed, the assemblers who performed each task and the inspection (both EOS and JPL evidence of satisfactory completion).

Visual aids will be prepared to assist assemblers and inspectors in performing their task. These will be used to supplement the process specifications and inspection instructions where appropriate. Production charts will be prepared to indicate the status of fabrication, projected fabrication schedule versus actual fabrication output.

For example, detail charts on submodule fabrication will be maintained which indicate the fabrication rates, number of defects, types of defects, etc. This information is used to determine adherence to schedule and to provide corrective actions necessary (both schedule and technical). This data is reviewed on a weekly basis during the program meeting.

Items that are reworkable at the manufacturer's option will be identified during the program. For each item of rework, a rework MO is prepared which again includes a detail step-by-step procedure with the appropriate inspection buyoffs. Certain items will be identified as reworkable only by direction from the cognizant engineer. Further items will require MRB action prior to rework authorization. Process specifications are used for certain critical rework items such as repair of insulation sheet, replacement of solar cells, etc.

SECTION 7

PRELIMINARY TEST PLAN

7.1 INTRODUCTION

This section describes the test program proposed for qualifying the JPL/SPA for the environments of sterilization, storage and transportation, launch, flight, Mars landing, and one Earth year on the Martian surface. Included are tests of components where they represent substantial innovations and tests to be performed during fabrication to determine acceptability of subassemblies. Additional tests not listed will be performed as required to qualify materials and manufacturing techniques.

We have developed a large body of special techniques for the testing of solar panels, many of which will have direct application to the JPL/SPA program.

7.1.1 DEFINITIONS

Substrate (or "substrate segment"): Any one of the three cell-support structures which compose each half of the cell array, without cells, or with dummy cells.

Panel (or "solar panel" or "solar panel segment"): Any one of the substrate segments with all circuits applied and wired - a functioning unit.

Substrate Assembly: The assembly of three mating substrate segments which composes one-half of the cell array (without cells or with dummy cells.)

Panel Assembly: The assembly of three mating solar panels with wiring which composes a functioning half of the cell array.

Flight Stowage and Deployment Linkage: One of two support structures required in each solar planetary array. These are identical structures, one of which supports each panel assembly during launch, flight, and landing in a stowed position and deploys and supports it in operating position after landing.

Array (or "solar array", or "solar planetary array"): The complete power system including panel assemblies and flight stowage and deployment linkages. (At one stage of testing, one-half of the cell array will be composed of substrate segments with dummy cells).

Cell Array: The full complement of six solar panels or substrates (the two "assemblies") distinguished from the flight stowage and deployment linkages.

7.2 SOLAR ARRAY TESTS

A summary of the test programs for sample modules, substrates, panels, deployment linkages, and the array are provided in Table 7-1.

7.2.1 DEVELOPMENT ENGINEERING TEST EVALUATION

The items to be used for these tests shall be at least 4 sample modules (6 cells parallel by 6 cells series), 1 each of 2 typical substrate segments with dummy cells (left, and center), 1 each of 2 typical solar panel segments (flight capable units), and one set (2 units) of flight stowage and deployment linkages.

Performance and environmental testing shall be accomplished to establish advance confidence in fabrication techniques, testing, and environmental requirements prior to conducting formal qualification tests. Performance and environmental test data shall be recorded and maintained. Table 7-II shows the testing sequence for each test.

TABLE 7-I

Test Program Summary

Table	Item	Quantity	Test
7-II-A	Sample Module	4	Engineering evaluation
7-II-B	Prototype substrate segment	2 (1 ea. of left and center segments)	Engineering and test evaluation
7-II-C	Prototype substrate assembly with flight stowage and deployment linkage.	1	Engineering and test evaluation
7-II-D	Prototype solar panel	2 (1 ea. of left and center segments)	Engineering and test evaluation
7-II-E	Prototype solar array	1	Engineering and test evaluation
7-III	Qualification solar panel	1	Formal Acceptance Tests
7-IV	Qualification solar panel	1	Formal Qualification Tests
7-V	Qualification solar panel	1	Formal Reliability Tests
(7-III)	Flight solar panels	12 (4 ea. of left, right, and center segments)	Acceptance Tests

TABLE 7-II-A

Engineering Evaluation Test Sequence

Item: Sample Module

Quantity: Four

1. Mechanical inspection
2. Simulator test
3. Application of cover film
4. Mechanical inspection
5. Simulator test
6. Sterilization
7. Mechanical inspection
8. Simulator test
9. Rapid decompression
10. Mechanical inspection
11. Simulator test
12. Mars environment
    - 7 millibars pressure
    - 270 mph wind
    - 1 to 100μ abrasive, conductive dust
13. Mechanical inspection
14. Simulator test
15. Accelerated weathering
16. Mechanical test
17. Simulator test

TABLE 7-II-B

Engineering and Test Evaluation Sequence

Item: Substrate, left segment, with dummy cells

Quantity: One

1. Mechanical inspection
2. Vibration (Sinusoidal)
3. Mechanical inspection
4. Vibration (random)
5. Mechanical inspection
6. Sterilization
7. Mechanical inspection
8. Rapid decompression
9. Mechanical inspection
10. Temperature cycling
11. Mechanical inspection

Repeat this sequence with center segment with dummy cells.

TABLE 7-II-C

ENGINEERING AND TEST EVALUATION SEQUENCE

Item: Substrate assembly with deployment linkage

Quantity: One

1. Mechanical inspection
2. Deployment - horizontal
3. Mechanical inspection
4. Deployment 34^{o} upward
5. Mechanical inspection
6. Deployment 34^{o} downward
7. Mechanical inspection
8. Deployment 34^{o} oblique
9. Mechanical inspection

10 through 15. Repeat steps 4 through 9 in a 23 mph wind (1 atmosphere pressure).

16 through 21. Repeat steps 10 through 15 with wind from another direction.

22 through 27. Repeat steps 10 through 15 with wind from a third direction.

TABLE 7-II-D

ENGINEERING AND TEST EVALUATION SEQUENCE

Item: Solar Panel, left segment

Quantity: One

1. Mechanical inspection
2. Sunlight test
3. Sterilization
4. Mechanical inspection
5. Sunlight test
6. Vibration, transverse axis (sinusoidal and random)
7. Mechanical inspection
8. Rooftop test
9. Vibration, lateral axis (sinusoidal and random)
10. Mechanical inspection
11. Vibration, vertical axis (sinusoidal and random)
12. Mechanical inspection
13. Rooftop test
14. Shock (general) ±transverse axis
15. Mechanical inspection
16. Shock (general) ±lateral axis
17. Mechanical inspection
18. Shock (general) ±vertical axis
19. Mechanical inspection
20. Rooftop test
21. Accoustics test
22. Mechanical inspection
23. Rooftop test
24. Temperature/vacuum

TABLE 7-II-D

ENGINEERING AND TEST EVALUATION SEQUENCE (contd)

25. Mechanical inspection
26. Rooftop test
27. Temperature/cycle
28. Mechanical inspection
29. Rooftop test
30. Rapid decompression
31. Mechanical inspection
32. Sunlight test

Repeat test sequence 7-II-D with center panel segment.

TABLE 7-II-E

ENGINEERING AND TEST EVALUATION SEQUENCE

Item: Solar Array

a. One substrate assembly (with dummy cells)

b. One panel assembly

c. Two flight stowage and deployment linkages

Quantity: One

1. Mechanical inspection
2. Rooftop test
3. Vibration - transverse axis (sinusoidal and random)
4. Mechanical inspection
5. Vibration - lateral axis (sinusoidal and random)
6. Mechanical inspection
7. Vibration - vertical axis (sinusoidal and random)
8. Mechanical inspection
9. Rooftop test
10. Shock (general) ±transverse axis
11. Mechanical inspection
12. Shock (general) ±lateral axis
13. Mechanical inspection
14. Shock (general) ±vertical axis
15. Mechanical inspection
16. Rooftop test
17. Disassembly
18. Mechanical inspection
19. Sunlight test

7.2.2 ACCEPTANCE TEST

The electrical and environmental test data shall be recorded and maintained. All sunlight and rooftop tests include diode reverse leakage and insulation resistance tests.

EOS will perform the acceptance tests in the sequence shown in Table 7-III. The acceptance test will be performed on the qualification solar panel segment and on each panel segment of all flight units.

7.2.3 QUALIFICATION TEST

To be performed on one solar panel segment which shall have been used previously in Acceptance Tests (7.2.2)

All individual tests shall lbe performed without any adjustments and/or repairs being accomplished during such tests. In the event of a test failure, EOS will stop all further testing and shall not proceed before notifying JPL. All data taken during electrical and environmental testing shall be recorded and maintained.

Prior to any qualification testing, the solar panel segment shall have satisfactorily passed the electrical and environmental requirements of acceptance testing.

Table 7-IV shows the qualification test sequence.

TABLE 7-III

ACCEPTANCE TEST SEQUENCE

To be performed on one solar panel segment not previously tested.

1. Sunlight test
2. Acoustic test
3. Mechanical inspection
4. Rooftop test
5. Temperature cycling
6. Mechanical inspection
7. Sunlight test

TABLE 7-IV

QUALIFICATION TEST SEQUENCE

To be performed on one solar panel segment (used in Acceptance Test sequence above).

1. Sunlight test
2. Relative humidity
3. Mechanical inspection
4. Rooftop test
5. Sterilization
6. Mechanical inspection
7. Sunlight test
8. Vibration - transverse axis (sinusoidal and random)
9. Mechanical inspection
10. Vibration - lateral axis (sinusoidal and random)
11. Mechanical inspection
12. Vibration - longitudinal axis (sinusoidal and random)
13. Mechanical inspection
14. Rooftop test
15. Shock ±transverse axis
16. Mechanical inspection
17. Shock ±lateral axis
18. Mechanical inspection
19. Shock ±longitudinal axis
20. Mechanical inspection
21. Rooftop test
22. Acoustic
23. Mechanical inspection
24. Rooftop test
25. Temperature vacuum

TABLE 7-IV

QUALIFICATION TEST SEQUENCE (contd)

26. Mechanical inspection
27. Rooftop test
28. Temperature cycling
29. Mechanical inspection
30. Rooftop test
31. Rapid decompression
32. Mechanical inspection
33. Sunlight test

7.2.4 RELIABILITY TEST

EOS will perform the reliability test using the panel segment previously used during qualification testing.

The panel segment shall be subjected to a total of 30 days of environmental conditions. Every 120 hours the unit shall be removed from its environment and rooftop tested.

Table 7-V shows the test sequence for the reliability tests.

NOTE

If wind-tunnel test of deployed array shows substantial vibration or oscillation, a reliability test may be required to evaluate this parameter.

7.2.5 SHIPPING CONTAINER TEST

The test shall consist of three drops from an elevation of 12 inches. The container shall be dropped once in each plane as follows:

a. Flat
b. Edgewise (long edge)
c. Edgewise (short edge)

The object of these tests is to determine that no physical damage occurs to the SPAs which may be in the container. All data shall be recorded and maintained.

TABLE 7-V

RELIABILITY TEST SEQUENCE

To be performed on one solar panel segment (used in Qualification Test sequence above).

1. Sunlight test
2. Temperature cycle (5 days)
3. Rooftop test
4. Temperature cycle (same as 2.)
5. Rooftop test (same as 3.)
6. Temperature cycle (same as 2.)
7. Rooftop test (same as 3.)
8. Temperature cycle (same as 2.)
9. Rooftop test (same as 3.)
10. Temperature cycle (same as 2.)
11. Rooftop test (same as 3.)
12. Temperature cycle (same as 2.)
13. Sunlight test (same as 1.)

7.3 TEST EQUIPMENT AND FIXTURES

EOS has maintained the latest in test equipment to record and resolve data within the parameters of present day requirements.

Three basic means of data acquisition for performance testing of solar devices are employed: digital voltmeters, digital printers, and X-Y recorders. Sun simulators are used to illuminate some of the solar devices; these will be discussed later.

The latest in test equipment is employed for environmental requirements. Digital voltmeters, temperature recorders, and electronic control equipment are a few of those utilized for controlling, resolving, and recording data and/or functions. Presently being used are environmental chambers capable of reaching pressures of 1×10^{-6} torr and simulating space environment conditions of solar panel testing.

Fixtures for vibration and shock, acoustic, temperature cycling, humidity tests, and altitude temperature tests will be specially designed.

7.4 PERFORMANCE TESTING (Sunlight, Rooftop, and Solar Simulator)

EOS will make performance tests for the purpose of acceptance during fabrication levels and final acceptance. The following paragraphs discuss the individual tests in greater detail.

7.4.1 SINGLE CELL TESTING

Individual cell measurements will be made under a tungsten iodine light source, calibrated to an intensity of 46 mW/cm^2 (AM1 Mars). A standard cell, typical in spectral response to cells being fabricated into SPAs, shall be calibrated against a JPL balloon flown standard.

7.4.2 SUBMODULE TESTING

The submodule testing is performed under the same tungsten iodine simulator discussed in Subsection 7.4.1.

The submodules are tested for I_{sc} (short circuit current) and the current at 485 mV. These tests are performed while the submodule is at a temperature of $77^{\circ} \pm 2^{\circ}F$. Calibration of the submodule area (2 cm x 7 cm) will be performed with a standard cell and set for an intensity of 46 mW/cm^2. Area uniformity will be held to within ±1% or less.

The test fixture has the standard 4-point probe electrical contact system, and also employs a vacuum system to aid in securing the submodule to the base.

7.4.3 SAMPLE MODULE TESTING

The 6 x 6 cell sample module used in the test sequence of Table 7-II-A will be tested under a xenon solar simulator.

7.4.4 PANEL TESTING

EOS will test the SPAs in sunlight. An I-V curve will be produced for each circuit on the panel.

"Sunlight" tests will be performed at Table Mountain, California. "Rooftop" tests will be performed at the Pasadena facility.

The I-V plots will be drawn with an X-Y recorder and points (I_{sc}, I at the V_{oc}) will be checked against a digital voltmeter. Data acquired during testing (temperature, intensity, panel electrical outputs, date, time, etc.) will be properly recorded and maintained.

Sunlight performance tests are performed when the following conditions exist:

- Sky radiation — 10 percent or less
- Sun intensity — approximately 100 mW/cm^2

Data obtained during testing of solar panels is extrapolated from AM1 Earth (100 mW/cm^2) to AM1 Mars (46 mW/cm^2).

Tests will be performed to determine the characteristic temperature response of the cells and that data will be used to derive panel temperature from open circuit voltage.

I_{sc} corrections must be made to correct for sun intensity losses through the earth's atmosphere. An equation for I_{sc} correction is as follows:

$$I_{scp_1} = I_{scp_2} \times \frac{I_{scuc}}{I_{scn}}$$

Where: I_{scp_1} = the corrected short circuit current for a circuit

I_{scp_2} = the recorded short circuit current for a circuit during testing

I_{scuc} = the standard cell, uncollimated, short circuit current reading during testing

I_{scn} = the calibrated AM0 short circuit current for the standard cell

SECTION 8

SUMMARY

This report finalizes the detailed analysis and demonstrates the feasibility of the first of three array concepts of a planetary photovoltaic solar array for operation on the Martian surface.

The system presented here is a nontracking, deployed, truncated conical array meeting all the packaging constraints imposed on the design by JPL in their drawing No. 1002-3236A. The basis of this concept was to present to JPL a system which was optimized for the best compromise in power versus weight, but without the encumberance of complicated orientating or tracking mechanisms. This system, once released from its locked, launched and flight position will require no power from the lander system for deployment or continuous operation for the mission life of one year.

This system, as recognized initially in its conception, will not meet the desired goal of 20 W/lb (1AU) and under worst case conditions be under the minimum power requirements of 200W of electrical power at solar noon. Figures 8-1 and 8-2 show that in the large majority of the cases the power output exceeds the minimum requirement of 200W. The worst case minimum power is 5 percent low at 190W. The best case condition is 35 percent high at 256W. The average noon power outputs of the limiting conditions shown is 17 percent high at 223W.

At the higher solar intensities occurring at spring and fall seasons the power level is above 200W for all conditions.

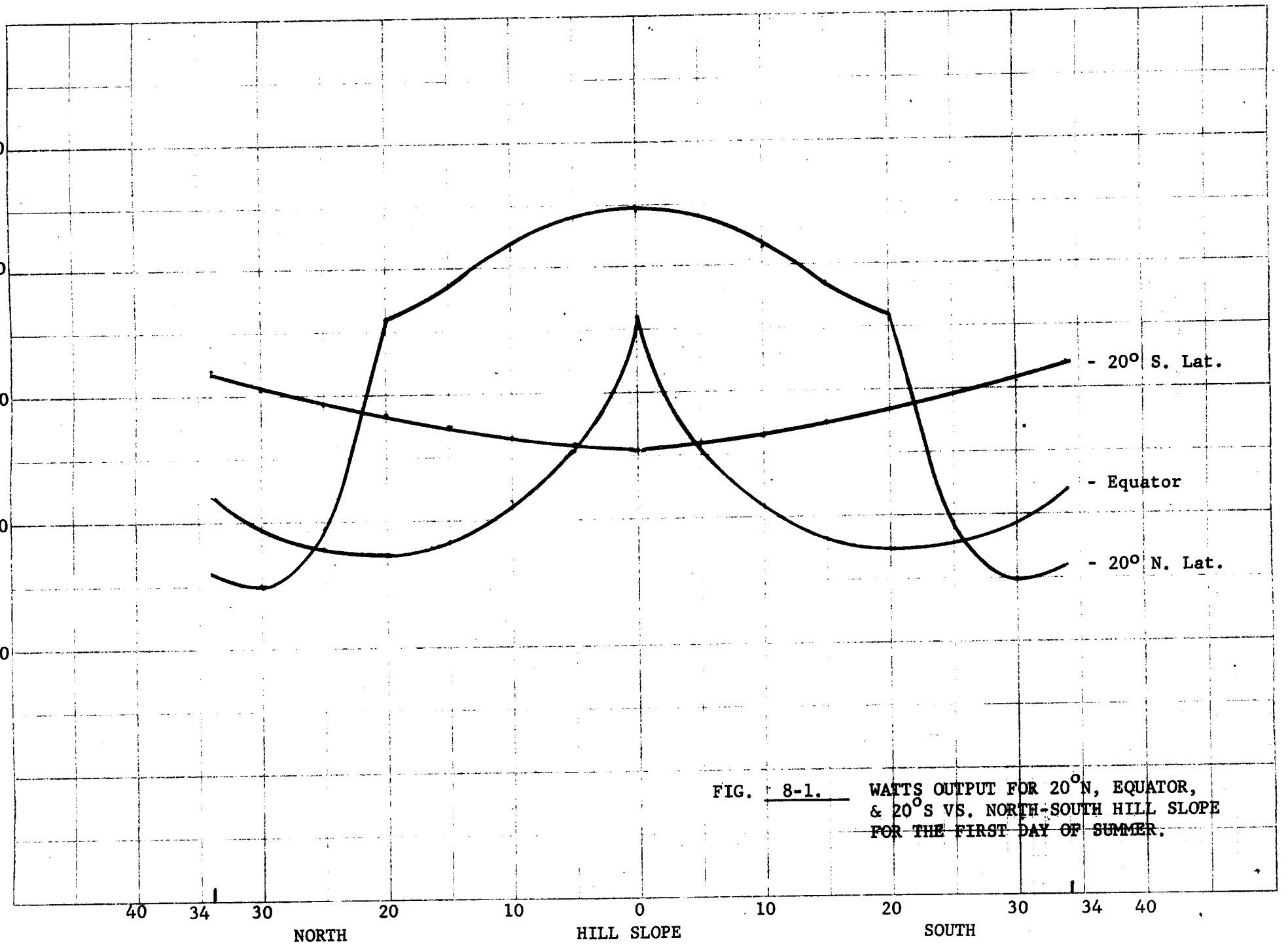

FIG. 8-1. WATTS OUTPUT FOR 20°N, EQUATOR, & 20°S VS. NORTH-SOUTH HILL SLOPE FOR THE FIRST DAY OF SUMMER.

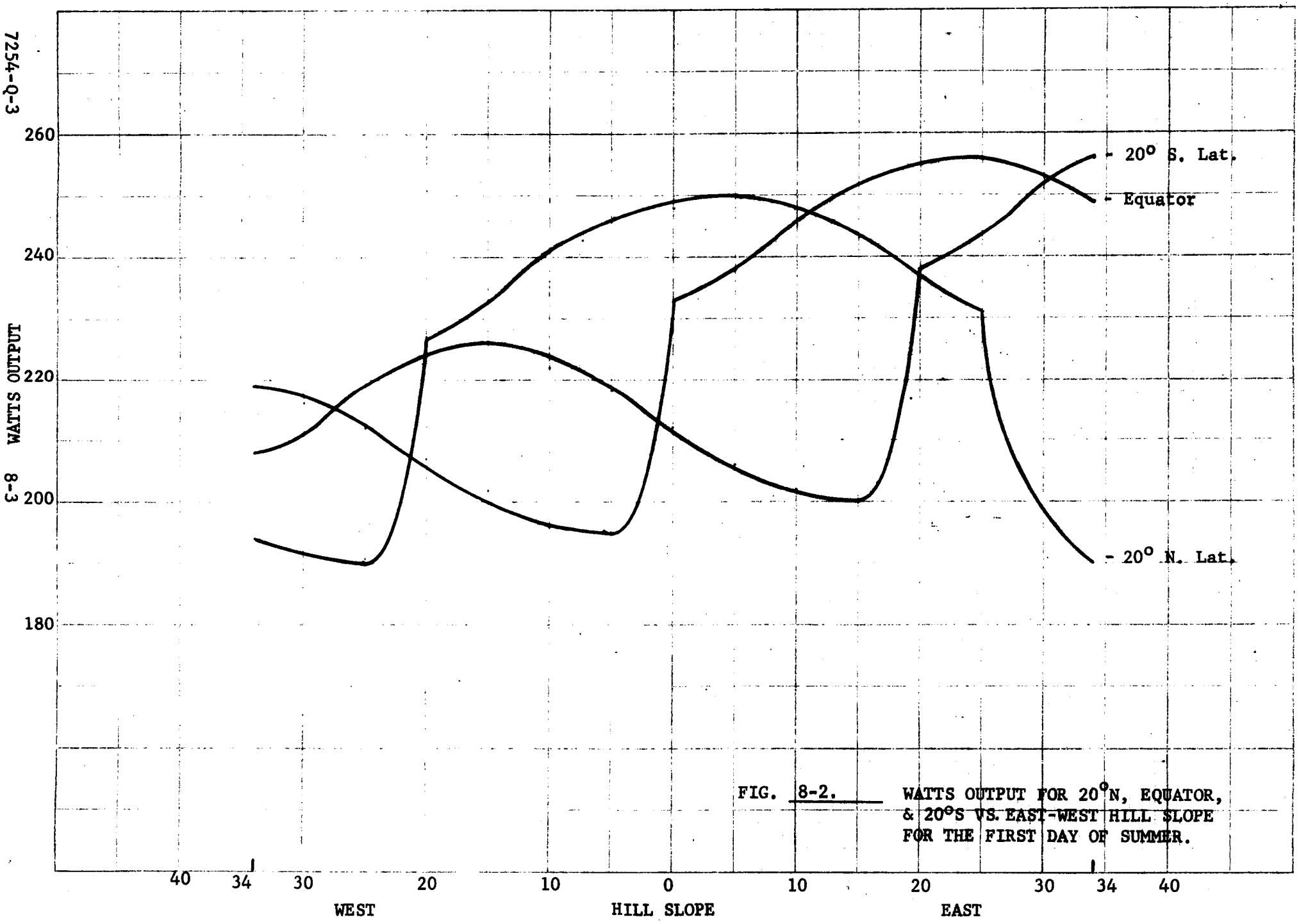

FIG. 8-2. WATTS OUTPUT FOR 20°N, EQUATOR, & 20°S VS. EAST-WEST HILL SLOPE FOR THE FIRST DAY OF SUMMER.

A summary of the system is as follows:

a. Type of cell - 0.010 thick, 2 x 2 cm, N/P, top contact, 1-3 ohm-cm, solderless
b. Output of cell - 58W at 485mV (AMO)
c. Number of cells/circ. - 6P x 57S
d. Number of circuits/panel - 15
e. Number of panels/array - 6
f. Total number of cells - 30,780
g. Number of deployment mech. - 2
h. Deployment mode - torsion springs and snubbers
i. Weight summary: (lbs)

(1) Mechanical		
(a) Solar panel -		14.65
(b) Adhesives -		0.49
(c) Sub's support -		3.08
(d) Space frame -		5.16
(e) Pivotal depl. mech. -		3.18
(f) Miscellaneous -		6.51
Subtotal		33.07
(2) Electrical		
(a) Solar panel		18.63
(b) Adhesives		4.74
Subtotal		23.37
Total system weight		56.44 lbs

The power-to-weight ratio varies with the power output of the array at noon at a specific Martian location. The range of power outputs for the first day of summer (lowest solar intensity) are shown for the noon condition in Figs. 8-1 and 8-2.

The specific power output is based on the equivalent power at 1 AU, and taking the power output at the worst case condition of 50 mW/cm^2 (summer) the following limits are obtained from Section 3.0.

Summer (maximum) = 256W
Summer (minimum) = 190W

Converting to 1 AU by the ratio of 46/140 = 0.328

256/0.328 = 780W (1 AU)
190/0.328 = 580W (1 AU)

Therefore the specific power would lie between the range of,

780/56.44 = 13.8 W/lb
580/56.44 = 10.3 W/lb

APPENDIX A

ANGLE OF INCIDENCE OF SUNLIGHT ON TRUNCATED CONE FOR SEVERAL LOCATIONS AND ORIENTATIONS ON THE MARTIAN SURFACE

The angle of incidence of sunlight on the solar-paneled truncated cone is defined in Fig. A-1. Here, $-\frac{\pi}{2} \leq \varphi \leq \frac{\pi}{2}$. We are interested in determining this angle for any location (i.e., latitude) and orientation of the cone on the Martian surface, and for any time of day and year. Let λ = latitude of the cone's position on the Martian surface, and let β, δ be the polar angles of the cone's axis measured relative to the local vertical and the north-south meridian, respectively. Refer to Fig. A-2. Here, $-90^{o} \leq \lambda \leq 90^{o}$, $0 \leq \beta \leq 90^{o}$, and, $-180^{o} \leq \delta \leq 180^{o}$. We shall let θ denote the time of the Martian year, and α the time of the Martian day. Table A-I shows values of θ corresponding to the first day of each Martian season.

TABLE A-I

θ	Time of Martian Year
0	1st day of Spring
90^{o}	1st day of Summer
180^{o}	1st day of Fall
270^{o}	1st day of Winter

The Martian seasons are defined for the northern Martian hemisphere. The three times during the Martian day which are of greatest interest are dawn, noon and sunset. For any value of θ, the values of α for these three times of day are as follows:

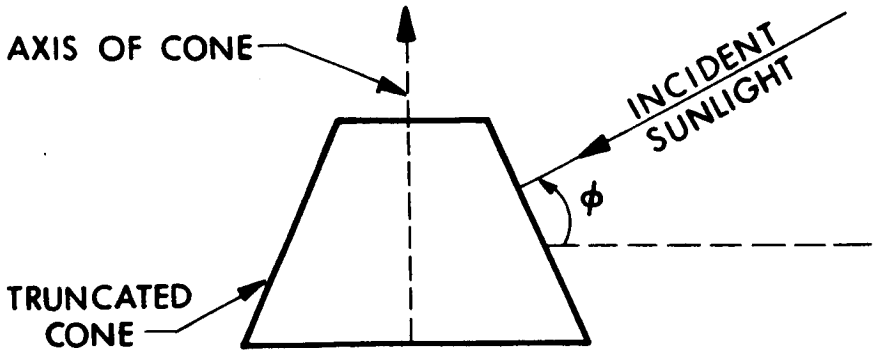

Figure A-1. Definition of φ

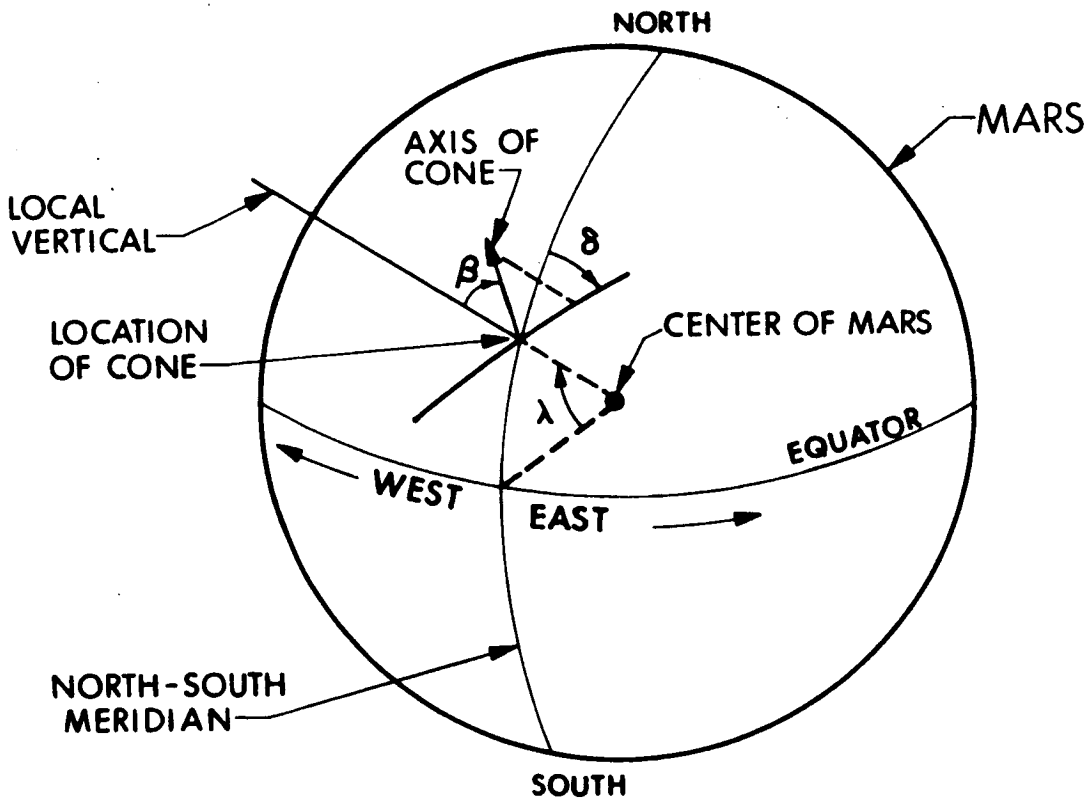

Figure A-2. Definition of λ, β, δ

827

Dawn: $\alpha = \theta - 90^{o}$

Noon: $\alpha = \theta$

Sunset: $\alpha = \theta + 90^{o}$

It is not difficult to show that the angle φ is given as follows:

$$\varphi = 90^{o} - \Psi$$

where,

$$\cos \Psi = \cos \theta \, [\cos \alpha \, (\cos \lambda \cos \beta - \sin \lambda \sin \beta \cos \delta) - \sin \alpha \sin \beta \sin \delta] + \cos \gamma \sin \theta \, [\sin \alpha \, (\cos \lambda \cos \beta - \sin \lambda \sin \beta \cos \delta) + \cos \alpha \sin \beta \sin \delta] + \sin \gamma \sin \theta \, (\sin \lambda \cos \beta + \cos \lambda \sin \beta \cos \delta)$$

Here, γ = inclination of Mar's equator to its orbital plane = 24^{o}, and $0 \leq \Psi \leq 180^{o}$.

Table A-II shows several values of φ computed for the first day of summer ($\theta = 90^{o}$). The values were computed for the three latitudes $\lambda = -20^{o}, 0^{o}, 20^{o}$, at dawn, noon and sunset. At each latitude, β was assigned values in the range $0 \leq \beta \leq 34^{o}$, for $\delta = 0, 180^{o}, 90^{o}, -90^{o}$. The axis of the cone leans in a northerly, southerly, easterly, westerly direction when $\delta = 0, 180^{o}, 90^{o}, -90^{o}$, respectively (when, $\beta = 0$). Figure A-3 shows a plot of φ versus β for the values $\delta = 0, 180^{0}$ in Table A-II, i.e., for the north-south inclination of the cone axis. Figure A-4 shows a plot of φ versus β for the values $\delta = 90^{o}, -90^{o}$ in Table A-II, i.e., for the east-west inclination of the cone axis.

Table A-III shows several values of φ computed for the first day of Spring ($\theta = 0$). Figure A-5 shows a plot of φ versus β for the values $\delta = 0, 180^{o}$ in Table A-III, and Fig. A-6 shows φ versus β for the values $\delta = 90^{o}, -90^{o}$, also in Table A-III.

TABLE A-II

$\theta = 0$

α	λ	δ	β	φ
0 (dawn)	20°	–	0	8°
		0	17°	$14^\circ\ 9'$
			34°	$19^\circ 12'$
		π	17°	$1^\circ 13'$
			34°	$-5^\circ 38'$
		$\pi/2$	17°	$23^\circ 35'$
			34°	$38^\circ 42'$
		$-\pi/2$	17°	$-7^\circ 42'$
			34°	$-23^\circ 15'$
	0	–	0	0
		0	17°	$6^\circ 50'$
			34°	$13^\circ\ 7'$
		π	17°	$-6^\circ 50'$
			34°	$-13^\circ\ 7'$
		$\pi/2$	17°	$15^\circ 29'$
			34°	$30^\circ 40'$
		$-\pi/2$	17°	$-15^\circ 29'$
			34°	$-30^\circ 40'$
	-20°	–	0	-8°
		0	17°	$-1^\circ 13'$
			34°	$5^\circ 38'$
		π	17°	$-14^\circ\ 9'$
			34°	$-19^\circ 12'$
		$\pi/2$	17°	$7^\circ 42'$
			34°	$23^\circ 15'$
		$-\pi/2$	17°	$-23^\circ 35'$
			34°	$-38^\circ 42'$

α	λ	δ	β	φ
$\pi/2$ (noon)	20°	–	0	86°
		0	17°	77°
			34°	60°
		π	17°	69°
			34°	52°
		$\pi/2$	17°	$72^\circ 22'$
			34°	$55^\circ 37'$
		$-\pi/2$	17°	$72^\circ 22'$
			34°	$55^\circ 37'$
	0	–	0	66°
		0	17°	83°
			34°	80°
		π	17°	49°
			34°	32°
		$\pi/2$	17°	$60^\circ 56'$
			34°	$49^\circ\ 7'$
		$-\pi/2$	17°	$60^\circ 56'$
			34°	$49^\circ\ 7'$
	-20°	–	0	46°
		0	17°	63°
			34°	80°
		π	17°	29°
			34°	12°
		$\pi/2$	17°	$43^\circ 24'$
			34°	$36^\circ 30'$
		$-\pi/2$	17°	$43^\circ 24'$
			34°	$36^\circ 30'$

α	λ	δ	β	φ
π (sunset)	20°	–	0	8°
		0	17°	$14^\circ\ 9'$
			34°	$19^\circ 12'$
		π	17°	$1^\circ 13'$
			34°	$-5^\circ 38'$
		$\pi/2$	17°	$-7^\circ 42'$
			34°	$-23^\circ 15'$
		$-\pi/2$	17°	$23^\circ 35'$
			34°	$38^\circ 42'$
	0	–	0	0
		0	17°	$6^\circ 50'$
			34°	$13^\circ\ 7'$
		π	17°	$-6^\circ 50'$
			34°	$-13^\circ\ 7'$
		$\pi/2$	17°	$-15^\circ 29'$
			34°	$-30^\circ 40'$
		$-\pi/2$	17°	$15^\circ 29'$
			34°	$30^\circ 40'$
	-20°	–	0	-8°
		0	17°	$-1^\circ 13'$
			34°	$5^\circ 38'$
		π	17°	$-14^\circ\ 9'$
			34°	$-19^\circ 12'$
		$\pi/2$	17°	$-23^\circ 35'$
			34°	$-38^\circ 42'$
		$-\pi/2$	17°	$7^\circ 42'$
			34°	$23^\circ 11'$

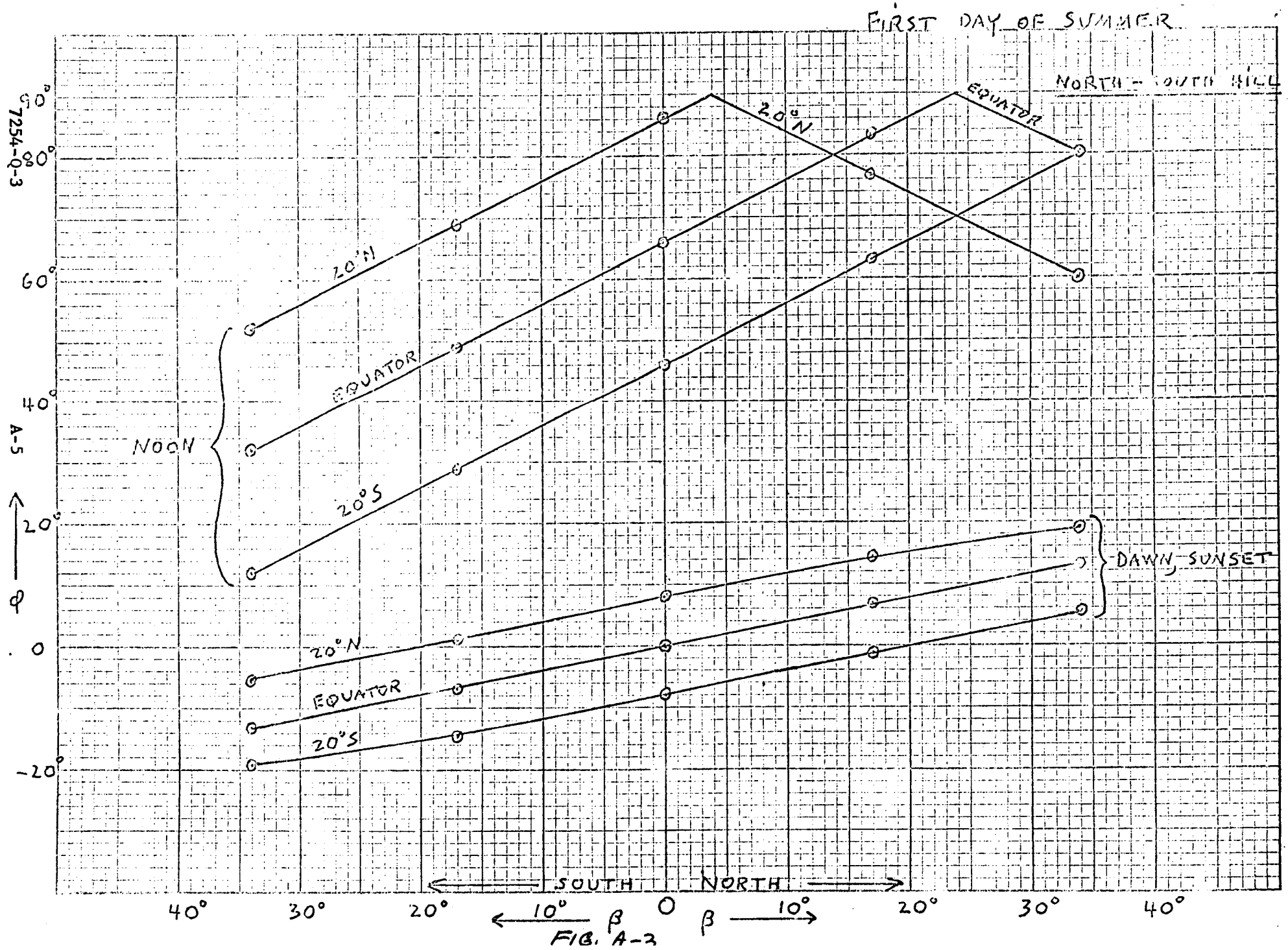

FIG. A-3

KEUFFEL & ESSER CO.

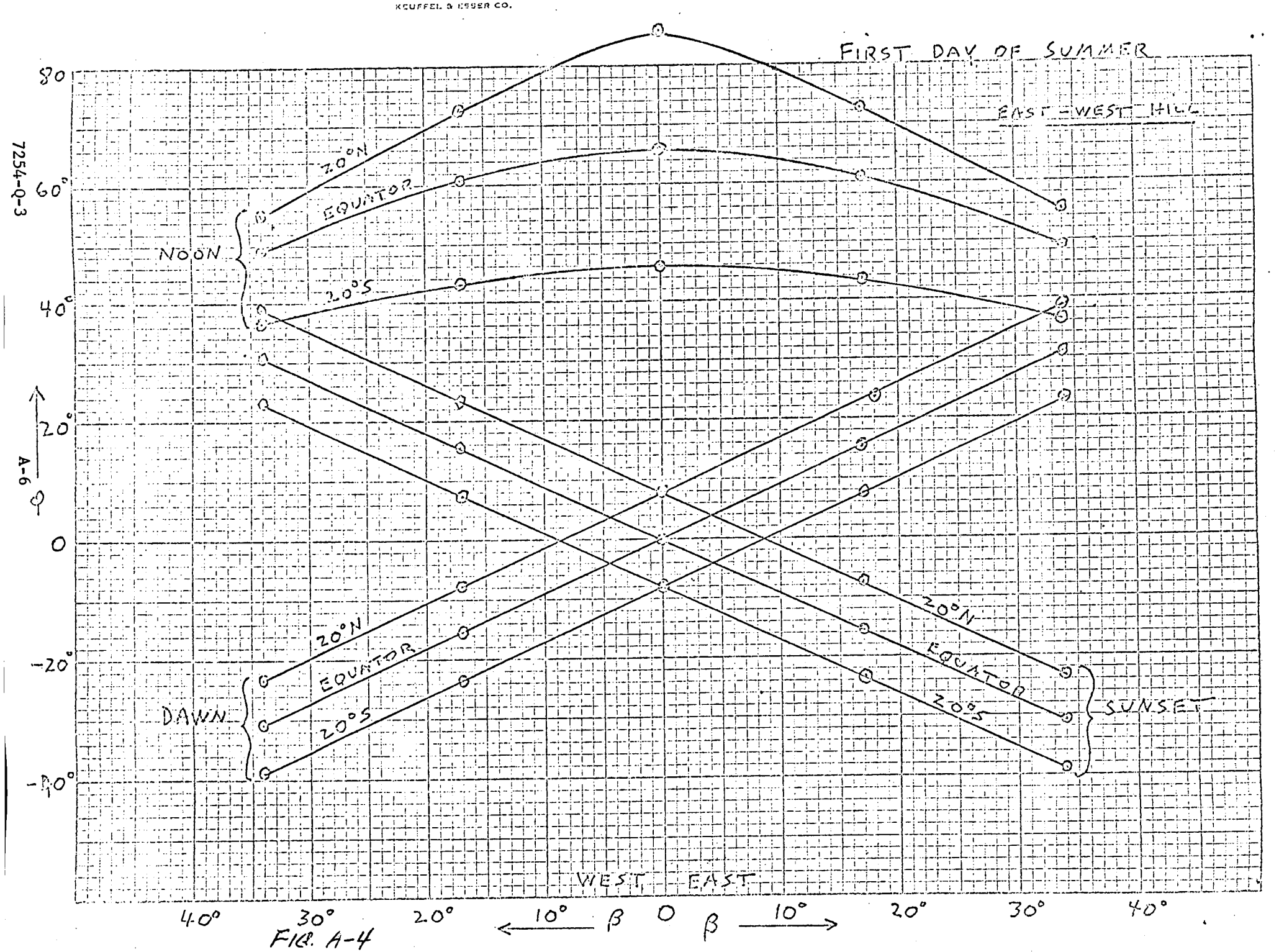

7254-Q-3

A-6

FIG. A-4

TABLE A-III

$\theta = 90^\circ$

α	λ	δ	β	φ	α	λ	δ	β	φ	α	λ	δ	β	φ
$-\pi/2$	20°	—	0	0	0	20°	—	0	70°	$\pi/2$	20°	—	0	0
(dawn)		0	17°	0	(noon)		0	17°	53°	(sunset)		0	17°	0
			34°	0				34°	36°				34°	0
		π	17°	0			π	17°	87°			π	17°	0
			34°	0				34°	76°				34°	0
		$\pi/2$	17°	17°			$\pi/2$	17°	$63^\circ 50'$			$\pi/2$	17°	-17°
			34°	34°				34°	$51^\circ 10'$				34°	-34°
		$-\pi/2$	17°	-17°			$-\pi/2$	17°	$63^\circ 50'$			$-\pi/2$	17°	17°
			34°	-34°				34°	$51^\circ 10'$				34°	34°
	0	—	0	0		0	—	0	90°		0	—	0	0
		0	17°	0			0	17°	73°			0	17°	0
			34°	0				34°	56°				34°	0
		π	17°	0			π	17°	73°			π	17°	0
			34°	0				34°	56°				34°	0
		$\pi/2$	17°	17°			$\pi/2$	17°	73°			$\pi/2$	17°	-17°
			34°	34°				34°	56°				34°	-34°
		$-\pi/2$	17°	-17°			$-\pi/2$	17°	73°			$-\pi/2$	17°	17°
			34°	-34°				34°	56°				34°	34°
	-20°	—	0	0		-20°	—	0	70		-20°	—	0	0
		0	17°	0			0	17°	87°			0	17°	0
			34°	0				34°	76°				34°	0
		π	17°	0			π	17°	53°			π	17°	0
			34°	0				34°	36°				34°	0
		$\pi/2$	17°	17°			$\pi/2$	17°	$63^\circ 50'$			$\pi/2$	17°	-17°
			34°	34°				34°	$51^\circ 10'$				34°	-34°
		$-\pi/2$	17°	-17°			$-\pi/2$	17°	$63^\circ 50'$			$-\pi/2$	17°	17°
			34°	-34°				34°	$51^\circ 10'$				34°	34°

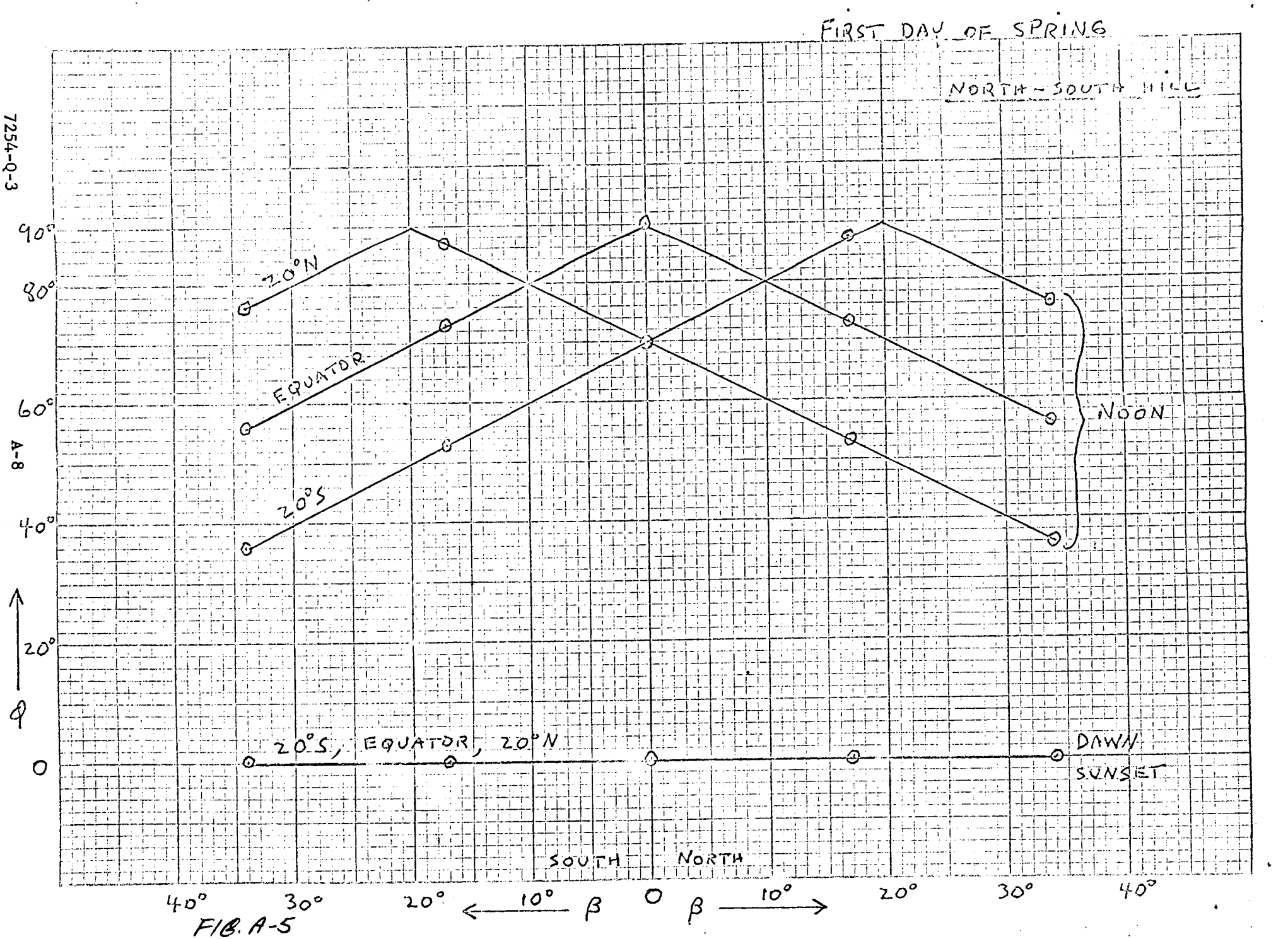

FIG. A-5

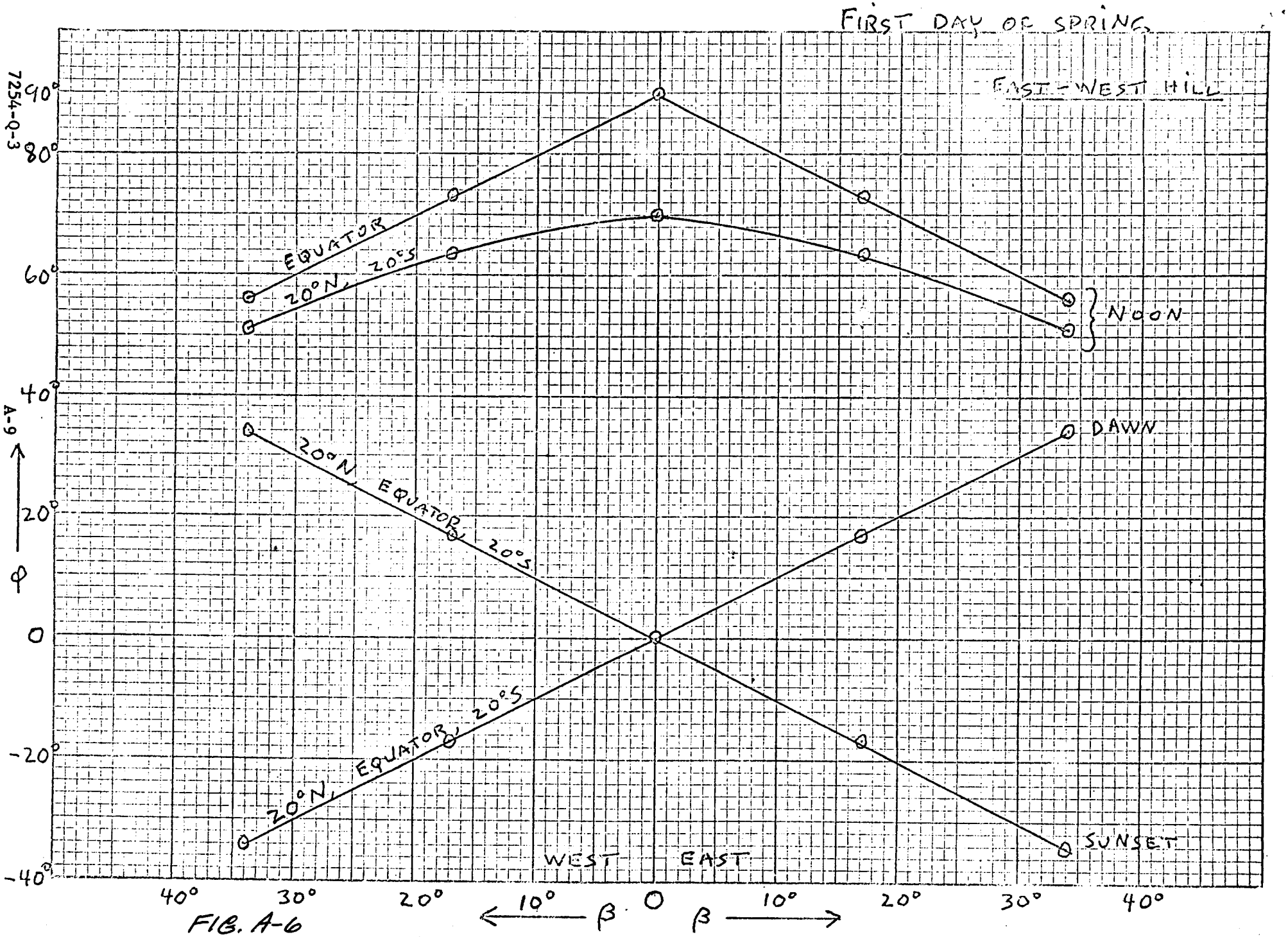

FIG. A-6

APPENDIX B

SOLAR PANEL HEAT BALANCE EQUATIONS

The array was assumed to rest on a fully illuminated surface with the sun's vector making a vertical angle ϕ with the base plane of the spacecraft. A heat balance on an isolated portion of the panel perpendicular to the sun in the horizontal plane is described below.

For the cell side of the panel (in words):

> Solar heating - converted to electricity + sunlight reflected from surface = heat radiated to space + heat radiated to upper atmosphere + heat radiated to surface + heat conducted to rear surface of panel. (Convection has been omitted for simplicity.)

In symbols: (See Table of Nomenclature at the end of this Appendix.)

$$\alpha_{s1} F G_s \cos(\phi - 23.8^\circ) - \alpha_{s1} F G_s \eta \cos(\phi - 23.8^\circ) + \bar{A}_m G_s F F_{1-m} \alpha_{s1} =$$

$$(1 - F_{1-m})\, t\epsilon_1 \sigma T^4_1 + (1 - F_{1-m})(1-t)\, \epsilon_1 \left(\sigma T^4_1 - \sigma T^4_a\right) +$$

$$F_{1-m}\, \epsilon_1 \left(\sigma T^4_1 - \sigma T^4_m\right) + C(T_1 - T_2) \qquad (1)$$

For the back side of the panel (in words):

> Heat conducted from front + sunlight reflected from surface = heat radiated to space + heat radiated to atmosphere + heat radiated to surface.

In symbols:

$$C(T_1 - T_2) + F_{2-R}\bar{A}_n G_s F\alpha_{s2} = \epsilon_2 F_{2-s} t\sigma T^4_2 + \epsilon_2 F_{2-s}(1-t)(\sigma T^4_2 - \sigma T^4_a) + F_{2-m}\,\epsilon_2 \left(\sigma T^4_2 - \sigma T^4_m\right) \quad (2)$$

Setting $T_1 = T_2$ (for a panel with a high thermal conductance) assuming $\epsilon_1 = \epsilon_2$, combining terms and simplifying results in:

$$FG_s \left[\alpha_{s1}(1-\eta) \cos(\phi - 23.8^\circ) + (\alpha_{s1}F_{1-m} + \alpha_{s2}F_{2-R})\,\bar{A}_m\right] + (1 - F_{1-m} + F_{2-s})(1-t)\,\epsilon\sigma T^4_a + (F_{1-m} + F_{2-m})\,\epsilon\sigma T^4_m = \sigma T^4_\epsilon\,(1 + R_{2-s} + F_{2-m}) \quad (3)$$

For a given Ta and Tm (see the Table of Assumed Temperatures below), Eq. 3 can be written as a function of cos ϕ and T^4:

$$\sigma T^4 = K_1 \cos(\phi - 23.8^\circ) + K_2 \quad (4)$$

where K_1 and K_2 are constants. The curves of Fig. 5-1 in Section 5 of this report are plots of T versus ϕ over the possible range of ϕ as determined by the geometric analysis (see Appendix A).

For Fig. 5-2, the solar intensity varies as the cosine of the horizontal sun angle ω, and an equation of the form of Eq. 4 was plotted around one-half of the truncated cone. An estimate of change due to convection was made and plotted as the dotted line in Fig. 5-2. This change is proportional to the difference between panel temperature and ambient temperature and was based on convection estimates discussed in the second quarterly report.

TABLE OF ASSUMED BACKGROUND TEMPERATURES

	First Day of Spring, Equator	First Day of Summer, 20°N Latitude
Solar Constant (G_s)	60 mw/cm^2	50 mw/cm^2
Average Sky Temperature	220°K (-53°C)	208°K (-65°C)
Dawn Temperature	240°K (-33°C)	238°K (-35°C)
Noon Temperature	285°K (12°C)	281°K (8°C)
Sunset Temperature	270°K (-3°C)	267°K (-6°C)

TABLE OF NOMENCLATURE

σ_{s1} = solar absorptivity cell side = 0.81

σ_{s2} = solar absorptivity back side = 0.30 (white paint)

F = transmission factor to sunlight = 0.92

G_s = solar constant at Mars orbit

η = solar panel efficiency

$\overline{A}_m$ = Mars surface albedo

F_{1-m} = cell side view factor of Mars surface

t = atmospheric transmissivity to Mars radiation = 0.90

σ = Boltzmann's Constant, 36.6×10^{-12} w/in^2 $^oK^4$

T_1 = cell side temperature

T_a = sky temperature

T_m = surface and ambient atmosphere temperature

h = heat transfer coefficient, watts/in. ^oC
(reference: first quarterly report)

C = conductance of solar panel

T_2 = back side surface temperature

ϕ = vertical sun vector angle

ω = horizontal sun vector angle